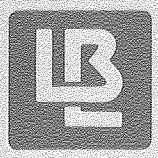

Lawrence Berkeley Laboratory
UNIVERSITY OF CALIFORNIA

Materials & Molecular Research Division

To be published as a Chapter in Man and Stratospheric Ozone, Vol. 1., Richard B. Ward and Frank A. Bower, eds., Boca Raton, FL.: Chemical Rubber Company, Inc.

ODD NITROGEN PROCESSES

Harold S. Johnston

January 1980

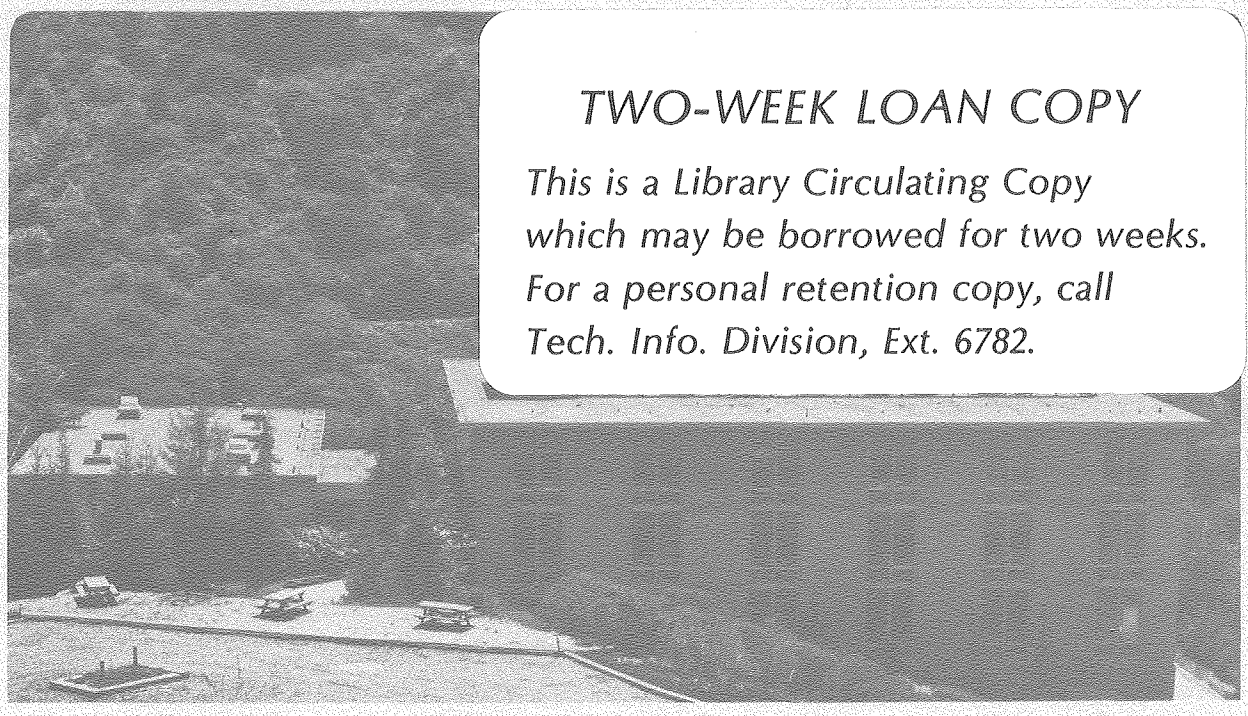

Prepared for the U.S. Department of Energy under Contract W-7405-ENG-48

DISCLAIMER

LBL-10585

MAN AND STRATOSPHERIC OZONE

CHAPTER 4

Odd Nitrogen Processes

Author:

Harold S. Johnston

Department of Chemistry, University of California, and Materials and Molecular Research Division of Lawrence Berkeley Laboratory, Berkeley, California

Table of Contents

Page

I. STRATOSPHERIC OBSERVATIONS AND INTERPRETATIONS

A. Introduction

In 1970 Murcray et al.[1] measured four vertical profiles of nitric acid vapor between about 15 and 28 km. These observations are as valid today as they were in 1970, and they are used later in this chapter to check the results of current theories. Also in 1970 some modelers calculated the vertical distribution of stratospheric ozone using photochemical models, which involved no atmospheric motions. Both the 1970 photochemistry and the neglect of motions are regarded as unacceptable now, and one would not cite the results of these calculations as being significant in current discussions. These two examples point up a distinction between observations in the stratosphere and model calculations for the stratosphere: (1) Although each observation is piecemeal, the information derived from stratospheric measurements is cumulative, is of long-lasting value, and leads directly to interpretations. (2) A dynamical and photochemical model must be complete, at least within a certain domain, in order to lead to any statements; and a change of any of its input quantities (rate coefficients, solar radiation intensity, parameterization of atmospheric motions, etc.) in principle modifies all of its results and in fact can lead to important changes in its predictions. Observations lead to cumulative, permanently valid interpretations, but are incapable of making future predictions. Models are susceptible to being outdated as new laboratory and atmospheric data are developed, but they are capable of making future predictions. This chapter is in three parts. The first concerns interpretations that can be made

from atmospheric observations, the second reviews some predictions made by atmospheric models, and the third compares between certain model results and atmospheric measurements with an emphasis on detecting evidence of significant disagreements.

B. Interpretation of Atmospheric Observations

1. Stratosphere Temperature and Ozone Distributions

Two observable quantities of especial interest in this context are atmospheric temperature and ozone, for which standard profiles are given by Figure 4.1. The latitudinal and vertical dependences of temperature are given by a zonal-average contour map in Figure 4.2, and, similarly, mixing ratios for ozone are shown in Figure 4.3. These two figures are based on Dütsch's[2] data published in 1978 and supplied in tabular form to this laboratory; these figures are the three-month averages for September, October, and November. Several zonal-average figures appear later in this chapter based on these distributions of temperature and ozone.

2. Catalytic Cycles and Null Cycles

The detailed development of this approach is given by a long recent article by Johnston and Podolske,[3] and certain high points are recapitulated here. Ozone is present in the stratosphere with mixing ratios of parts per million (Figure 4.3). There are a number of free radicals HO_x (H, HO, HOO), NO_x (N, NO, NO_2, NO_3), and ClX (Cl, ClO)* that

---

* There are a number of different conventions used in this context. In this Chapter the terms HO_x, NO_x, and ClX are used for the chemically active free radicals as listed above. The free radicals plus photochemically reversible molecular reservoirs for the free radicals are often defined as HO_y(H, HO, HOO, H_2O_2, HNO_3, $HOONO_2$, HOCl), NO_y (N, NO, NO_2, NO_3, N_2O_5, HNO_3, $HOONO_2$, $ClONO_2$) and ClY (Cl, ClO, HCl, HOCl, $ClONO_2$). These families do not include the parent substances, H_2O, N_2O, or organic chlorine compounds.

react with ozone, but these are present in the stratosphere with mixing ratios of parts per billion or less. Because of this great disparity in number a one-way reaction of free radicals with ozone would have only a small effect on ozone, for example

$$NO + O_3 \rightarrow NO_2 + O_2 \qquad (4.1)$$

	NO	O_3
Before	10^{-9}	10^{-6}
After	0	0.999×10^{-6} .

If the trace species reacts in a cyclic manner, such as

$$NO + O_3 \rightarrow NO_2 + O_2 \qquad (4.1)$$

$$O_3 + h\nu \rightarrow O_2 + O \qquad (4.2)$$

$$NO_2 + O \rightarrow NO + O_2 \qquad (4.3)$$

$$\text{net: } 2\ O_3 + h\nu \rightarrow 3\ O_2 \quad (\text{catalyzed by } NO_x) \qquad (4.4)$$

it can have a significant effect on ozone:

	NO	O_3
Before	10^{-9}	10^{-6}
After one cycle	10^{-9}	0.998×10^{-6}
After two cycles	10^{-9}	0.996×10^{-6}
After 100 cycles	10^{-9}	0.8×10^{-6} .

The way free radicals can have a significant effect on ozone is to act as catalysts in processes that are cyclic in free radicals and destructive or productive of ozone. Cyclic, catalytic processes are disproportionately important.

This simplifying principle is immediately confronted by the need for qualifying statements. Reaction (4.1) itself is catalyzed both by the HO_x and ClX free radicals

$$HO + O_3 \rightarrow HOO + O_2 \qquad (4.5)$$

$$HOO + NO \rightarrow HO + NO_2 \qquad (4.6)$$

$$\text{net:}\quad NO + O_3 \rightarrow NO_2 + O_2 \quad \text{(catalyzed by } HO_x\text{)} \qquad (4.7)$$

$$Cl + O_3 \rightarrow ClO + O_2 \qquad (4.8)$$

$$ClO + NO \rightarrow Cl + NO_2 \qquad (4.9)$$

$$\text{net:}\quad NO + O_3 \rightarrow NO_2 + O_2 \quad \text{(catalyzed by ClX)} \qquad (4.10)$$

These reactions tend to couple the NO_x, HO_x, and ClX systems. Reactions (4.1), (4.7), and (4.10) are not always followed by reaction (4.3), which leads to ozone destruction, but rather they are usually (altitude dependent) followed by photolysis of nitrogen dioxide and regeneration of ozone:

$$NO + O_3 \rightarrow NO_2 + O_2 \qquad (4.1, 4.7, 4.10)$$

$$NO_2 + h\nu\ (300 < \lambda < 400\ \text{nm}) \rightarrow NO + O \qquad (4.11)$$

$$O + O_2 + M \rightarrow O_3 + M \qquad (4.12)$$

$$\text{net}\quad \text{null reaction} \qquad (4.13)$$

The situation can be summarized by the diagram

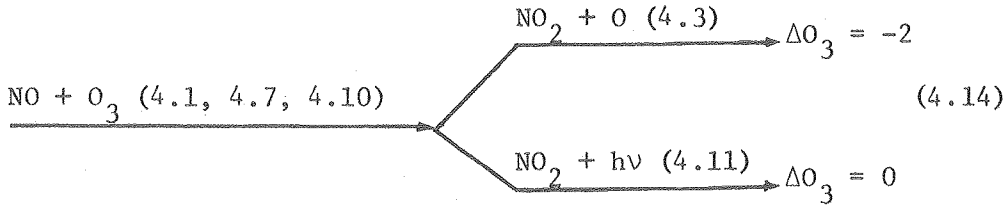

(4.14)

Thus reaction (4.3) is the bottleneck or the rate-determining step for the destruction of ozone by NO_x in the complex coupled N-H-Cl system of reactions (4.1 - 4.12). In the NO_x system, this identification of the rate-determing step becomes an important, valid, simplifying principle

in the interpretation of atmospheric observations and in the interpretation of the results of model calculations: the rate of destruction of ozone by the oxides of nitrogen is given as an excellent approximation by twice the rate of reaction (4.3)

$$2\ k_3\ [NO_2][O] \tag{4.15}$$

where k is the rate constant and square brackets refer to the concentration of the corresponding species. As shown in reference 3, there are several other very small terms that contribute to ozone destruction by the oxides of nitrogen, but these may be neglected relative to reaction (4.3), at least in the middle and upper stratosphere.

3. Ozone Production and Loss in the O_x Family of Reactions

In the middle and upper stratosphere, ozone is formed almost exclusively by the photolysis of molecular oxygen with short-wavelength ultraviolet radiation

$$O_2 + h\nu\ (\lambda < 244\ nm) \rightarrow O + O \tag{4.16}$$

$$2\ (O + O_2 + M \rightarrow O_3 + M) \tag{4.12}$$

$$\text{net:}\quad 3\ O_2 + h\nu \rightarrow 2\ O_3 \quad . \tag{4.17}$$

The rate determining step in this couplet of reactions is (4.16), so that the rate of ozone formation in the stratosphere is primarily

$$2\ j_{16}\ [O_2] \tag{4.18}$$

where j is the photochemical coefficient.

Ozone is photolyzed at a rate much faster than that for photolysis of oxygen; however, the photolysis of ozone does not lead to ozone destruction since it is usually followed by recombination:

$$O_3 + h\nu\ (\lambda > 310\ nm) \rightarrow O_2 + O \qquad (4.19)$$

$$O + O_2 + M \rightarrow O_3 + M \qquad (4.12)$$

net: null

$$O_3 + h\nu\ (\lambda < 310\ nm) \rightarrow O_2 + O(^1D) \qquad (4.20)$$

$$O(^1D) + M \rightarrow O + M \qquad (4.21)$$

$$O + O_2 + M \rightarrow O_3 + M \qquad (4.12)$$

net: null .

These processes have relaxation times of less than one second over almost all of the stratosphere, and they rapidly set up steady state concentrations of singlet atomic oxygen and of ground-state atomic oxygen.

$$O(^1D) = j_{20}[O_3]/k_{21}[M] \qquad (4.22)$$

$$O = (j_{20} + j_{19})[O_3]/k_{12}[M][O_2] \quad . \qquad (4.23)$$

The destruction of ozone by the O_x [O_3, O, $O(^1D)$] family of reactions occurs through the sequence

$$O_3 + h\nu \rightarrow O_2 + O$$

$$O_3 + O \rightarrow O_2 + O_2 \qquad (4.24)$$

net: $2\ O_3 + h\nu \rightarrow 3\ O_2$. (4.25)

In this case, reaction (4.24) is the rate determining step, and the rate of ozone destruction by O_x reactions is

$$2\ k_{24}[O][O_3] \quad . \qquad (4.26)$$

Similar processes occur with $O(^1D)$ but the concentration of $O(^1D)$ is so small that this rate is small compared to the rate of reaction (4.24).

4. The Method of Instantaneous Rates[4]

The atmosphere of the globe may be divided into a three-dimensional grid with intervals of 10° latitude, 15° longitude, and 1 km altitude (from 0 to 50 km). The intensity of solar radiation has been measured above the atmosphere.[5,6,7] By means of molecular absorption of radiation, Rayleigh scattering of radiation,[8] and an assumed albedo of 0.3 for the surface of the earth and tropospheric clouds, one may calculate the intensity of radiation at each wavelength between 170 and 700 nm in each volume element as defined above. This distribution of radiation depends on longitude, latitude, and altitude of the volume element. The rate of production of ozone from photolysis of molecular oxygen, Equation (4.18), was calculated in each volume element for the observed average ozone distribution given by Figure 4.4, and these rates were averaged around 360 degrees of longitude at each latitude and altitude to give the zonal average rates of ozone formation, Figure 4.5. The contours of this figure are given on a linear scale to emphasize the regions of large gross photochemical formation of ozone. The maximum rate of ozone production is above the tropical region and between 35 and 45 km. Rates at 10 percent of the maximum rate occur down to 25 km at the equator and out to ± 85° latitude at 40 km. Figure 4.5 is not the result of a model calculation; rather it comes from the observed distribution of ozone, oxygen, and solar radiation above the atmosphere and an independent, one-step calculation. Figure 4.5 is only one step removed from being the "observed" rate of gross ozone production.

Another one-step calculation leads to a useful interpretation. The local concentration of ozone (Figure 4.4) is divided by the local, zonal-average (360° longitude) rate of ozone formation (Figure 4.5) to give a fictitious ozone photochemical replacement time, Figure 4.6.

$$\tau = [O_3]/2\ j_{16}[O_2] \quad . \tag{4.27}$$

This time is how long it would take locally to produce an amount of ozone equal to that locally present and with the rest of the atmosphere having the ozone distribution given by Figure 4.4. The rate of air transport and mixing rates in the stratosphere are independently measured from the dissipation of radioactivity from nuclear bomb tests and from a number of meteorological considerations. A comparison of air transport times and ozone photochemical replacement times, such as Figure 4.6, leads to the conclusion that so far as the local distribution of ozone is concerned, photochemistry is dominant in the upper stratosphere, air motions are dominant in the lower stratosphere, and air motions and photochemistry are of comparable importance in the middle stratosphere.

Another example of the use of observational data to interpret certain aspects of stratospheric ozone is given by superimposing the zonal-average rate of ozone production (Figure 4.5) on the contour map of ozone concentration (Figure 4.4), and this is done in Figure 4.7. As has been known for several decades, the location of high rate of ozone production is substantially different from that of maximum ozone concentration. In temperate and polar regions, the peak ozone concentrations occur in volumes of air where the rate of ozone

production is exceedingly slow (compare Figure 4.6). Figure 4.7 implies the occurrence of atmospheric motions as a mechanism for transporting ozone from the region of fast production to the region of high concentration. The input to Figure 4.7 involved no explicit consideration of atmospheric motions, but involved only measured ozone concentrations and solar intensities. Actual three-dimensional motions in the atmosphere are demonstrated by the observed static ozone distribution.

The rate of ozone destruction by O_x species,* Equation (4.26), was calculated in each volume element (including zero rates on the dark side of the earth) and the zonal average rates as given in Figure 4.8 with the same scale of contour lines as in Figure 4.5. Simple visual inspection of Figures 4.5 and 4.8 shows that the O_x destruction of ozone is very much less than the photochemical production of ozone. The "ozone production region," which supplies the "ozone storage zone," compare Figure 4.7, is presumably at and below the maximum ozone mixing ratio, Figure 4.3. At most latitudes this maximum is at 35 to 40 km, but at some latitudes and seasons it extends almost to 45 km. For this reason, it has been judged appropriate to compare the global rate of ozone production between 15 and 45 km, Figure 4.5, with the corresponding integrated loss from O_x reactions, Figure 4.8. Over this altitude range, the global ozone loss to O_x reactions is only 15 percent of the rate of ozone production from solar radiation. For the last 15 years, the large discrepancy between ozone formation and ozone destruction by O_x reactions has required the search for other sources of ozone destruction, and these searches have led to catalytic cycles based on trace HO_x, NO_x, and ClX species.

---

*O_x = odd oxygen, O and O_3.

C. Source of Stratospheric Oxides of Nitrogen

Nitrous oxide, N_2O, is produced in soils and waters at the surface of the earth by biological processes (compare Chapter 9), and it is produced as a by-product in some combustion processes.[9,10] Away from the earth's surface, nitrous oxide is inert in the troposphere. Air motions transport nitrous oxide into the stratosphere where it is destroyed by ultraviolet radiation[11]

$$N_2O + h\nu \rightarrow N_2 + O \qquad (4.28)$$

and it is also destroyed by reaction with singlet oxygen atoms[12,13]

$$N_2O + O(^1D) \rightarrow N_2 + O_2 \qquad (4.29)$$

$$N_2O + O(^1D) \rightarrow NO + NO \qquad (4.30)$$

The reaction of singlet atomic oxygen with nitrous oxide is the principal source of natural stratospheric nitrogen oxides, and it appears to be very nearly the exclusive source.

The vertical profiles of nitrous oxide between 0 and about 35 km have been measured by balloon flights at a wide range of latitudes[14,15,16] and the concentrations of nitrous oxide between 40 and 60 km have been measured at one latitude by two rocket flights.[17] The data available through early 1978 were interpolated and extrapolated to produce an estimate of the global distribution of atmospheric nitrous oxide from 0 to 50 km.[18] The distribution of nitrous oxide mixing ratios for spring-fall conditions is given as Figure 4.9. Although this figure is based on observations, there are very few observations in the important tropical half of the globe, 30°N to 30°S, and there are few observations

above 35 km. This figure leads to some perspective on the global distribution of nitrous oxide and of its photochemical reactions, but one should not take literally its fine structure (or its lack of fine structure). The figure shows large values of nitrous oxide mixing ratios in the tropical stratosphere relative to values at corresponding altitudes in temperate and polar zones, and these features are consistent with the classical global circulation model of large injection of tropospheric air into the tropical stratosphere, horizontal transport to temperate and polar regions, and return of stratospheric air to the troposphere at polar zones and at discontinuities in the tropopause in temperate zones.[19]

With the qualifications stated above, Figure 4.9 gives an estimate of the observed three-dimensional distribution of stratospheric nitrous oxide. The rate of photolysis of this nitrous oxide in all volume elements of the sunlit half of the earth was evaluated, and the global zonal average is given[18] by Figure 4.10. At each latitude, the altitude of maximum photolysis rate is very nearly 30 km, and the photolysis rate is approximately symmetrical about this altitude. There is very little photolysis below 20 km or above 40 km. As a function of latitude, the photolysis rate is a strong maximum in the tropical zone.

The rate of reaction of nitrous oxide with singlet atomic oxygen to produce nitric oxide [reaction (4.30)], was calculated over the atmosphere, and the zonal average rate over the globe is given[18] by Figure 4.11. The altitude of maximum rate of nitric oxide production is roughly parallel to and slightly above the altitude of maximum ozone concentration (Figure 4.4); it is about 26 km at the equator, 23 km over temperate zones, and 20 km in polar regions. The formation of nitric oxide from nitrous oxide (Figure 4.11) has a different latitude

dependence than the photolysis of nitrous oxide (Figure 4.10). The global rate of nitric oxide production based on Figure 4.11 is 1.4×10^{27} molecules s^{-1}, 2.3×10^{12} g (NO) yr^{-1}, or 1.06×10^{12} g (N) yr^{-1}. The global rate of loss of nitrous oxide [photolysis plus both channels of $O(^1D)$ reaction] is 6.4×10^{27} molecules s^{-1}, 14.7×10^{12} g (N_2O) yr^{-1}, or 9.4×10^{12} g (N) yr^{-1}. The global inventory of N_2O from Figure 4.10 is 3.5×10^{37} molecules, 2550×10^{12} g (N_2O), or 1620×10^{12} g (N). The nitrous oxide average "residence time with respect to photochemistry," defined as the ratio of global inventory to global loss rate, is 175 years. Although extensive measurements of stratospheric nitrogen oxides (NO, NO_2, HNO_3) have been made, they are sufficient to permit only a rough estimation of the global inventory of the sum of these species. This global inventory divided by the global rate of formation of NO from N_2O (Figure 4.11) gives an average stratospheric residence time of 1 to 3 years for nitrogen oxides. They are presumably removed from the stratosphere by transport into the troposphere and rainout there, largely as nitric acid.

D. Solar Proton Event

This section concerns observations associated with the large solar proton event of August 4 to 8, 1972. During a solar proton event, a stream of high energy protons are emitted from the sun, and they are focused by the earth's magnetic field into the polar regions, primarily above 60° latitudes. In August 1972, the largest solar proton event within 25 years occurred. At the time one orbiting satellite[20] measured the magnitude and velocity of the incoming protons above the earth's atmosphere, and another satellite was making continual global measurements

of stratospheric ozone from backscattered solar ultraviolet radiation. From the nature of the incoming beam of solar protons, it can be calculated that the protons and secondary energetic electrons derived from their interactions with air would penetrate deep into the stratosphere. From laboratory measurements of the effect of energetic protons and electrons on air, it is calculated that the August 1972 solar proton event formed about 4.5×10^{33} molecules of HO and HOO free radicals and about 3×10^{33} molecules of nitric oxide.[20,21,22] As discussed in the preceding section, the stratospheric residence time for nitrogen oxides is 1 to 3 years, but the residence time for HO and HOO radicals is the order of magnitude of 1 hour in the mid-stratosphere. The photochemical relaxation times for ozone are given in Figure 4.6, although one needs to look at the comparable figure for summer,[23] in which case one sees that these times in the summer polar regions are about a month at 27 km, a week at 30 km, a day at 36 km, and 10 hours at 41 km. Thus one should look at the ozone record to see if there was a fast (1 hour) change and recovery from the HO_x radicals and to see if there was a prompt, sustained effect high in the stratosphere and a slowly appearing effect in the middle stratosphere caused by the increased NO_x.

In 1975 Crutzen et al.[24] compared the calculated vertical profile of natural nitrogen oxides in the polar region with the vertical profile of nitric oxide calculated to be produced from the observed flux of solar protons, and these two vertical profiles are given by Figure 4.12. At about 40 km the natural NO_x concentration was suddenly doubled, at 50 km the NO_x concentrations were increased by a factor of five, and at 30 km the NO_x concentrations were increased by 20 percent. Since

April 1970 and at the time of the solar proton event, the Nimbus 4 satellite had circled the earth about the poles in a sun-synchronous circular orbit; and it had been measuring backscattered solar ultraviolet radiation, from which vertical ozone profiles above about 24 km can be derived. In 1975 the ozone data from the Nimbus 4 satellite had not yet been interpreted, and Crutzen predicted that the data should show a sudden decrease of local ozone in the 35 to 45 km altitude range above the summer polar cap. In 1977, Heath et al.[21] published three series of direct ozone observations by the satellite for about one month before to one month after the solar proton event. The predicted ozone decrease was conspicuously present at 75° to 80°N latitude above the 4 mbar pressure surface. For this chapter, Crutzen donated a large amount of data from the Nimbus 4 satellite, that is, observed ozone columns above various pressure surfaces for a wide range of latitudes. A portion of these data are presented as ozone columns above certain altitudes (approximately 24, 32, 35, 39, 44, and 49 km) as a function of day of the year of 1972 for one month before and one month after the solar proton event: Figure 4.13 for 75° to 80°N, Figure 4.14 for 65° to 75°N, and Figure 4.15 for 45° to 55°N. The main solar proton event occurred on day 217 and further pulses occurred during 4 subsequent days.

Heath et al.[21] analyzed the Nimbus 4 satellite data for July and August of 1970, 1971, and 1973 in order to compare them with the record for 1972. They reported that the normal seasonal trend in the upper stratosphere at these times was a slow ozone increase at 55°N to 65°N and that stratospheric ozone was essentially constant around 75°N

to 80°N. The solar protons came into the stratosphere primarily above 60° latitudes, but there were some longitude-dependent irregularities and an exponentially decreasing input at latitudes lower than 60°.

It is interesting to examine the direct data in Figures 4.13 - 4.15. The records give observed ozone columns above various pressure surfaces (here translated to approximate altitudes); the cross represents the 24-hour-average observed value and the vertical bar associated with each datum includes both the imprecision of the measurement and the longitude-dependent variations of ozone. At 75° to 80°N before the solar proton event, there appears to be a slow decrease of ozone for the total atmosphere and for the columns above 24, 32, and 35 km; there appears to be a slow increase in ozone columns above 44 and 49 km; and the column above 39 km was very nearly constant for about 3 weeks before the solar proton event. After the solar proton event at 75° to 80°N, the observations indicate a sharp decrease of the ozone columns above 32, 35, 39, and 44 km, and the decreases seem to persist for the rest of the month of August. Simple inspection of the data do not reveal any conspicuous changes for the entire atmosphere nor for the column above 49 km.

Six panels of primary data for 65° to 75°N are given by Figure 4.14. For a month before the solar proton event the data show little or no systematic trends in the various ozone columns. Immediately after the solar proton event, one can see ozone decreases for the columns above 35 km, above 39 km, above 44 km, and perhaps above 49 km. For the month after the solar proton event, there is a slow increase in ozone for each case where there was an ozone decrease; by the end of August

ozone was restored to its average July values; but above 44 km there appears to be an increase of ozone to a value above the July average.

Seven panels of primary data are given for 45° to 55°N latitude in Figure 4.15. At no altitude was there a large or conspicuous effect of the solar proton event. If one looks very closely at the record, certain small trends and effects can be perceived, but it would be difficult to argue that these effects are outside the experimental error of the measurement. The panels showing the ozone columns above 32, 35, and 49 km seem to show steady ozone before the solar proton event, a small decrease immediately after the solar proton event, and a slow increase later in August restoring the July value by the end of August. Above 39 and 44 km, there appears to be a slow increase in ozone during July, a slight downward break in this decrease immediately after the solar proton event, and a continuation of the increase during the rest of August. For the total atmosphere and for the column above 24 km, the observations show more noise and variability than for the other cases.

The Nimbus satellite itself was bombarded by the solar protons and one should ask whether the large changes in ozone shown in Figure 4.13 merely represent a change in the calibration of the instrument by the strong ionization caused by the solar protons. A comparison of Figures 4.13 and 4.15 rules out this interpretation. The measurements at 50°N were made (several times each day) within a few minutes of the measurements at 80°N, and a change in calibration would show up at all latitudes.

A somewhat more sensitive test than visual inspection of the observed ozone columns was carried out. The satellite measures the

total ozone column C above a series of altitudes i (or pressure surfaces). From the difference in successive columns divided by the difference in the corresponding altitudes, one can evaluate the average change in ozone concentration between the two altitudes. For adjacent levels, i and i+1, the difference in ozone columns

$$\Delta C_i = C_i - C_{i+1} \tag{4.31}$$

was evaluated for each day from day 210 to day 235, which is one week before, 4 days during, and two weeks after the solar proton event. The average value of ΔC_i was calculated for the 24 days of observations for each altitude interval, and the local percentage change in ozone is defined as

$$\Delta O_3, \text{ percent} = 100 \frac{\Delta C_i - \Delta C_{AVE}}{\Delta C_{AVE}} \quad . \tag{4.32}$$

These percentage changes in local ozone are given for 75°N to 80°N in Figure 4.16 and for 65°N to 75°N in Figure 4.17. On day 218 the ionization caused by the stream of protons disabled the instrument and during the 4 days after the initial solar proton event there are occasional irregularities that should probably be dismissed as instrument noise.

The data in Figure 4.16 at 75°N to 80°N show large local percentage ozone changes. The biggest effect is shown at 39 to 44 km. There appears to be an ozone reduction of almost 25 percent. The reduction appears within two days and persists for at least 17 days. These changes are consistent with a change in ozone from one photochemical steady-state before the solar proton event to another

photochemical steady-state involving an increased rate of ozone destruction after the solar proton event. The photochemical ozone relaxation time is about 7 to 14 hours over this altitude range and at this season. The long persistence of the effect is consistent with the long residence time of NO_x in the stratosphere, and it indicates no rapid mixing of this stratospheric air with air at lower latitudes. The two records at 32 to 35 km and 35 to 39 km are similar and are discussed together. There is a prompt initial decrease in ozone and about a week after the end of the solar proton event there is a further decrease of ozone. In the 32 to 35 km range, the photochemical relaxation time for ozone is about a week. The later ozone decrease is consistent with slow photochemistry (photolysis of the nitric acid formed from the hydroxyl radicals produced by the solar proton event) or it could be due to atmospheric motions interchanging ozone poor air for the local ozone rich air. The case at 24 to 32 km is of especial interest even though there are two quite different explanations. At 24 to 32 km, ozone appears to go down a small amount immediately after the solar proton event and continuously to go down further over the two-week period. At 24 km the ozone photochemical relaxation time at 75°N in the summer is about 4 months, and at 32 km it is about 5 days. The slow decrease in ozone indicated in Figure 4.16 for the range of 24 to 32 km could be slow photochemical ozone reduction from the added NO_x catalysts from the solar proton event, or it could be a natural trend associated with air transport. At these altitudes the characteristic times for horizontal air transport and for ozone photochemistry are of comparable magnitude, and a slow effect such as that shown here is consistent with either photochemistry or air transport or both.

The local percentage changes in ozone at 65 to 75°N at various altitudes are given by Figure 4.17. One should ignore the large erratic changes during the first four days after the initial solar proton shower. Within the scatter of data, the record at 44 to 49 km shows little or no effect from the solar proton effect, but there is an increase of ozone that starts about one week after the completion of the solar proton event. The photochemical relaxation time for ozone is a small number of hours at this altitude, latitude, and season; and it is difficult to ascribe any feature in this panel to local photochemistry. Between 39 and 44 km, the record shows a sharp ozone decrease, which is less than that seen at 80°N; and there appears to be a slow increase in ozone during the two weeks after the solar proton event. Between 35 and 39 km, there appears to be a prompt, sustained, ozone decrease after the solar event. Between 32 and 35 km there are a number of short-term ozone changes, but there appears to be no systematic change related to the solar protons. Between 24 and 32 km there appears to be a small sustained ozone reduction after the solar proton event. As a group, the five panels in Figure 4.17 for 70°N show greater day-to-day variations than the examples in Figure 4.16 for 80°N. The solar proton beams and associated cascading electrons had irregularities with longitude. These irregularities overlapped some of the latitudes of 65° to 75°N, but stratospheric air at 75° to 80°N was well inside the region uniformly affected by the solar proton event. Both the initial irregular pattern of the solar proton event at 65° to 75°N and the mixing of air between strongly and weakly affected regions during the two weeks after the solar proton event could explain some of the irregularities of Figure 4.17.

The solar proton event may be interpreted as a direct demonstration of stratospheric ozone destruction by a long-chain catalytic process. Over each altitude interval for 75° to 80°N in Figure 4.16, the ratio of observed ozone decrease to calculated nitrogen oxides increase was evaluated, and the component data are given in Table 4.1. The average concentration of ozone over each interval was obtained, from Figure 4.4 for example. The percentage change in the ozone column for one week before the solar proton event relative to one week after the end of the event was obtained by inspection of Figure 4.16 and listed in Table 4.1. The average (over altitude) increase in nitrogen oxides from the solar proton event was obtained from Figure 4.12. The next to last column in Table 4.1 gives the ratio in ozone decrease to NO_x increase for each altitude band. Between 32 and 44 km this ratio is very nearly 50, which can be interpreted as the minimum catalytic chain length demonstrated by this event. As can be seen from Figure 4.6 or rather from similar figures for summer-winter conditions,[23] the ozone replacement time is less than one week over most of these altitudes, and the minimum chain lengths should be increased by an altitude dependent factor. A rough, order-of-magnitude correction for this effect is the duration of the period of reduced ozone (the period of one week is arbitrarily selected) divided by the ozone replacement time. With this correction, one obtains an estimate of the catalytic chain length ($NO + O_3 \rightarrow NO_2 + O_2$, $NO_2 + O \rightarrow NO + O_2$) over a period of one week; these numbers are rounded to the nearest 100 and entered as the last column of Table 4.1. These chain lengths for a period of one week vary between 100 ± 100 in the lowest altitude band to 600 ± 100 in range of 39 to 44 km.

The importance of the solar proton event of August 1972 is that it demonstrated a conspicuous and unambiguous ozone reduction (Figures 4.13 and 4.16) in the middle and upper stratosphere following the sudden, natural introduction of ozone-destroying catalysts at concentrations 100 to 1000 fold less than that of ozone itself. These observations apply to a specific season, latitude, altitude range, and catalyst (NO_x); and they should not be uncritically extended to other seasons, latitudes, altitudes, or catalysts. However, the facts in the case deserve to be understood by all who are interested in stratospheric science.

E. Nitrogen Oxides in the Global Ozone Balance[23]

1. Ozone Destruction by the Oxides of Nitrogen in the Natural Stratosphere

The catalytic destruction of ozone by the oxides of nitrogen including interactions with the HO_x and ClX families of free radicals is summarized as follows:

Step I

$$NO + O_3 \rightarrow NO_2 + O_2, \text{ direct} \qquad (4.1)$$

$$NO + O_3 \rightarrow NO_2 + O_2, \text{ catalyzed by } HO_x \qquad (4.7)$$

$$NO + O_3 \rightarrow NO_2 + O_2, \text{ catalyzed by ClX} \qquad (4.10)$$

Step II

$$NO_2 + O \rightarrow NO + O_2, \text{ rate determining step} \qquad (4.3)$$

OVERALL:

$$O + O_3 \rightarrow O_2 + O_2, \text{ catalyzed by } NO_x .$$

Since the atom of oxygen in (4.3) was provided by ozone photolysis, the net effect of reaction (4.3) is the loss of two ozone molecules. The gross rate of ozone destruction by the oxides of nitrogen is $2\ k_3[O][NO_2]$, to an excellent degree of approximation. Both atomic oxygen and nitrogen dioxide have been measured in the stratosphere, and the rate constant k_3 has been measured by several different groups in the laboratory and is regarded to be known to about 10 percent at stratospheric temperatures. Thus the rate of ozone destruction by NO_x in any volume element could be derived purely from observations if atomic oxygen and nitrogen dioxide were measured simultaneously. However, it is rare to have simultaneous measurements of trace species in the stratosphere. Fortunately atomic oxygen measured in the stratosphere agrees with the amount calculated to be there from considerations of local ozone and light intensities. To the extent that atomic oxygen can be accurately calculated from observed local ozone, the rate of ozone destruction by NO_x is

$$\underset{\text{OBS}}{2\ k_3} \quad \underset{\text{CALC}}{[O]} \quad \underset{\text{OBS}}{[NO_2]} \qquad . \tag{4.33}$$

2. Observation of Nitrogen Dioxide

Noxon[25] and co-workers measured, from the ground, the vertical column of nitrogen dioxide over a wide range of latitudes, Figure 4.18. Four vertical columns of nitrogen dioxide as found from balloon-based observations are included on the figure.

Using a special-purpose model, Solomon et al.[23] calculated the shapes of the NO_2 profiles as a function of time during the

day, but the magnitude of the NO_2 column was taken from Noxon's observations at each latitude. By this method, Noxon's observed NO_2 columns were translated into a three-dimensional distribution of nitrogen dioxide over the sunlit half of the globe. The daytime average NO_2 mixing ratios derived in this way are given by Figure 4.19, and the corresponding concentrations of nitrogen dioxide as a function of latitude and altitude are given by Figure 4.20.

3. Rates of Ozone Destruction by NO_x

The concentrations of atomic oxygen were calculated in each volume element of the sunlit globe, and the rate of ozone destruction throughout the sunlit atmosphere was calculated as $2\ k_3[O][NO_2]$. Complete zonal averages or 24 hour averages of these rates were evaluated and are given by Figure 4.21. The contour lines of ozone destruction by NO_x in Figure 4.21 are to the same, linear scale as those showing ozone formation from photolysis of molecular oxygen, Figure 4.5, and it is instructive to compare these two figures. The altitude of maximum rate of ozone destruction by NO_x is about 38 km, which is just below the altitude of maximum rate of ozone formation, which is about 41 to 43 km, Figure 4.5. Another interesting comparison of altitudes can be made; the altitude of maximum ozone mixing ratios is about 35 to 38 km, Figure 4.3; and the altitude of maximum rate of ozone destruction by NO_x is about 38 km. Presumably the net source of ozone to the lower stratosphere is a downward transport of ozone more or less down the mixing-ratio gradients of Figure 4.3. The cosine weighted integral (equal weight to equal area of earth's surface) of ozone destruction between 15 and 45 km

(Figure 4.21) is 45 percent of the corresponding integral for ozone formation (Figure 4.5). It will be recalled (Figure 4.8) that the corresponding integrated rate of ozone destruction by O_x reactions was 15 percent. All of these numbers are subject to substantial uncertainties, but the present state of knowledge indicates that the nitrogen oxides are the most important single cause of ozone destruction in the natural stratosphere. However, HO_x destruction of ozone, or ClX destruction of ozone, or both are quite important in the natural ozone balance, apparently contributing about 40 percent to the total destruction of ozone below 45 km.

F. Consideration of Magnitudes in the Stratosphere

This section has been devoted to observations in the atmosphere and to the interpretations that can be derived from these observations with a minimum input of theory. The next section concerns possible future changes of stratospheric ozone as a result of human activities, and such predictions are, of course, entirely theoretical (it is impossible, literally, to carry out any observations or experiments in the future itself). Before ending this section, a slightly whimsical discussion will be given for the various masses and species in the atmosphere. Such masses may be regarded as observed quantities, and the object of this exercise is to see if any general statements can be made as to the plausibility or implausibility of proposed "threats to stratospheric ozone."

For this discussion the unit of mass will be taken to be the global human mass (GHM), a whimsical unit as promised above. Assuming three billion people in the world and further assuming an average mass of 50 kg per person, one estimates the global human mass to be about

1.5×10^{14} g. A series of masses and relative masses is given in Table 4.2.

The mass of the entire atmosphere is 35 million-fold greater than the mass of all the people in the world. The mass of atmospheric oxygen is more than 7 million times greater than the global human mass, and the stratosphere exceeds the human mass by a factor of over 4 million. There are no human activities underway or proposed that would add or subtract a significant fraction of such large masses as these.

The mass of carbon dioxide is 7 thousand times greater than the human mass. In recent decades carbon dioxide has been increasing at a rate of about 9×10^{15} grams per year,[26] or about 60 global human masses per year. If this increase is caused in large measure by human activity, that is all the combustion processes in the world, then this perturbation of the atmosphere probably represents about the upper limit of what the human race can do at this time. The total mass of atmospheric ozone is about 24 fold greater than the global human mass, and as can be seen by comparison with carbon dioxide it would require an extremely great effort for human activity directly to manufacture or to consume a large fraction of atmospheric ozone.

The global inventory of nitrogen dioxide, taken to be twice the amount in the sunlit hemisphere, is about one percent of the global human mass. The mass of nitric oxide produced in the atmosphere by the solar proton event of August 1972 is about one-tenth of one percent of the global human mass. This unusual unit of mass gives some readily grasped perspective as to the quantities of the major, minor, and trace species in the stratosphere.

In the natural atmosphere, nitrogen dioxide at about one percent of the global human mass destroys roughly half the ozone photochemically produced between 15 and 45 km. During the solar proton event of 1972 the introduction of nitric oxide in a restricted portion of the stratosphere at 0.001 global human masses, appears to have caused large local reduction of ozone (Figure 4.13 and 4.16). These quantitative considerations offer a reasonable guideline as to which proposed perturbations of the stratosphere deserve serious consideration. If a proposed human activity would globally add ozone-destroying catalysts in quantities comparable to the order of magnitude of natural stratospheric nitrogen dioxide, then such a proposal should be taken quite seriously. It should be assumed that such an addition of ozone-destroying catalysts would reduce stratospheric ozone until and unless deep study of the problem reveals special features, such as a buffering action, that show the added ozone-destroying catalysts to have no significant effect. On the other hand, if a proposed human activity would add ozone-destroying catalysts to the stratosphere in masses very small compared to that of natural NO_2, then it should be assumed that such an addition to the stratosphere would have negligible effect on ozone until and unless deep study of the problem revealed that this substance would have an exceptionally large special effect on ozone. These simple considerations based on the magnitude of substances in the stratosphere should provide some model-independent guidelines as to what attitude one should take toward possible or proposed perturbations of the stratosphere. As an example, military aircraft add and have added NO_x to the stratosphere in amounts far less than the natural source rate,[27] and such a source

can be regarded as probably negligible on this basis alone. On the other hand a large fleet (500 or so) of large supersonic transports operating at 20 km are expected to add NO_x to the stratosphere at a rate comparable to the natural rate (10 to 100 percent, depending on auxiliary assumptions). Thus it is plausible that this case should receive careful consideration (see Chapter 7 and Section II. B. 1. below).

Although these considerations provide preliminary guidelines, it requires a detailed mathematical model of the atmosphere to come up with a prediction as to the effect of a perturbation.

II. RESULTS OF MODEL CALCULATIONS

A. Introduction

The advantage of model calculations is that, taking present knowledge and information, the models can make future predictions. The vulnerability of model predictions is that present knowledge is, to some degree, incomplete and incorrect; and new discoveries or the correction of wrong data may lead to substantial changes in the future predictions. A model of stratospheric dynamics, radiation balance, and photochemistry may involve several hundred input parameters, a calculation may involve a long and expensive computer run, but the discovery of some new effect or the revision of some numerical value in the input parameters may render obsolete the entire expensive computation. In problems of stratospheric ozone models since 1970, significant new or revised factors have appeared more or less every six months, major changes have appeared every couple of years, and the end of this process is not yet in sight. By the time a major model calculation is refereed and published in a journal, some new fact has developed that modifies its conclusions. Referees and editors accept this situation, and model calculations are published recognizing that they represent the expectations as of a certain date. Although articles may become obsolete in some respect by the time they are published, they still retain considerable value; and the history of various predictions as a function of new information is a vital part of the present knowledge of the subject. This section focuses not so much on the latest model developments as on the recent history of certain model predictions.

B. Recent History of Model Calculations

1. Stratospheric Perturbations by NO_x

Between 1971 and 1977 models of stratospheric ozone predicted that the injection of nitric oxide at 20 km altitude would reduce stratospheric ozone, and the amount of NO that would be injected by certain large fleets of supersonic transports (see Chapter 7) using engines comparable to present-day models would reduce global ozone between 5 and 20 percent, although some models gave results above and some below this range.[27,28] Since early 1978, the same model input of nitric oxide at 20 km has led to predictions of very small changes of the ozone vertical column and of uncertain sign. Most models predict a small increase in the column of ozone. This situation is illustrated by Figure 4.22, which is derived from Rundel et al.[29] This figure presents the calculated ozone reduction as a function of NO injection at 20 km altitude using the same mathematics and physics for each curve but using 1976 chemistry in one case and 1978 chemistry in the other case. For chemistry as it was understood to be in 1976, any injection of NO_x at 20 km would cause a reduction of ozone; for moderate to large rates of NO_x injection the ozone decrease would be directly proportional to the NO_x injection; and for the larger NO_x injections ozone column reduction shows the beginning of saturation of the effect (Figure 4.22). For chemistry as it was understood to be in 1978, small injections in NO_x at 20 km would cause very small ozone column increases; for moderate to large NO_x injections the calculated curve is essentially flat showing a buffered situation where the ozone column is unaffected one way or another by changes of NO_x injection rate; and very large NO_x injections would cause large ozone

decreases approaching the magnitude predicted with 1976 rate constants (Figure 4.22).

In recent decades the fixation of nitrogen to make fertilizer has increased exponentially and at present the total rate of nitrogen fixation by human activities approaches or perhaps equals the global natural rate of nitrogen fixation (see Chapter 9). In the natural nitrogen cycle there is a balance between the fixation of nitrogen and the return of fixed nitrogen to the atmosphere, part of which appears as nitrous oxide. Although time scales and magnitudes remain very uncertain, large increases in atmospheric nitrous oxide have been predicted for certain scenarios.[30] Duewer and Wuebbles[31] calculated the ozone reduction to be expected with 1979 chemistry from a doubling of the flux of nitrous oxide from the earth's surface, and they showed the calculated changes of both ozone and the nitrogen oxides as a function of altitude, Figure 4.23. Doubling the flux of nitrous oxide, leads to about a 40 percent increase in stratospheric nitrogen oxides. There is a large ozone increase between 0 and 26 km and a large ozone decrease between 26 and 45 km. These large local increases and decreases of stratospheric ozone are very nearly equal, and the net effect is the small difference of two large numbers.

W. H. Duewer carried out special calculations for the sake of this chapter giving results for doubling the N_2O flux on the basis of three different sets of chemical rate constants, those as understood to be in 1976, March 1979, and September 1979. The three calculations used the same 1979 model with respect to vertical eddy diffusion function, treatment of solar radiation, list of chemical species, and boundary

conditions. The 1976 model used rate constants from Hampson and Garvin,[32] taking their upper limit for the rate constant for the reaction HO + HOO → $H_2O + O_2$, and the total stratospheric chlorine was 1.2 ppbv. The early 1979 model takes total chlorine (ClY)* to be 1.9 ppbv, and there are some differences in 90 rate constants between this and the 1976 model. The late 1979 model takes ClY to be 1.2 ppbv, there are minor changes in 40 rate coefficients, but the largest effect comes from a three-fold reduction in the rate of NO photolysis in the upper stratosphere. The calculated changes in the ozone vertical profile for these three cases are given by Figure 4.24.

A doubling of the N_2O flux according to 1976 chemistry (curve A in Figure 4.24) would cause a reduction in ozone at all altitudes between 0 and 50 km. The maximum reduction in local ozone concentration is 5.7 x 10^{11} molecules cm^{-3} at 26 km. According to the early 1979 model (curve B), doubling the N_2O flux increases ozone between 0 and 26 km with a maximum increase in local ozone concentration at 20 km; and it decreases ozone between 26 and 50 km with maximum reduction at 33 km. According to the September 1979 model, the situation is essentially the same as the March 1979 between 0 and 25 km, that is, an equal calculated ozone increase; but the late 1979 model (curve C) calculates a larger ozone reduction between 25 and 50 km by increased N_2O. Curve A, representing 1976 chemistry, corresponds to an 11 percent decrease of the ozone column. For the March 1979 model, the area of ozone increase very nearly balances the area of ozone decrease, and the net effect is an increase of the ozone column by 0.5 percent. Curve C, representing September 1979 chemistry, also shows large ozone increases at low altitudes and decreases at high altitudes, but the net effect is a two percent decrease in the vertical ozone column.

---

*See footnote on p. 000.

2. Stratospheric Perturbations by ClX

Since chlorine chemistry has a direct impact on nitrogen-oxide perturbations, it is necessary to mention chlorine effects in this chapter on nitrogen oxides. For example, Rundel et al.[29] made a calculation for the chlorine perturbation of ozone by way of chlorofluoromethanes, Figure 4.25. Figure 4.25 shows the calculated ozone reduction for both 1976 and 1978 chemistries as a function of increasing tropospheric chlorofluoromethanes (CFM) but expressed as long-term increase in stratospheric ClY mixing ratio, that is for $Cl + ClO + HCl + ClONO_2$. For both cases, the model predicts an ozone decrease for any value of chlorine increase. There is very nearly a linear relation between percentage reduction of the ozone vertical column and increased stratospheric ClX, although for large increases there is a slight negative curvature for the 1978 models and a slight positive curvature for the 1976 model. For a given chlorine perturbation, the calculated ozone reduction with the 1978 model of chemistry is about twice as great as that for the 1976 model. The changes in the values of the chemical rate coefficients between 1976 and 1978 had opposite effects on the predicted ozone reduction due to NO_x increases and to ClX increases.

Rundel et al.[29] provided a breakdown of the effect of increased chlorine (from CFM) on ozone as a function of altitude, Figure 4.26. Rundel's model using 1976 chemical rate constants predicted that an increase in CFM would slightly increase local ozone between 15 and 27 km and strongly decrease local ozone between 28 and 45 km, with a maximum local effect at 35 km. The reason that the 1976 model predicted a local ozone increase in the lower stratosphere is that

added stratospheric chlorine caused additional amounts of the active oxides of nitrogen to be tied up temporarily in the inert reservoir species chlorine nitrate, $ClONO_2$. Chlorine tended to reduce the ozone-reducing power of NO_x, and this double negative caused a small positive effect on local ozone. The model using 1978 rate constants shows a reduction in ozone at all altitudes between 15 and 45 km as the long-term (centuries) effect of the addition of CFM to the atmosphere. The increased sensitivity of ozone to chlorine perturbations as calculated between 1976 and 1978 (Figure 4.25) largely depends on effects in the lower stratosphere, 15 to 30 km (Figure 4.26).

3. Relations Between NO_x and ClX Perturbations

a. Importance of Hydroxyl Radicals

The model-predicted increase in ozone sensitivity to chlorine (Figure 4.25) and decrease in sensitivity to nitrogen oxides (Figure 4.22) between 1976 and 1978 are not unrelated topics, but rather two sides of the same coin. The destructive effect of nitrogen oxides on stratospheric ozone is reduced as the active species NO_2 is reversibly tied up as nitric acid

$$NO_2 + HO \xrightarrow{M} HNO_3 \qquad (4.34)$$

$$HNO_3 + h\nu\ (UV) \longrightarrow HO + NO_2 \quad . \qquad (4.35)$$

The destructive effect of chlorine radicals on stratospheric ozone is reduced as the active species Cl is reversibly tied up as hydrogen chloride

$$Cl + CH_4 \rightarrow CH_3 + HCl \qquad (4.36)$$

$$HO + HCl \rightarrow H_2O + Cl \quad . \qquad (4.37)$$

Note the opposite effect of hydroxyl radicals on the NO_x and ClX family of reactions: the hydroxyl radical directly ties up the active nitrogen dioxide to form inert nitric acid; and the hydroxyl radical breaks down the inert hydrogen chloride releasing the active atomic chlorine.

In 1974 there were some high temperature studies that indicated the rate constant for the reaction

$$HO + HOO \rightarrow H_2O + O_2 \qquad (4.38)$$

to be around 1 to 2 x 10^{-11} cm^3 $molecules^{-1}$ s^{-1} and there were two separate low temperature studies that indicated the values 1.5 x 10^{-10} and 2 x 10^{-10} for this rate constant. Hampson and Garvin[32] could not find a basis to resolve this major difference, they presented 2 x 10^{-11} and 2 x 10^{-10} as of equal apparent validity, and they recommended that modelers use both values. The value 2 x 10^{-10} was the more recent; all concerned in the Climatic Impact Assessment Program (CIAP) were very busy trying to reach the Congressionally mandated completion of the program by the end of 1974; hence Hampson and Garvin's recommendation to use both 2 x 10^{-11} and 2 x 10^{-10} was not acted upon until after the conclusion of CIAP. Then it was found that the low value led to larger amounts of the HO_x radicals than the previously used high value, and use of the low value simultaneously decreased the predicted effect of NO_x on ozone and increased the predicted effect of ClX on ozone.

b. Interactions Between NO_x and ClX Catalytic Cycles

The oxides of nitrogen interact with species in the chlorine system of reactions. The reaction ($NO + ClO \rightarrow NO_2 + Cl$) plays an interesting double role. An increase in ClX tends to increase the rate of the non-rate-determining step in the NO_x catalytic cycle (reactions 4.8, 4.9, 4.10), so that ClX weakly increases the rate of NO_x destruction of ozone. On the other hand, the chlorine catalyzed destruction of ozone

$$\begin{array}{lll} & Cl + O_3 \rightarrow ClO + O_2 & \\ & ClO + O \rightarrow Cl + O_2 & \text{rate determining step} \\ \hline \text{net:} & O_3 + O \rightarrow O_2 + O_2 & \text{catalyzed by ClX} \end{array} \qquad (4.39)$$

is diverted into its null channel by nitric oxide

$$\begin{array}{lll} & Cl + O_3 \rightarrow ClO + O_2 & \\ & ClO + NO \rightarrow NO_2 + Cl & \text{rate determining step} \\ & NO_2 + h\nu \rightarrow NO + O & \\ & O + O_2 + M \rightarrow O_3 + M & \\ \hline \text{net:} & \text{null} & \end{array} \quad . \qquad (4.40)$$

Thus an increase in nitric oxide acts as a double negative; it reduces the chlorine-catalyzed reduction of ozone; and an increase in NO_x tends in this way to increase ozone. The inert reservoir compound, chlorine nitrate, ties up key species in both the NO_x and ClX systems

$$ClO + NO_2 \underset{h\nu}{\overset{M}{\rightleftharpoons}} ClONO_2 \quad . \qquad (4.41)$$

4. Relations Between NO_x and HO_x Reactions

a. Interactions Between NO_x and HO_x Catalytic Cycles

The interactions between the NO_x and HO_x systems are even more extensive. Probably the major interaction is the formation of nitric acid (Equations 4.34, 4.35). A similar but apparently much less important process is the formation of peroxy-nitric acid

$$HOO + NO_2 \underset{h\nu}{\overset{M}{\rightleftharpoons}} HOONO_2 \quad . \tag{4.42}$$

As in the chlorine system, the HO and HOO radicals catalyze the non-rate-determining step in the NO_x catalytic cycle (reactions 4.5, 4.6, 4.7), and thus an increase in HO_x weakly increases the rate of the NO_x catalyzed destruction of ozone. The reaction of the hydroperoxyl radical with nitric oxide (analogous to ClO + NO)

$$HOO + NO \rightarrow HO + NO_2 \tag{4.6}$$

is the key step in determining whether several catalytic cycles destroy ozone or lead to null cycles; one example is

$$\begin{array}{ll} HO + O_3 \rightarrow HOO + O_2 & \\ HOO + O_3 \rightarrow HO + O_2 + O_2 & \text{rate determining step} \\ \hline \text{net:} \quad 2\,O_3 \rightarrow 3\,O_2 & \text{catalyzed by } HO_x \end{array} \tag{4.43}$$

$$\begin{array}{ll} HO + O_3 \rightarrow HOO + O_2 & \\ HOO + NO \rightarrow HO + NO_2 & \text{rate determining step} \\ NO_2 + h\nu \rightarrow NO + O & \\ O + O_2 + M \rightarrow O_3 + M & \\ \hline \text{net:} \quad \text{null} & \end{array} \quad . \tag{4.44}$$

The increase in NO_x has the double negative effect in this system; it reduces the rate of ozone reduction by HO_x.

b. Methane-Smog Reactions

During CIAP it was recognized[33,34] that the oxides of nitrogen catalyzed ozone formation from the methane smog reactions, and it was pointed out[35] that below 13 km at midlatitudes the formation of ozone from the NO_x-methane smog reactions equaled or exceeded the rate of ozone destruction by the NO_x catalytic cycle. Some CIAP models did not fully include the methane-smog reactions, but recent models have usually done so.

The detailed chemical reactions in this complicated system are written out by Johnston and Podolske,[3] and they are simplified and abbreviated here. Hydroxyl radicals, singlet atomic oxygen, or atomic chlorine convert methane to the methyl free radical

$$CH_4 \xrightarrow{HO,\ O(^1D),\ Cl} CH_3 \qquad (4.45a)$$

In rapid sequence, the carbon-containing free radical reacts with oxygen, nitric oxide, and oxygen to produce formaldehyde and perhydroxyl radical

$$CH_3 \xrightarrow{O_2} CH_3OO \xrightarrow{NO} CH_3O \xrightarrow{O_2} H_2CO + HOO \qquad (4.45b)$$

Formaldehyde is photolyzed along two product channels to give hydrogen, carbon monoxide, and perhydroxyl radical

$$H_2CO \xrightarrow{h\nu} HCO + H \xrightarrow{2O_2} CO + 2HOO \qquad (4.45c)$$

$$H_2CO \xrightarrow{h\nu} H_2 + CO \qquad (4.45d)$$

Both hydrogen and carbon monoxide undergo reactions leading to additional perhydroxyl radicals

$$H_2 + HO \longrightarrow H_2O + H \xrightarrow{O_2} HOO \qquad (4.45e)$$

$$CO + HO \longrightarrow CO_2 + H \xrightarrow{O_2} HOO \qquad (4.45f)$$

In all these sequencies HOO is produced, and competition between the reactions

$$HOO + NO \longrightarrow HO + NO_2$$

$$HOO + O_3 \longrightarrow HO + 2O_2$$

determines whether the smog reactions produce ozone or destroy ozone. This feature will be illustrated by the carbon monoxide smog reactions, which are the last portion of the methane smog reactions. Consumption of carbon nomoxide leads to ozone formation by this sequence of reactions

$$\begin{array}{ll} CO + HO \rightarrow CO_2 + H & \\ H + O_2 + M \rightarrow HOO + M & \\ HOO + NO \rightarrow HO + NO_2 & \text{rate determining step} \\ NO_2 + h\nu \rightarrow NO + O & \\ O + O_2 + M \rightarrow O_3 + M & \\ \hline \text{net:} \quad CO + 2\,O_2 \rightarrow CO_2 + O_3 & \end{array} \quad . \qquad (4.46a)$$

However, consumption of carbon monoxide leads to ozone destruction if the sequence is

$$\begin{aligned} &CO + HO \rightarrow CO_2 + H \\ &H + O_2 + M \rightarrow HOO + M \\ &HOO + O_3 \rightarrow HO + O_2 + O_2 \qquad \text{rate determining step} \\ \text{net:}\quad &CO + O_3 \rightarrow CO_2 + O_2 \end{aligned} \qquad . \qquad (4.46b)$$

The methane system shows these features illustrated by the carbon monoxide smog reactions. The process is catalytic in HO_x and NO_x radicals, but it is limited by the supply of fuel, CH_4 or CO. It leads to ozone formation if the intermediate HOO radical (or the CH_3OO radical) reacts with NO to form NO_2, but there is ozone destruction if the HOO radical reacts with ozone.

The methane-smog reactions are important in the troposphere and lower stratosphere.

c. Revised Rate Constant for HOO + NO Reaction

Before 1977 the rate constant for the reaction

$$HOO + NO \rightarrow HO + NO_2 \qquad (4.6)$$

was thought to be[32] about 2×10^{-13} cm^3 $molecule^{-1}$ s^{-1}. Then Howard and Evenson[36] found the rate to be forty times larger or 8×10^{-12} cm^3 $molecules^{-1}$ s^{-1}. With hindsight, one can see why the old values were incorrect. When HOO and NO are mixed together and the above reaction starts to occur, many other reactions become possible

$$\begin{aligned} &HO + NO_2 \rightarrow HNO_3 \\ &HO + HOO \rightarrow H_2O + O_2 \\ &HO + NO \rightarrow HONO \\ &HOO + NO_2 \rightleftarrows HOONO_2 \end{aligned} \qquad . \qquad (4.47)$$

At room temperature peroxynitric acid forms and then decomposes quite rapidly. The presence of peroxynitric acid was not recognized in

this system until quite recently.[37] Peroxynitric acid temporarily delayed the appearance of NO_2, the product of reaction (4.6), making the reaction seem slower than it actually is. When large errors are made in measured rate constants, the cause is often the presence of some unidentified species or the occurrence of other, parallel, unrecognized reactions.

The fast rate of reaction (4.6) led directly to larger calculated values of hydroxyl radicals in the stratosphere, larger calculated values of nitric acid concentrations and larger HNO_3/NO_2 ratios, lower calculated values for hydrochloric acid concentrations and lower HCl/ClX ratios, and higher rates for ozone production by the methane smog reaction. The net effect was simultaneously to reduce the calculated impact of NO_x on stratospheric ozone and to increase the calculated impact of ClX on ozone. These effects are the major differences in the 1976 and 1979 predictions, Figures 4.22 - 4.26, and these differences occur primarily in the region 10 to 25 km, Figures 4.24, 4.26.

C. Model Predictions for Very Large NO_x Perturbations

As can be seen from Figure 4.22, current atmospheric models predict large ozone decreases in the event of very large increases of stratospheric NO_x. The double-negative effects become saturated, and the methane-smog production of ozone is limited by the available methane. After these finite effects are saturated, added NO_x is predicted to reduce the ozone column. A possible example of such a situation would be a full-scale nuclear war with calculated ozone reductions as large as 60 percent (dependent on altitude of cloud stabilization in the stratosphere).[31] Solar proton events at a time of reversal of the earth's magnetic field could cause very large additions of nitric oxide

to the stratosphere[38] with large ozone reductions calculated to follow. Supernovae, depending on distance from the earth and the magnitude of the event, could add — or in the past every few hundred million years may have added — very large amounts of NO_x to the stratosphere,[39] which is calculated to cause very large ozone reductions (35 to 65 percent), even with 1979 chemistry.[31,40]

III. CHECKING CERTAIN ASPECTS OF MODEL CALCULATIONS AGAINST ATMOSPHERIC OBSERVATIONS

A. Nitric Oxide Injection Experiments

It would be very desirable to have an historical event where large amounts of nitrogen oxides were injected into the stratosphere and simultaneous measurements were made of both ozone and total NO_x before and after the injection. Two recent events meet many but not all of the requirements of this desirable experiment. (1) The nuclear bomb tests of 1961-62 injected large amounts of NO_x in the stratosphere[41] the distribution of this NO_x in the stratosphere can be associated with the observed distribution of excess carbon-14, which was observed before, during, and after the bomb tests[42]; and there were scores of ground-based Dobson meters over the globe that made daily (weather permitting) observations of the total overhead ozone column. (2) As discussed in Section I-D, the large solar proton event of August 1972 injected large amounts of ionizing radiation in the polar caps of the earth, the intensity of this radiation was measured by satellite, the degree of NO production from the radiation is readily calculated, and the Nimbus 4 satellite measured the coarse ozone profile all over the globe for several years before and after this sudden nitric oxide injection. The comparisons of model calculations and atmospheric observations for these two cases are discussed in this section.[43,44]

1. Calculated and Observed Effects of the Nuclear Bomb Tests of 1961-1962

Foley and Ruderman[41] in 1973 calculated the approximate mass of nitrogen oxides expected to be formed by the high-temperature fireballs of the nuclear explosives, and they pointed out that most of the debris from large nuclear bombs is lifted into the stratosphere. Johnston et al.[42] proposed that the NO_x from the nuclear bombs should be located in the stratosphere at about the same places as the radioactive debris such as ^{90}Sr and ^{14}C, which were observed by the U.S. Atomic Energy Commission for several years. On the basis of a theoretical proportionality factor between bomb-produced carbon-14 and bomb-produced nitrogen oxides, a stratospheric distribution of NO_x for January 1963 is given by Figure 4.27. A large cloud of NO_x is seen to spread from the North Pole to the equator between 10 and 25 km.[27] This picture of "observed" NO_x is to be interpreted with caution: (i) The area below 21 km was extensively sampled by U-2 flights, but the area above 21 km was sampled by balloon for carbon-14 only at 30°N and only to 35 km height. (ii) Debris from the 60 MT bomb of October 1961 may be largely above the region of sampling. (iii) The latitude scale in Figure 4.27 is not proportional to equal surface area for equal distance along the abscissa.

Using a list of chemical reactions and rate constants as they were understood to be in 1973 and using Figure 4.27 as the NO_x perturbation, Johnston et al.[42] estimated the latitude dependent maximum pzone reductions of 1 to 6 percent. Chang and Duewer[45] in 1973 calculated the time dependent, hemispherical-average ozone decreases as given in Figure 4.28, which includes the

1957-59 test series as well as the 1961-62 tests. The maximum ozone decrease was calculated to be 4 percent in 1963, becoming 2 percent in 1966, and 1 percent by 1968 (using later lists of chemical reactions and rate constants, Chang et al.[46] in 1979 have calculated other time-dependent ozone changes from these tests, but this review uses Chang and Duewer's 1973 result in order to examine the observability of such a pulsed change in the ozone records).

Komhyr et al.[47] examined the ozone records as observed at several stations using Dobson instruments over the period 1961-1970, and at a large number of stations they found a perplexing increase of ozone over much of this period. Their results for observed ozone for a given month minus the 10-year average for the same month is given for five stations in Figure 4.29. The noise of the data was such that one cannot precisely determine when the increase began nor how long it lasted, but the average trend for these stations was an increase of about 2 to 10 percent for the decade.

Johnston et al.[42] posed the hypothesis that the ozone increase reported by Komhyr et al.[47] might be the atmosphere recovering from an ozone decrease in 1962-63 caused by the nuclear bomb tests. Chang and Duewer's[45] calculated ozone decreases (from Figure 4.28) are plotted to the same scale as the ozone records in Figure 4.29. The observed and calculatec changes in ozone are of comparable magnitude. Subsequently, however, Birrer[48]

went to the original ozone records at Arosa, Switzerland and recalculated all the observations from 1926 through 1971 on a consistent basis. His results for 1942 through 1971 are given in Figure 4.30; again the theoretical ozone changes of Figure 4.28 are entered to the same scale as a dashed line on Figure 4.30. Birrer pointed out that the ozone record at Arosa had shown increases and decreases that sometimes lasted several years and that were comparable to or larger than the 1961-1970 trend. The long-term record did not support an hypothesis that a bomb-produced ozone decrease could be demonstrated.

Goldsmith et al.[49] considered the problem of nitric oxide produced by nuclear bomb tests. They discussed the quantity of NO_x injected into the stratosphere by these tests, but they did not calculate or consider the magnitude of the expected effect on ozone. They looked at the noisy, forty-year records at Arosa and at Oxford, and they concluded that the failure of these records to display a conspicuous ozone depletion positively disproved the theory that additional stratospheric nitrogen oxides would reduce stratospheric ozone.

Goldsmith et al.[49] and Angell and Korshover[50] examined this question by pooling the data from a number of ozone-observing stations and by carring out various averaging and smoothing operations. The combined, smoothed data were compared to Chang and Duewer's theoretical ozone decreases (Figure 4.28), no similarities were seen, and the result was interpreted as demonstrating that NO_x from the nuclear bombs had little or no effect on ozone. Angell and Korshover in 1976[50] concluded that any ozone reductions caused by the nuclear test series must have been less than 1 to 2 percent.

It is argued here that these investigators did not make a proper comparison between theory and observation. To illustrate this contention, their procedure is repeated here. For the sake of this review, J. Angell provided a large block of his data as monthly-mean ozone columns. For seven European stations (Aarhus, Arosa, Cagliari-Elmas, Lerwick, Messina, Oxford, Rome) the monthly deviations from monthly means are averaged for the seven stations and plotted for the period 1957 to 1974 as the curve marked "observed" in Figure 4.31. Chang and Duewer's theoretical function (Figure 4.28) was scaled by the factor 5/4.* The observed ozone record at each station was modified by this theoretical function to generate what the observed record would have looked like subject to four different hypotheses. These modified records were processed in the same way that the observed records were treated.[49,50] Average deviations from the long-term monthly mean were evaluated for each month and at each station and these deviations were averaged for the seven stations. In this way a uniform treatment was given to each of four cases: (i) What the observed record would have looked like in the absence of nuclear bomb tests on the assumption that the observed record included ozone decreases with a history as Figure 4.28 but with a maximum 10 percent ozone reduction. (ii) What the observed record would have looked like in the absence of nuclear bomb tests assuming a 5 percent maximum ozone reduction. (iii) What the observed ozone record would look like on the assumption of zero effect by the nuclear bombs, that is, the actual observed record. (iv) What the observed ozone record would have looked like if the nuclear bombs had produced ozone with a history as Figure 4.28 but with a maximum ozone production of 5 percent. There was, of course, only a single observed

*Scaling factors used in this examination and Figure 4.31 are arbitrary and intended to provide a large effect for this examination.

record. Figure 4.31, however, poses a test for four hypotheses. If one is judging the situation simply by inspection, as Goldsmith et al.[49] and as Angell and Korshover[50] did, one should ask whether there is any geophysical principle that would exclude any of the four records in Figure 4.31 from being a satisfactory history of unperturbed ozone at these stations. If one cannot make such an exclusion, then the ozone records cannot, by simple inspection, prove or disprove the destruction or formation of ozone according to a function like Figure 4.28.

Goldsmith et al.[49] and Angell and Korshover[50] also apply various smoothing techniques to remove some of the fluctuations from the monthly records, and the smoothed records failed to show a decrease in ozone in association with the nuclear bomb tests. The four cases in Figure 4.31 were subjected to such smoothing processes and are given in Figures 4.32 and 4.33. In Figure 4.32 monthly deviations are combined to quarters and subjected to a running 1-2-1 smoothing process. In Figure 4.33 the monthly deviations of Figure 4.31 are subjected to a running 29 month smoothing function. In each of Figure 4.32 and 4.33 the four panels contain various multiples of the theoretical ozone-reduction function, Figure 4.28; but the final smoothed curves do not resemble or reveal the presence of these perturbed ozone functions. It seems quite incorrect to smooth the observed record and then compare it to an unsmoothed theoretical function such as Figure 4.28.[50]

In terms of analyses and arguments presented so far, it seems that the long-term ozone records (1) do not support an hypothesis that a bomb-produced ozone change can be demonstrated and (2) do not exclude that there was a transient ozone change comparable to Figure .28. It is frustrating that this historical injection experiment does not lead to a definite answer, one way or another; but such seems to be the case.[43]

2. Calculated and Observed Effects of the Solar Proton Event of 1972

Within a few days, the solar proton event of August 1972 formed 0.2×10^{12} g NO, primarily in the two polar caps above 60° latitude with a profile calculated to be that of Figure 4.12. At that time the southern hemisphere was still in or just emerging from the winter night, and there was a major sudden stratospheric warming in July, so that meaningful measurements of ozone by the Nimbus 4 satellite could not be made over the south pole. In the northern hemisphere, some of the observed changes in ozone are given by Figures 4.13 - 4.17. In the month of observations after the solar proton event, there was sure to be some North-South air transport in and out of the source region. It is clear that one needs to have a time-dependent two-dimensional or three-dimensional model properly to handle this case. Brief publications have appeared giving results of calculations with two different two-dimensional models.[20,51]

Heath et al.[20] used Crutzen's two-dimensional model, which incorporated 1975 values for rate constants and did not include chlorine species. At 75°N to 80°N, the model in general calculated less ozone reduction than that observed, about 30 percent less in the 35 to 45 km range and very much less (factor of 5 to 10) in the 25 to 33 km range. At 30° to 40°N, the model calculated greater ozone reductions than those observed,

28 days after the solar proton event. The underestimation of ozone reduction inside the NO source region (75° to 80°N) and overestimation of ozone reduction outside the source region (30° to 40°N) were interpreted by Heath et al. as evidence that their 2-D model had too fast North-South air transport. Below 32 km, there appears to be a substantial disagreement between observations and theory, with more ozone reduction being observed than calculated. Above 35 km, the theory gave a reasonable estimate of the magnitude and altitude of maximum effect, provided allowance is made for too fast horizontal transport in the model.

Fabian et al.[51] examined the detailed time behavior of the ozone column at altitudes above the 4 mbar surface, using the Oxford 2-D model. They, too, included only O-H-N chemistry, whereas chlorine chemistry is surely important at these altitudes. During the month of August, their model calculated too slow a recovery of ozone at 50°N to 60°N relative to observations and too rapid a recovery at 70°N to 80°N, indicating that their model (like Crutzen's) had too fast mixing of air in the horizontal dimension. Even at the high altitudes of their example (above about 39 km), they calculated ozone reductions much less than those observed, and they interpreted this result to mean that the solar proton event deposited more NO than that calculated by Crutzen. Since their model omitted chlorine chemistry, it seems premature to ascribe the disagreement between their theory and experiment to any single feature.

As of September 1979, there appears to be no published comparison of theory and observations that utilizes contemporary chemistry in a time-dependent two-dimensional model. In a field where millions of dollars are being spent each year to obtain new data and to carry out novel model studies, it seems unfortunate that more effort is not devoted to this

test for stratospheric ozone models. In this case there was a sudden injection of ozone-destroying catalysts, and ozone was observed to decrease in amounts that varied with altitude and latitude. It seems particularly important to test theories against these observations.

B. Checking Model Calculations Against the Observed Distribution of Some Atmospheric Species

In checking model calculations against observations of species in the atmosphere, one must be very careful on several scores. One of the most difficult aspects is that one-dimensional (1-D) models can apply only to long-term global averages, and an atmospheric observation is usually made at a specific location on a certain day. To test 1-D models one needs global data from satellites, and such data are just beginning to become available. Wherever possible, it is desirable to check specific observations against a 2-D model, matching latitude and season. The models are required to specify a large number of boundary conditions; in some cases the boundary conditions are, appropriately, fitted to atmospheric observations; but then the model cannot be verified by comparing calculated and observed values of such quantities near the boundary. Sometimes stratospheric models set up a buffer zone, perhaps in the lower troposphere or above the stratosphere; unrealistic physical assmptions may be tolerated in these buffer regions whose function is to remove the arbitrarily specified boundary conditions far enough from the stratosphere so that errors are not propagated from the boundary into the region of interest. In such a case, the failure of a calculated property to agree with observations in the buffer zone is a matter of no consequence.

1. Calculated and Observed Total Stratospheric Nitrogen Oxides

In one-dimensional stratospheric models the calculated mixing ratios of total nitrogen oxides are about 0.1 ppb in the lowest stratosphere, rapidly increase to attain a more or less uniform value over the middle stratosphere, and decline slowly from this uniform value in the upper stratosphere. The rapid build up of nitrogen oxides with altitude occurs where nitrous oxide reacts with singlet atomic oxygen (compare Figure 4.11). The slow decrease in the upper stratosphere is caused by photolysis of nitric oxide

$$NO + h\nu \rightarrow N + O \tag{4.48}$$

and the reaction of atomic nitrogen with nitric oxide

$$N + NO \rightarrow N_2 + O \quad . \tag{4.49}$$

The total nitrogen oxides consist of NO, NO_2, HNO_3, $ClONO_2$, N_2O_5, and possibly $HOONO_2$. It is very rare that an investigator measures NO, NO_2, and HNO_3 at once; and of the other three species, only $ClONO_2$ has been detected in the stratosphere.[52] High in the stratosphere, HNO_3, $ClONO_2$, N_2O_5, and $HOONO_2$ are rapidly destroyed by solar radiation, and the total oxides of nitrogen are well approximated by $NO + NO_2$. At 50 km, the observed ratio[53] of NO_2 to NO is 0.1, so the total nitrogen oxides are given to a good approximation by 1.1 times the observed nitrix oxide. Including three cases where NO_2 is calculated at 43 and 50 km, six examples of observed nitrogen oxides ($NO_x = NO + NO_2$)

in the upper stratosphere[53-57] are given in Table 4.3. These values were obtained at midlatitude. The mixing ratios vary from 5 to 14 ppbv, and the average of the set is 9.4 ppbv.

Anderson[58] quotes six values of total nitrogn oxides as calculated for 50 km altitude by various modelers. These values and the original references[46,58-63] are also included in Table 4.3. The mixing ratios of NO_x at 50 km vary between 13 and 25 ppbv, and the average value is 19 ppbv, which is about twice the average value of the observed values quoted in Table 4.3. Apparently these calculations were made during or before the spring of 1979. Meanwhile in the summer of 1979, Frederick and Hudson[64] reevaluated the photolysis rate of nitric oxide in the upper stratosphere, and they found it to be much slower than it had previously been regarded to be. When these new photolysis rates are put in the models, there is less calculated destruction of NO_x, reactions (4.48) and (4.49); and the calculated mixing ratio of NO_x in the upper stratosphere increases.[65] As of the fall of 1979, it appears that one-dimensional models systematically overestimate the mixing ratios of total nitrogen oxides in the upper half of the stratosphere; a comparison of observations and calculations in the lower half of the stratosphere is made difficult by lack of enough simultaneous measurements of NO, NO_2, and HNO_3 in this region, plus the uncertainty about $ClONO_2$ and $HOONO_2$.

Although this discrepancy between observations and theory is identified in the upper stratosphere, it is probably caused by effects in the middle and lower stratosphere. Nitric oxide is produced

from nitrous oxide and singlet atomic oxygen; at midlatitudes the altitude of maximum rate is about 25 km; rates of half the maximum value occur at 18 and 32 km, (Figure 4.11). A possible cause of this disagreement between measurements and models is that the models calculate too high a rate of NO formation from nitrous oxide and singlet atomic oxygen.

2. Calculated and Observed Stratospheric Nitric Acid

A comparison between observed nitric acid columns as a function of latitude and a contemporary (March 1979) two dimensional model by Widhopf and Glatt[66] indicates another disagreement between current theory and observations. Figure 4.34 shows the nitric acid vertical column above 12 to 16 km as measured by Murcray et al.;[67] their cases for the HNO_3 columns above 18 km are omitted from the figure. The measurements were the total vertical column of nitric acid above an aircraft; the circles are for January 1974 and the triangles are for April 1974. Nitric acid vertical columns above 12 km were obtained by summing over vertical profiles observed from balloons. These vertical columns are plotted as squares enclosing the initial of the observer: L for Lazrus and Gandrud,[68] M for Murcray et al.,[1] E for Evans et al.[57] The balloon data are also identified by the month of the observation. Figure 5.34 also includes the calculated vertical HNO_3 column above 12 km for four seasons by Widhopf's 2-D model. Also at 30°N latitude, the vertical column of HNO_3 above 12 km as calculated by the Lawrence Livermore Laboratory 1-D model[69] is included as a cross on the figure. The 1-D calculation is in good

agreement with the 2-D calculation, but there is a major disagreement between these models and observed nitric acid vertical columns.

The Livermore 1-D model has atmospheric and radiative properties associated with 30° latitude. The detailed nitric acid vertical profile from the Livermore Model 69 is given in Figures 4.35 and 4.36; Lazrus' observed profiles for spring conditions at 34°S and 32°N are included in Figure 4.35; and profiles corresponding to Murcray's largest and smallest columns at 30°N are included on Figure 4.36. In general, although not in every instance, the calculated profiles show much more nitric acid than the observed nitric acid profiles.

Simultaneous measurements have been made of HNO_3 and NO_2 by Evans et al.[57] at 59°N and by Harries[70] at 44°N. The observed ratio of HNO_3/NO_2 as reported by Evans et al. is presented as a smooth curve on the left-hand panel of Figure 4.37, and Harries' three local values of this ratio are entered as circles on this figure. The calculated ratio of HNO_3 to NO_2 at 60°N according to Widhopf's 2-D model is included as a smooth curve.[66] It can be seen that Widhopf's calculated value for this ratio at 60°N is larger by a factor of about five than Evans' observations at 59°N. The right-hand panel of Figure 4.37 gives the ratio of $(HNO_3/NO_2)_{CALC}$ to $(HNO_3/NO_2)_{OBS}$ for 59° and 60°N. Over the region 25 to 35 km, the calculated ratio exceeds the observed ratio by factors between 2 and 6, averaging about 3. Between 16 and 25 km, the calculated ratio exceeds the observed ratio by factors between 4 and 10.

Although natural variations of stratospheric species make it very difficult to compare observations and model calculations,

a pattern seems to be emerging that 1979 stratospheric models calculate more NO_x ($NO + NO_2 + HNO_3$) than that observed, calculate more HNO_3 than that observed, and calculate too large a ratio of HNO_3/NO_2.

3. Calculated and Observed Shape of the ClO Profile

This topic is covered in Chapter 6, but it is mentioned here because it may be related to the apparent discrepancies between observations and model calculations for NO_x. The ClO profile discrepancy concerns the shape of the vertical profile. The absolute magnitude of this calculated profile is determined by the boundary conditions assumed for organic chlorides (CH_3Cl, CFM, etc.). Figure 4.38 gives six vertical profiles as measured at midday at 31°N by Anderson et al.[58] at various seasons. The heavy dashed line corresponds to the Livermore model[69] with 1.2 ppbv for total atmospheric chlorine. The ratio of calculated ClO at 35 km to calculated ClO at 25 km is 3.9. For the observed ClO profiles, the ratios of values at 35 km to 25 km are in order of increasing value at 25 km: 21, 26, 13, 12, 6, 9 (where the value of 13 was based on an extrapolation of the observed profile from 26 to 25 km). Between 35 and 25 km the observed ClO profiles decrease more rapidly than the calculated ClO profile.

C. Discussion of Apparent Discrepancies Between Observations and Model Calculations

The first point to make is that these discrepancies may only be apparent and may not be real. One-dimensional models represent long-time global averages, and the quoted observations may be too small

a sample to give such averages. At one location a given method measuring a single quantity typically shows large variations from one measurement to the next, for example, compare the six measured ClO profiles in Figure 4.38. These variations could be natural fluctuations, or they could be unrecognized systematic errors in the measuring techniques.

In comparing observations and model calculations, one needs to examine the full range of observations and the full range of model calculations, and one needs to keep alive multiple hypotheses about apparent disagreement — or agreement, for that matter — between observations and theory. If the models are in error, the trouble is not likely to be in the numerical computation, since many modelers using various numerical methods get similar results; the difficulty is expected to be in the input data or in the concepts of the model itself. The models specify a list of chemical and photochemical reactions, boundary values for all independent species, a theory of global-average vertical mixing, and a method of calculation the distribution of radiation. The input data are based on observations in the laboratory or in the atmosphere, and any measurement is susceptible to having unsuspected systematic error. The great uncertainty always hanging over any model calculation concerns the unrecognized features that have been omitted.

Recognizing that these discrepancies may be only apparent and not real, one can nevertheless list the several conflicts between observations and model calculations noted in this review:

(i) The solar proton event caused a larger reduction in ozone below 32 km at 80°n than that predicted by models.

(ii) The limiting mixing ratio of total nitrogen oxides in the upper stratosphere is overestimated by the models.

(iii) The observed vertical columns of nitric acid vapor are much less at all latitudes than the values calculated by 2-D models, and the observed value at 30° latitude is much less than the value calculated by 1-D models.

(iv) The observed ratio of nitric acid to nitrogen dioxide, $[HNO_3]/[NO_2]$, is generally, but not always, less than that calculated in the lower half of the stratosphere.

(v) The models calculate more ClO at 25 km relative to 35 km than that observed.

Of these five indicated discrepancies between theory and observations, it appears that the one concerning the solar proton event below 32 km is the least well established. For the sake of discussion, these discrepancies between theory and observation will be regarded as real, and possible, multiple reasons for the differences will be discussed.

All five discrepanices noted above would tend to be resolved if, for some reason, the models overestimate the concentration of singlet atomic oxygen in the lower half of the stratosphere. A lower concentration of $O(^1D)$ would cause less production of nitric oxide (Figure 4.11)

$$N_2O + O(^1D) \rightarrow 2\ NO \qquad (4.30)$$

with consequent greater photolysis of nitrous oxide (Figure 4.10), and thus the models would calculate less NO_x in the upper stratosphere (item ii, above). A lower concentration of $O(^1D)$ in the lower stratosphere would result in a reduced rate of production of hydroxyl radicals

$$H_2O + O(^1D) \rightarrow 2\ HO \qquad (4.50)$$

and a lower steady-state concentration for the family of HO_x species. A reduced concentration of hydroxyl radicals would form less nitric acid

$$HO + NO_2 \xrightarrow{M} HNO_3 \qquad (4.34)$$

which would relieve the overcalculation of the nitric acid vertical column (item iii). The steady-state concentration of nitric acid is largely the resultant of formation as in Equation (4.34) and photolysis

$$HNO_3 + h\nu \rightarrow HO + NO \quad . \qquad (4.35)$$

The steady-state ratio of nitric acid to nitrogen dioxide is

$$\frac{[HNO_3]}{[NO_2]} = \frac{k(M)[HO]}{jHNO_3} \quad . \qquad (4.51)$$

Thus a reduction in hydroxyl radical concentration would reduce the ratio $[HNO_3]/[NO_2]$, which is item (iv). There are many reactions interchanging Cl, ClO, and HCl, but the dominant processes in the lower stratosphere are

a. $Cl + O_3 \rightarrow ClO + O_2$ (4.52)

b. $NO + ClO \rightarrow NO_2 + Cl$ (4.53)

c. $Cl + CH_4 \rightarrow HCl + CH_3$ (4.36)

d. $HO + HCl \rightarrow H_2O + Cl$ (4.37)

The steady state ratio between the ClO radical and the reservoir species HCl is

$$\frac{[ClO]}{[HCl]} = \frac{k_a[O_3]}{k_b[NO]} \frac{k_d[HO]}{k_c[CH_4]} \quad . \qquad (4.54)$$

In this case a reduction in the concentration of hydroxyl radicals around 25 km would cause a reduction in ClO, as is indicated by item (v) above. A reduced calculated $O(^1D)$ in the lower half of the stratosphere would also affect items (i), the unexpectedly large reduction of ozone below 32 km by the solar proton event. The principal difference in the calculated effect of NO_x on ozone between 1976 and 1978, Figure 4.22, resides in the higher concentrations of HO in the lower stratosphere according to the 1978 models. As can be seen in Figure 4.24, the calculated effect of increased NO_x went from a decrease of ozone in 1976 to an increase of ozone in 1978 as the calculated concentrations of hydroxyl radicals increased. A decrease in $O(^1D)$ in the lower stratosphere with a corresponding decrease in HO_x radicals would tend to change Figures 4.24 and 4.26 towards the 1976 shapes. An increased sensitivity of ozone towards reduction by NO_x in the 25 to 32 km range would relieve the possible discrepancy listed as item (i) above.

The steady-state concentration of singlet atomic oxygen is largely determined by the photolysis of ozone below 310 nm and the deactivation of excited atomic oxygen by oxygen and nitrogen of air

$$O_3 + h\nu \ (\lambda < 310 \text{ nm}) \rightarrow O_2 + O(^1D) \qquad (4.20)$$

$$O(^1D) + N_2 \rightarrow O(^3P) + N_2 \qquad (4.55)$$

$$O(^1D) + O_2 \rightarrow O(^3P) + O_2 \quad . \qquad (4.56)$$

These reactions have been measured several times in the laboratory,[71-78] but agreement between different workers is not good. The sense of the discrepancies in the stratosphere largely concern the relatively cold, high pressure lower stratosphere as opposed to the warmer, lower pressure upper stratosphere. If the temperature and pressure coefficients of the quantum yield (4.20) and/or the rate constants (4.55 and 4.56) are systematically wrong, then this error alone would tend towards relieving all five discrepancies noted above. Many of the laboratory observations were made at low pressures, far less than those in the lower stratosphere. The experiments are difficult, and large systematic errors might still be present. It is possible that some models use too high an intensity of solar radiation in the 250 to 310 nm range[79] and such an error in input data would lead to too high a concentration of $O(^1D)$ and to too high a production rate of HO and NO in the lower stratosphere.

Another possibility is that some process recombines HO_x radicals in the 15 to 30 km stratosphere much faster than current models indicate, thereby accounting for the discrepancies associated with the nitric acid columns, the HNO_3/NO_2 ratio, and the ClO/HCl ratio. For this to be true, it might be that the reaction $HO + HOO \rightarrow H_2O + O_2$ is, after all, much faster at stratospheric temperatures and pressures than the values now calculated. Or it might be that the catalytic cycles

$$\begin{array}{ll} & HOO + HOO \rightarrow H_2O_2 + O_2 \\ & HO + H_2O_2 \rightarrow H_2O + HOO \\ \hline \text{net:} & HO + HOO \rightarrow H_2O + O_2 \end{array} \qquad (4.57)$$

$$\begin{aligned} & HOO + NO_2 + M \rightarrow HOONO_2 + M \\ & HO + HOONO_2 \rightarrow H_2O + O_2 + NO_2 \\ \text{net:} \quad & HO + HOO \rightarrow H_2O + O_2 \end{aligned} \qquad (4.58)$$

at low temperatures are faster than they are now considered to be. Reaction (4.58) represents catalytic destruction of HO_x free radicals by the oxides of nitrogen. The rate constant for reaction, $HO + HOONO_2 \rightarrow H_2O + O_2 + NO_2$, is quoted to be 5×10^{-13} cm^3 $molecule^{-1}$ s^{-1} with a factor of 10 uncertainty.[80] If this rate constant should be at the upper end of its quoted uncertainty range, that is, 5×10^{-12}, then the NO_x catalyzed destruction of ozone (4.58) would be, by far, the fastest mechanism for HO_x destruction in the lower stratosphere. [Because of the occurrence of M in reaction (4.58), this effect decreases with increasing altitude.]

If these five discrepancies are real and if they are to be relieved by decreasing the calculated concentration of $O(^1D)$ in the lower stratosphere or by increasing the rate of recombination of HO_x species, then the revised models will probably move part-way in Figures 4.24 and 4.26 from the situation as shown for 1978 to the situation as shown for 1976. In particular, the sensitivity of the ozone column to NO_x perturbations would tend to increase, and the sensitivity of the ozone column to chlorine perturbations would tend to decrease.

As more observations are obtained, these apparent discrepancies may be swallowed up by the large range of natural variations of stratospheric species. On the other hand, these discrepancies may turn out to be real, and it seems worthwhile to give careful attention to the possibility that the models suffer from serious deficiencies in the 15 to 30 km altitude range.

Acknowledgment

This work was supported by the Division of Chemical Sciences, Office of Basic Energy Sciences, U.S. Department of Energy under Contract No. W-7405-Eng-48.

Many investigators generously supplied tables of observed data, tables of model calculations, or special figures for the sake of this chapter. For this invaluable aid, especial gratitude is expressed to P. J. Crutzen, W. H. Duewer, H. U. Dütsch, F. M. Luther, S. Solomon, J. Angell, and G. F. Widhopf.

References

1. Murcray, D. G., Goldman, A., Csoeke-Poeckh, A., Murcray, F. H., Williams, W. J., and Stocker, R. N., Nitric acid distribution in the stratosphere, *J. Geophys. Res.*, 78, 7033, 1973.

2. Dütsch, H. U., Vertical ozone distribution on a global scale, *Pure Appl. Geophys.*, 116, 511, 1978.

3. Johnston, H. S., and Podolske, J., Interpretations of stratospheric photochemistry, *Rev. Geophys. Space Phys.*, 16, 491, 1978.

4. Johnston, H. S., and G. Whitten, Instantaneous photochemical rates in the global stratosphere, *Pure Appl. Geophys.*, 106-108, 1468, 1973.

5. Ackerman, M., Ultraviolet solar radiation related to mesospheric processes, in *Mesospheric Models and Related Experiments*, Fiocco, G., Ed., D. Reidel, Hingham, Massachusetts, 1971, pp. 149-149.

6. Brueckner, G. E., Bartoe, J.-D. F., Moe, O. K., and Van Hoosier, M. E., Absolute solar ultraviolet intensities and their variations with solar activity, 1, The wavelength region 1750-2100 Å, *Astrophy. J.*, 209, 935, 1976.

7. Hudson, R. D., and Mahle, S. H., Photodissociation rates of molecular oxygen in the mesosphere and lower thermosphere, *J. Geophys. Res.*, 77, 2902, 1972.

8. Isaksen, I. S. A., Midtbö, K., Dunde, J., and Crutzen, P. J., A simplified method to include molecular scattering and reflection in calculations of photon fluxes and photodissociation rates, *Report 20*, Inst. for Geophys., University of Oslo, Oslo, Norway, 1976, pp. 1-21.

9. Pierotti, D., and Rasmussen, R. A., Combustion as a source of nitrous oxide in the atmosphere, *Geophys. Res. Lett.*, 3, 265, 1976.

10. Weiss, R. F., and Craig, H., Production of atmospheric nitrous oxide by combustion, *Geophys. Res. Lett.*, 3, 751, 1976.

11. Bates, D. R., and Hayes, P. B., Atmospheric nitrous oxide, *Planet. Space Sci.*, 15, 189, 1968.

12. Crutzen, P. J., Ozone production rates in an oxygen-hydrogen-nitrogen atmosphere, *J. Geophys. Res.*, 76, 7311, 1971.

13. Nicolet, M., and Vergison, A., L'oxyde azoteux dans la stratosphere, *Aerom. Acta*, 90, 1, 1971.

14. Schmeltakopf, A. L., Albritton, D. L., Crutzen, P. J., Goldan, P. D., Harrop, W. J., Henderson, W. R., McAfee, J. R., McFarland, M., Schiff, H., Thompson, T. L., Hoffman, D. J., and Kjome, N. T., Stratospheric nitrous oxide profiles at various latitudes, *J. Atmos. Sci.*, 34, 729, 1977.

15. Goldan, P. D., Kuster, W. C., Albritton, D. L., and Schmeltekopf, A. L., Stratospheric CF_3Cl, CF_2Cl_2, and N_2O height profile measurements at several latitudes, *J. Geophys. Res.*, in press, 1979.

16. Tyson, B. J., Vedder, J. F., Arveson, J. C., and Brewer, R. B., Stratospheric measurements of CF_2Cl_2 and N_2O, *Geophys. Res. Lett.*, 5, 369, 1978.

17. Ehhalt, D. H., Sample of stratospheric trace constituents, *Can. J. Chem.*, 52, 1510, 1974.

18. Johnston, H. S., Serang, O., and Podolske, J., Instantaneous global nitrous oxide photochemical rates, *J. Geophys. Res.*, 84, 5077, 1979.

19. Brewer, A. W., Evidence for a world-wide circulation provided by measurements of helium and water vapor distribution in the stratosphere, *Quart. J. Roy. Mat. Soc.*, 75, 351, 1949.

20. (a) Reagan, J. B., Imhof, W. L., Moughan, V. F., in *Collected Data Reports on August 1972 Solar Terrestrial Events*, Coffey, H. E., Ed., Report UAG 28, World Data Center A, Boulder, Colorado, 1973, Part III, p. 676.

(b) Kohl, J. W., Bostrom, C. O., and Williams, D. J., *ibid.*, Part II, p. 330.

21. Heath, D. F., Krueger, A. J., and Crutzen, P. J., Solar proton event: Influence on stratospheric ozone, *Science*, 197, 886, 1977.

22. Frederick, J. E., Solar corpuscular emission and neutral chemistry in the earth's middle atmosphere, *J. Geophys. Res.*, 81, 3179, 1976.

23. Solomon, S., Johnston, H. S., Kowalczyk, M., and Wilson, I., Instantaneous global ozone balance including observed nitrogen dioxide, *Pure Appl. Geophys*, accepted for publication, 1980.

24. Crutzen, P. J., Isaksen, I. S. A., Reid, G. C., Solar proton events: Stratospheric sources of nitric oxide, *Science*, 189, 457, 1975.

25. (a) Noxon, J. F., Whipple, E. C., Jr., and Hyde, R. S., Stratospheric NO_2. 1. Observational method and behavior at mid-latitude, *J. Geophys. Res.*, 84, 5047, 1979.

(b) Noxon, J. F., Stratospheric NO_2. 2. Global behavior, *J. Geophys. Res.*, 84, 5067, 1979.

26. Keeling, C. D., Bacastow, R. B., Bainbridge, A. E., Ekdahl, C. A., Guenther, P. R., Waterman, L. S., and Chin, J. S., Carbon dioxide variations at Mauna Loa Observatory, Hawaii, *Tellus*, 28, 538, 1976.

27. National Academy of Sciences-National Research Council, *Environmental Impact of Stratospheric Flight*, Climatic Impact Committee, 2101 Constitution Avenue, Washington, D.C., 1975.

28. Grobecker, A. J., Coroniti, S. C., and Cannon, R. H., Jr., *Report of Findings - The Effect of Stratospheric Pollution by Aircraft*, DOT-TST-75-50, National Technical Information Service, Springfield, Virginia, 1975.

29. Rundel, R. D., Butler, D. M., and Stolarski, R. S., Uncertainty propagation in a stratospheric model. 1. Development of a concise stratospheric model, *J. Geophys. Res.*, 83, 3063, 1978.

30. Hahn, J., and Junge, C., Atmospheric nitrous oxide: A critical review, *Zeitschrift f. Naturforschung*, 329, 190, 1977.

31. Duewer, W. H., and Wuebbles, D. J., Predictions of the effect on the stratosphere of changes in the oxides of nitrogen, NASA Stratospheric Workshop, Harper's Ferry, West Virginia, June 4-8, 1979.

32. Hampson, R. F., and Garvin, D., Chemical kinetic and photochemical data for modeling atmospheric chemistry, Technical Note 866, National Bureau of Standards, Washington, D.C., 1975.

33. Levy, H., Photochemistry of the lower stratosphere, *Planet. Space Sci.*, 20, 919, 1972.

34. Crutzen, P. J., Minor constituents in the stratosphere and troposphere, *Pure Appl. Geophys.*, 106-108, 1385, 1973.

35. Johnston, H. S., and Quitevis, E., The oxides of nitrogen with respect to urban smog, supersonic transports, and global methane, in *Radiation Research*, Proceedings of the Fifth International Conference on Radiation Research, Nygaard, O. F., Adler, H. I., and Sinclair, W. K., Eds., Academic Press, New York, 1975, pp. 1299-1313.

36. Howard, C. J., and Evenson, K. M., Kinetics of the reaction of HOO with NO, *Geophys. Res. Lett.*, 4, 473, 1977.

37. Graham, R. A., Winer, A. M., and Pitts, J. N., Jr., Pressure and temperature dependence of the unimolecular decomposition of HO_2NO_2, *J. Chem. Phys.*, 4505, 1978.

38. Reid, G. C., Isaksen, I. S. A., Holzer, T. E., and Crutzen, P. J., Influence of ancient solar-proton events on the evolution of life, *Nature*, 259, 177, 1976.

39. Ruderman, M. A., Possible consequences of nearby supernova explosions for atmospheric ozone and terrestrial life, *Science*, 184, 1079, 1974.

40. Whitten, R. C., Cuzzi, J., Borucki, W. J., and Wofe, J. H., Effect of nearby supernova explosions on atmospheric ozone, *Nature*, 203, 398, 1976.

41. Foley, H. M., and Ruderman, M. A., Stratospheric NO production from past nuclear explosions, *J. Geophys. Res.*, 78, 4441, 1973.

42. Johnston, H. S., Whitten, G., and Birks, J., Effect of nuclear explosions on stratospheric nitric oxide and ozone, *J. Geophys. Res.*, 78, 6107, 1973.

43. Bauer, E., and Gilmore, F. R., Effect of atmospheric nuclear explosions on total ozone, *Rev. Geophys. Space Phys.*, 13, 451, 1975.

44. Bauer, E., A catalog of perturbing influences on stratospheric ozone, *J. Geophys. Res.*, in press, 1979.

45. Chang, J. S., and Duewer, W. H., On the possible effect of NO_x injection in the stratosphere due to past atmospheric nuclear weapons tests, Paper presented at the AIAA-AMS Meeting, Amer. Inst. of Aeronaut. and Astronaut., Denver, Colorado, June 1973.

46. Chang, J. S., Duewer, W. H., and Wuebbles, D. J., The atmospheric nuclear tests of the 1950's and 1960's: A possible test of ozone depletion theories, *J. Geophys. Res.*, 84, 1755, 1979.

47. Komhyr, W. D., Barrett, E. W., Slocum, G., and Weickmann, H. K., Atmospheric total ozone increase during the 1960's, *Nature*, 233, 390, 1971.

48. Birrer, W. M., Some critical remarks on trend analysis of total ozone data, *Pure Appl. Geophys.* , 112, 523, 1974.

49. Goldsmith, P., Tuck, A. F., Foot, J. S., Simmons, E. L., and Newson, R. L., Nitrogen oxides, nuclear weapon testing, Concorde, and stratospheric ozone, *Nature*, 244, 545, 1973.

50. Angell, J. K., and Korshover, J., Quasi-biennial and long-term fluctuations in total ozone, *Mon. Weather Rev.*, 101, 426, 1973; Global analysis of recent total ozone fluctuations, *Mon. Weather Rev.*, 104, 63, 1976.

51. Fabian, P., Pyle, J. A., and Wells, R. J., The August 1972 solar proton event and the atmospheric ozone layer, *Nature*, 277, 458, 1979.

52. Murcray, D. G., Goldman, A., Williams, W. J., Murcray, F. H., Bonono, F. S., Bradford, G. M., Cole, G. R., Hanst, P. L., and Molina, M. J., *Geophys. Res. Lett.*, 4, 227, 1977.

53. Drummond, J. R., and Jarnot, R. F., Infrared measurements of stratospheric composition. II. Simultaneous NO and NO_2 measurements, *Proc. Roy. Soc. Lond.*, A 364, 237, 1978.

54. Horvath, J. J., and Mason, C. J., Nitric oxide mixing ratios near the stratopause measured by a rocket-bourne chemiluminescent detector, *Geophys. Res. Lett.*, 5, 1023, 1978.

55. Drummond, J. R., Rosen, J. M., and Hofman, D. J., Balloon-bourne chemiluminescent measurement of NO to 45 km, *Nature*, 265, 319, 1977.

56. Ackerman, M., Fontanella, J. C., Frimont, D., Girard, A., Louisnard, N., and Muller, C., Simultaneous measurement of NO and NO_2 in the stratosphere, *Planet. Space Sci.*, 23, 651, 1975.

57. Evans, W. F. J., Kerr, J. B., McElroy, C. T., O'Brien, R. S., Ridley, B. A., and Wardle, D. I., The odd nitrogen mixing ratio in the stratosphere, *Geophys. Res. Lett.*, 4, 236, 1977.

58. Anderson, J. G., Radicals, Chapter 4 in *The Stratosphere: Present and Future*, NASA Reference Publication to be published in 1980.

59. Miller, C. P., Meakin, P., Franks, G. E., and Jesson, J. P., The fluorocarbon theory. V. One dimensional modeling of the atmosphere: The base case, *Atmos. Environ.*, 12, 2481, 1978.

60. Herman, J. R., The response of stratospheric constituents to solar eclipse, sunrise, and sunset, *J. Geophys. Res.*, 84, 3701, 1979.

61. Turco, R. P., and Whitten, R. C., A note on the diurnal averaging of aeronomical models, *J. Atmos. Terr. Phys.*, 40, 13, 1978.

62. Logan, J. A., Prather, M. J., Wofsy, S. C., and McElroy, M. B., Atmospheric chemistry: Response to human influence, *Phil. Trans. Roy. Soc.*, 290, 187, 1978.

63. Liu, S. C., Donahue, T. M., Cicerone, R. J., and Chameides, W. L., Effect of water vapor on the destruction of ozone in the stratosphere perturbed by ClX or NO_x pollutants, *J. Geophys. Res.*, 81, 3111, 1976.

64. Frederick, J. E., and Hudson, R. D., Photodissociation of nitric oxide in the mesosphere and stratosphere, *J. Atmos. Sci.*, 36, 737, 1979.

65. Crutzen, P. J., Duewer, W. H., and Stolarski, R. S., private communications.

66. Widhopf, G. F., and Glatt, L., Two-dimensional description of the natural atmosphere including active water vapor modeling and potential perturbations due to NO_x and HO_x aircraft emissions, Report No. FAA-EE-79-07, National Technical Information Service, Springfield, Virginia, March 1979.

67. Murcray, D. G., Barker, D. B, Brooks, J. N., Goldman, A., and Williams, W. J., Seasonal and latitudinal variation of the stratospheric concentration of HNO_3, *Geophys. Res. Lett.*, 2, 223, 1975.

68. Lazrus, A. L., and Gandrud, B., Distribution of stratospheric nitric acid vapor, *J. Atm. Sci.*, 31, 1102, 1974.

69. Luther, F. M., private communication, 1978.

70. Harries, J. E., Ratio of HNO_3 to NO_2 concentrations in the daytime stratosphere, *Nature*, 274, 235, 1978.

71. Heidner, R. F., Husain, D., and Wiesenfeld, J. R., Kinetic investigation of electronically excited oxygen atoms, $O(^1D_2)$ by time-resolved attenuation of atomic resonance in the vacuum ultraviolet, *J. Chem. Soc. Faraday Trans. II*, 69, 927, 1973.

72. Davidson, J. A., Sadowski, C. M., Schiff, H. I., Streit, G. E., Howard, C. J., Jennings, D. A., and Schmeltekopf, A. L., Absolute rate constant determinations for the deactivation of $O(^1D)$ by time-resolved decay of $O(^1D) \rightarrow O(^3P)$ emission, *J. Chem. Phys.*, 64, 57, 1976.

72. Kajimoto, O., and Cvetanovic, R. J., Absolute quantum yield of $O(^1D_2)$ in the photolysis of ozone in the Hartley band, *Int. J. Chem. Kinetics*, 11, 605, 1979.

74. Fairchild, C. E., Stone, E. J., and Lawrence, G. M., Photofragment spectroscopy of ozone in the UV region 270-310 nm and at 600 nm, *J. Chem. Phys.*, 67, 3632, 1978.

75. Sparks, R. S., Carlson, L., Shobatake, K., Kowalczyk, M. L., and Lee, Y. T., Dynamics of photodissociation of O_3, Paper presented at 7th International Symposium on Molecular Beams, Riva Del Garda, Italy, May 28-June 1, 1979.

76. Streit, G. E., Howard, C. J., Schmeltekopf, A. L., Davidson, J. A., and Schiff, H. I., Temperature dependence of $O(^1D)$ rate constants for reactions with O_2, N_2, CO_2, O_3, and H_2O, *J. Chem. Phys.*, 65, 4761, 1976.

77. Lee, L. C., and Slanger, T. G., Observations on $O(^1D \rightarrow {}^3P)$ and $O_2(b^1\Sigma_g \rightarrow {}^3\Sigma_g)$ following O_2 photodissociation, *J. Chem. Phys.*, 69, 4053, 1978.

78. Amimoto, S. T., Force, A. P., and Wiesenfeld, J. R., Ozone photochemistry: Production and deactivation of $O(^1D_2)$ following photolysis at 248 nm, *Chem. Phys. Lett.*, 60, 40, 1978.

79. Levy, H., private communication, 1979.

80. DeMore, W. B., Laboratory measurements, Chapter 1 in The Stratosphere: Present and Future, NASA Reference Publication to be published in 1980.

Table 4.1. Initial decreases in ozone, increase in nitrogen oxides from solar proton event, and ratio for intervals in Figure 4.16, 75°N to 80°N.

Altitude Range, km	Ave. O_3 $cm^{-3}/10^{12}$	$\frac{-\Delta O_3}{O_3}$ Percent	ΔNO_x $cm^{-3}/10^9$	Catalytic Chain Length: Minimum $\frac{-\Delta O_3}{\Delta NO_x}$	Catalytic Chain Length: Corrected $\frac{-\Delta O_3}{\Delta NO_x}\frac{t}{\tau}$
44-49	0.14	12	2.5	7	300
39-44	0.41	24	2.2	45	600
35-39	0.84	12	1.8	56	400
32-35	1.3	6	1.5	52	200
24-32	2.3	3	0.9	77	100

Table 4.2. Various global masses in the atmosphere and relative masses.

Global Atmospheric Entity	Mass g	$\frac{\text{Mass}}{\text{GHM}^*}$
All air	5.3×10^{21}	35,000,000
Oxygen	1.1×10^{21}	7,400,000
Stratospheric air	6.3×10^{20}	4,200,000
Carbon dioxide	1.1×10^{18}	7,000
Ozone	3.6×10^{15}	24
Human race	1.5×10^{14}	1
NO_2 (twice Fig. 4.20)	1.8×10^{12}	0.01
NO from solar proton event	1.5×10^{11}	0.001

*Global human mass, taken to be 1.5×10^{14} g.

Table 4.3. Calculated and observed NO_x in the upper stratosphere.

A. Observed NO_x mixing ratios, ppbv.

Altitude km	NO	NO_2	NO_x	Authors	Ref. No.
50	obs.	obs.	14	Drummond and Jarnot	53
50	obs.	calc.	5.0	Horvath and Mason	54
50	obs.	calc.	9.7		54
43	obs.	calc.	7.7	Drummond et al.	55
36	obs.	obs.	11	Ackerman et al.	56
35	obs.	obs.	8.9	Evans et al.	57
		average	9.4		

B. Model calculated values of $NO_x = NO + NO_2$ at 50 km.

NO_x	Authors	Ref. No.
13	Miller et al.	59
13	Herman	60
15	Turco and Whitten	61
22	Logan et al.	62
24	Liu et al.	63
25	Chang et al.	46
average	19	

Figure Captions

Figure 4.1 Temperature and ozone profiles, based on averaged observations. Standard temperature profiles are given for tropical and temperate zones. At temperate latitudes, the standard profiles of ozone are given in terms of mixing ratio and concentration.

Figure 4.2 Zonal-average contour map of tropopshere and stratospheric temperatures. Three month average of data as supplied by Dütsch[2] for the months of September, October, and November.

Figure 4.3 Zonal average mixing ratios of ozone. Fall average as in Figure 4.2. Data supplied by Dütsch.[2]

Figure 4.4 Zonal average ozone concentrations for same data as in Figure 4.3

Figure 4.5 Zonal average (24-hour average) rate of ozone formation from the photolysis of molecular oxygen, as calculated from observed ozone distribution (Figure 4.4), observed temperature (Figure 4.2), and observed distribution of solar radiation above the atmosphere.

Figure 4.6 Ozone photochemical replacement times, an artificial concept defined as the ratio of local ozone concentration (Figure 4.4) divided by the local rate of ozone formation (Figure 4.5). From separate considerations one derives the time scales for horizontal air transport and for vertical air mixing, and interpretations follow concerning the relative rates of photochemistry and air transport.

Figure 4.7 An interpretation about air transport as derived from static observations in the atmosphere and instantaneous photochemical calculations. With a reduction in number of contours, Figure 4.5 is superimposed on Figure 4.3. The region of fast ozone formation is high in the tropical and temperate stratosphere, but the region of maximum ozone concentration is in the lower stratosphere, espcially in the lower polar stratosphere. As has been recognized for decades, this disparity implies large scale air transport of ozone from an "ozone production region" to "ozone storage regions."

Figure 4.8 Zonal-average rate of ozone destruction by the O_x family of reactions. These contour lines are the same scale as those for ozone formation in Figure 4.5. Simple inspection shows the O_x reactions to destroy ozone very much slower than it is formed. The weighted sum of ozone destruction between 15 and 45 km in this figure is 15 percent of the corresponding of ozone formation in Figure 4.5.

Figure 4.9 Contour maps of global nitrous oxide mixing ratios ppbv derived from observed nitrous oxide vertical profiles at various latitudes. Reproduced with permission of American Geophysical Union.[18]

Figure 4.10 Zonal average instantaneous rate of photolysis of nitrous oxide for spring-fall conditions. Reproduced with permission of American Geophysical Union.[18]

Figure 4.11 Zonal-average instantaneous rate of production of nitric oxide from singlet atomic oxygen and nitrous oxide. Reproduced with permission of American Geophysical Union.[18]

Figure 4.12 Natural background for nitrogen oxides in north polar regions during the summer, and the increase in nitric oxide from the solar proton event of August 1972 as derived from observed proton beam above the atmosphere, derived from Crutzen et al.[24]

Figure 4.13 Ozone vertical columns as observed from Nimbus 4 satellite between 75°N and 80°N as function of day number of 1972. The main solar proton event occurred on day number 217 and was followed by secondary proton streams up to day 221. The observations were made above pressure surfaces, but these are transcribed here to approximate altitudes.

Figure 4.14 As in Figure 4.13, observed between 65°N and 75°N.

Figure 4.15 As in Figure 4.13, observed between 45°N and 55°N.

Figure 4.16 Percent change in local ozone as derived from the observed data in Figure 4.13 for 75°N to 80°N. The average is with respect to the local ozone columns between days 210 and 234, one week before, four days during, and two weeks after the solar proton event.

Figure 4.17 As in Figure 4.16, as observed between 65°N and 75°N.

Figure 4.18 Observed latitude dependence of vertical columns of nitrogen dioxide. O, Noxon et al.; Δ, balloon flights (compare Ref. 23).

Figure 4.19 Zonal-average nitrogen dioxide mixing ratios for the sunlit hemisphere derived from the line in Figure 4.18 and local 1-D time-dependent model, which was used only to estimate the vertical profile and time dependence of NO_2 with prescribed vertical column.[23]

Figure 4.20 Zonal-average nitrogen dioxide concentrations (sunlit hemispherical average).

Figure 4.21 Zonal-average contour map of the rate of ozone destruction by NO_x reactions based on "observed" (Figures 4.18 and 4.20) nitrogen dioxide concentrations, calculated atomic oxygen concentrations, as $2\ k_3[O][NO_2]$.

Figure 4.22 Calculated reduction of the ozone vertical column as a function of injection of nitrogen oxides at a uniform global rate and at 20 km altitude. The dashed curve gives the calculated ozone reduction using chemical rate constants as they were understood to be in 1976, and the solid curve presents the same calculation with rate constants as they were understood to be in 1978. Rundel et al.[29]

Figure 4.23 Calculated local increases in stratospheric odd nitrogen ($NO + NO_2 + HNO_3 + ClONO_2$) and local changes in stratospheric ozone as a result of doubling the ground-level flux of nitrous oxide, using rate constants as of March 1979. Noteworthy features are ozone increases in the 0 to 27 km range and ozone decreases in the 28 to 50 km range. Duewer and Wuebbles[31]

Figure 4.24 Changes in local ozone concentration as a result of doubling the ground-level flux of nitrous oxide for a single physical model (Lawrence Livermore Laboratory, one-dimensional model) and for three different sets of chemical rate coefficients: A. Set as used in early 1976, including 1.2 ppbv ClX. B. Set as used in spring 1979 with 1.9 ppbv ClX. C. Set as used in fall 1979 with 1.2 ppbv ClX. The percentage change in the ozone vertical column for these three cases is: A. -11; B +0.5; C. -2 (W. H. Duewer[65]).

Figure 4.25 Calculated reduction of the ozone vertical column as a function of increased tropospheric chlorofluoromethanes, expressed as the long-term asymptotic increase in upper stratospheric odd chlorine ($Cl + ClO + HCl + ClONO_2$) mixing ratio. According to current theory, the long-term release of CFM at the 1974 rate would lead to an asymptotic-odd-chlorine mixing ratio of about 7 ppbv. As in Figure 4.22, the dashed line is calculated from 1976 rate constants and the solid line from 1978 rate constants. Rundel et al.[29]

Figure 4.26 Calculated local changes in stratospheric ozone in terms of 1976 rate constants and 1978 rate constants. A noteworthy feature of this figure is that it identifies the changes in Figure 4.25 as arising primarily from effects in the 15 to 30 km altitude range.

Figure 4.27 Zonal-average contour map of nuclear-bomb produced NO_x (molecules cm^{-3}) based on observed carbon-14, January 1963, including curves showing the photochemical ozone replacement times (compare Figure 4.6) of four months and 10 years (Ref. 27, p. 156).

Figure 4.28 Calculated changes in ozone in the northern hemisphere as a result of the nuclear-bomb tests of 1961-62, as calculated by Chang and Duewer.[45]

Figure 4.29 Observed increase in ozone during the 1960's as reported by Komhyr et al.[47], and the calculated ozone changes due to nuclear bomb tests (Figure 4.28).

Figure 4.30 Ozone record at Arosa, Switzerland from 1942-1971. Deviation in monthly ozone (milli-atmosphere-cm, where total column is 330 milli-atm cm) from 50 year monthly mean plotted against time.[48] The circles are January 1. The dashed line is the calculated ozone reduction shown in Figure 4.28.

Figure 4.31 Average monthly ozone deviations from seven European stations. All four panels are what the natural ozone record would have looked like in the absence of nuclear bomb tests subject to four hypotheses: ozone reduction (as in Figure 4.28) with a 10 percent maximum effect; ozone reduction (as in Figure 4.28) with a 5 percent maximum effect; nuclear bomb tests had no effect on ozone; ozone increases (as a negative of Figure 4.28) with a 5 percent maximum effect.

Figure 4.32 The same operations as in Figure 4.31 except for quarterly averaging before recalculating deviations and using 1-2-1 smoothing function.

Figure 4.33 The data in Figure 4.31 subjected to 29 month running average.

Figure 4.34 Observed and calculated vertical columns of nitric acid vapor above 12 km in most cases, above 16 km for a small number of Murcray's observations. Direct measurements of the total vertical column above an aircraft: O, January 1974; Δ, April 1974. Vertical profile derived from integration over balloon-observed profiles: [L], Lazrus and Gandrud;[68] [M], Murcray et al.;[1] [E], Evans et al.[57] The curves were calculated with a 2-D model by Widhopf and Glatt.[66] The cross was calculated by the Livermore 1-D model.[69]

Figure 4.35 Calculated and observed nitric acid profiles. Observed by Lazrus and Gandrud.[68] Calculated by Livermore 1-D model. Compare Figure 4.34.

Figure 4.36 Same as Figure 4.35. Observed by Murcray et al.[1] Compare the May and September points at 31°N latitude on Figure 4.34.

Figure 4.37 Calculated and observed local ratios of nitric acid to nitrogen dioxide. The left-hand panel gives Evans[57] observations at 59°N. The measurements were simultaneous but by different methods. The circles represent simultaneous daytime measurements by Harries[70] using a single method. The calculated curve is from Widhopf and Glatt's 2-D model.[66] The right-hand panel is a ratio of ratios; it is the ratio between the calculated and observed curves on the left-hand panel.

Figure 4.38 Six observed[58] and one calculated profile of ClO measured near midday at 32°N at various seasons. Calculation based on Livermore model[69] including 1.2 ppbv of total chlorine.

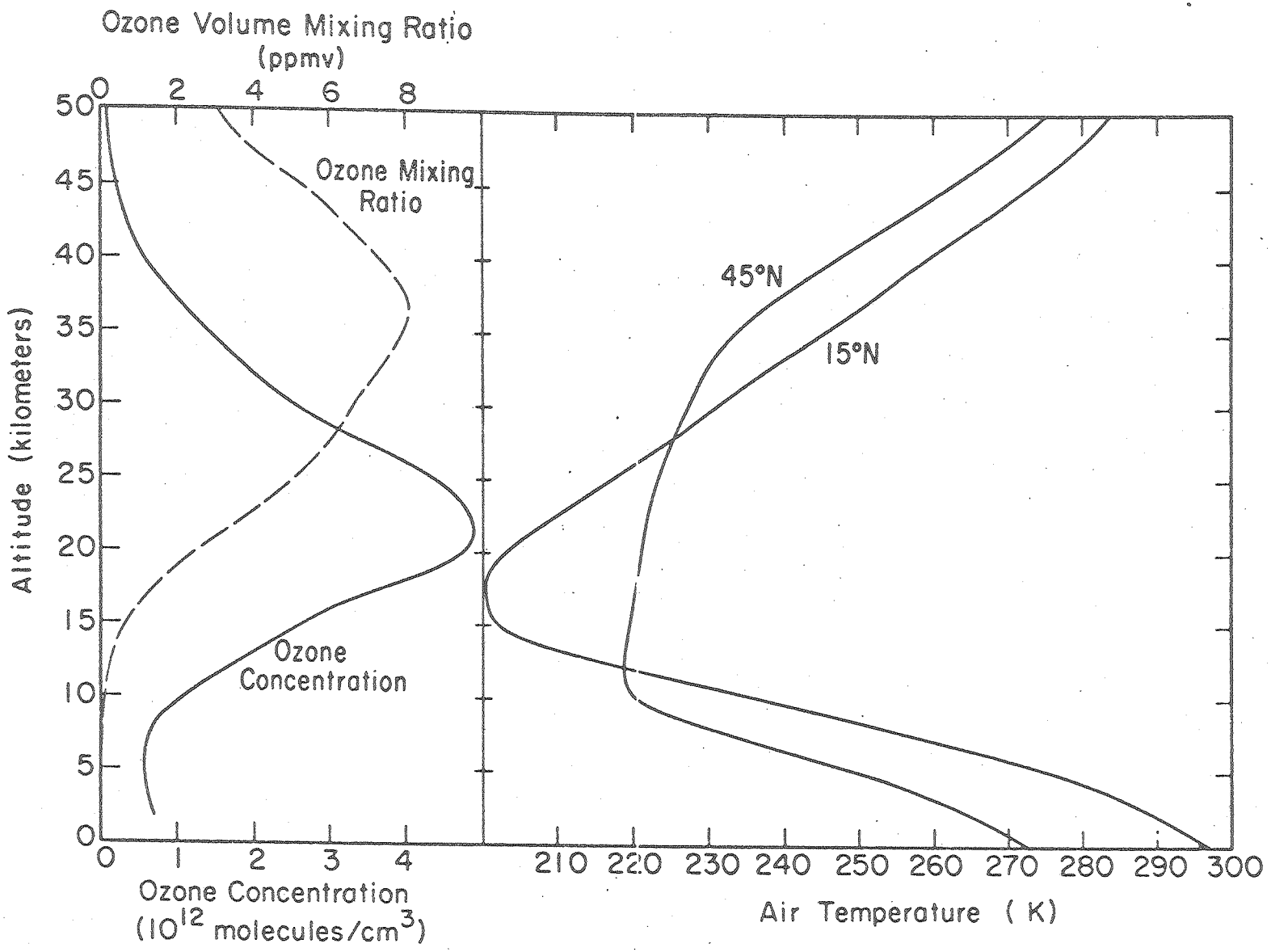

Fig. 4.1
H. S. Johnston

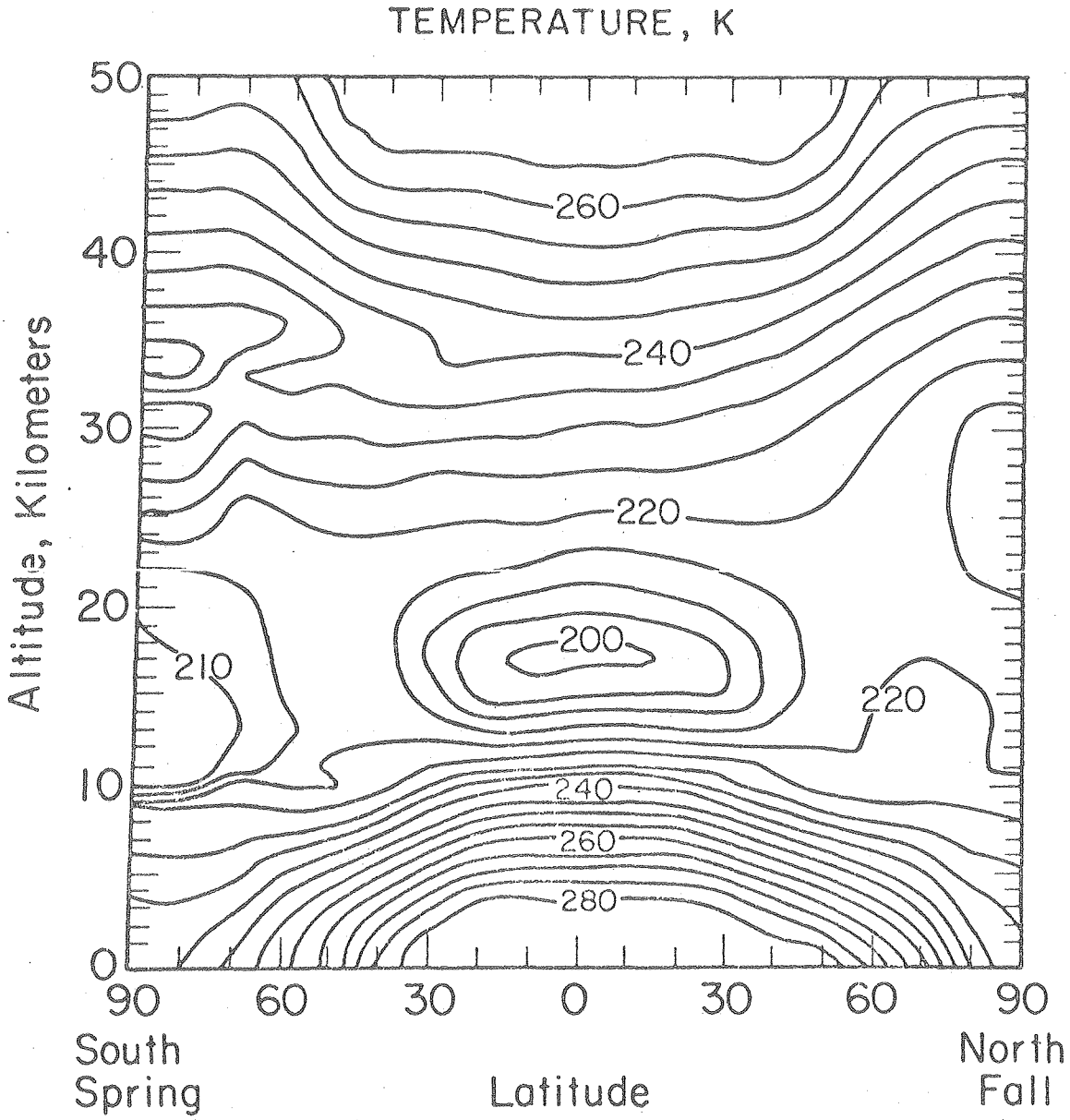

Fig. 4.2
H. S. Johnston

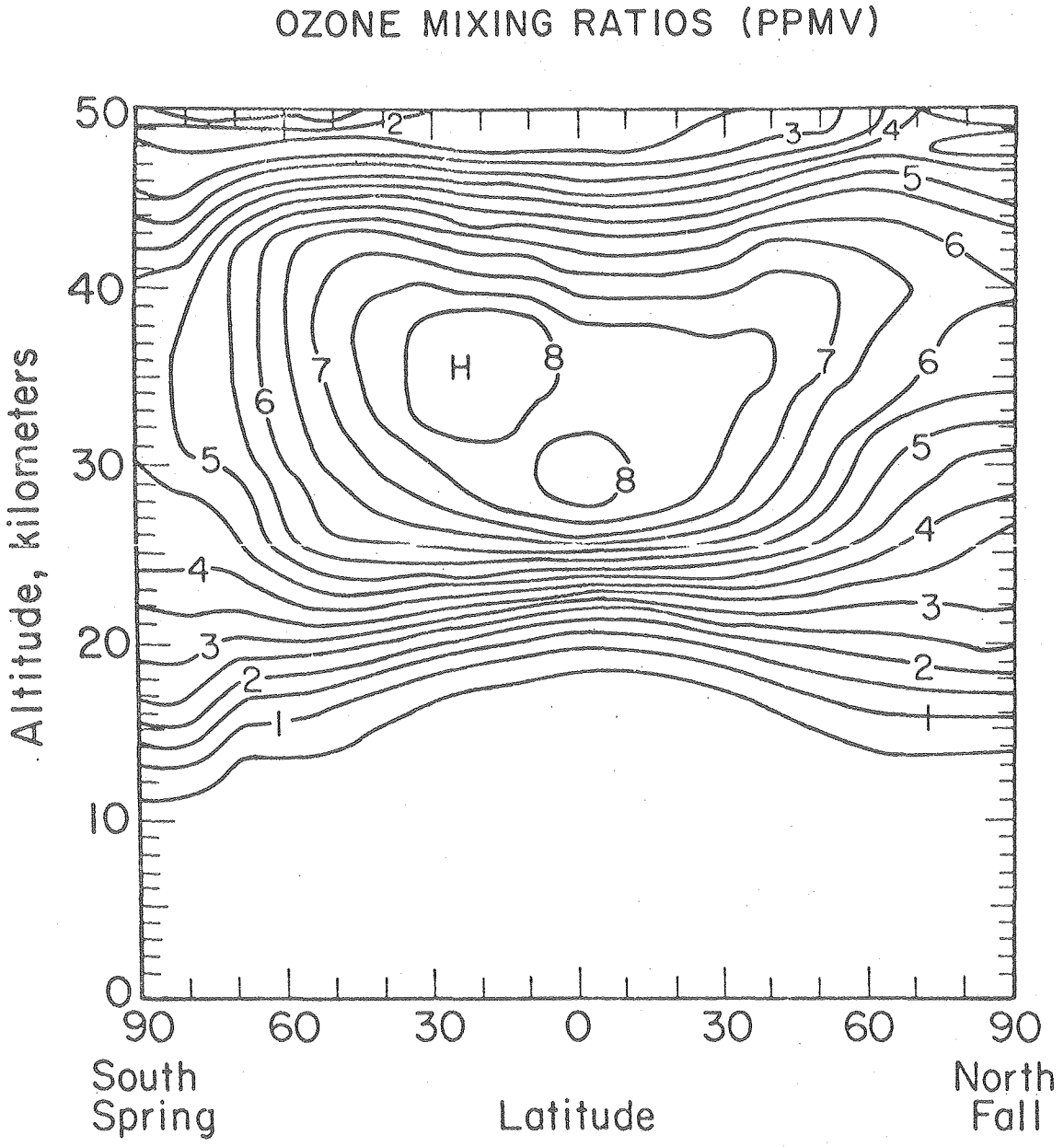

Fig. 4.3
H. S. Johnston

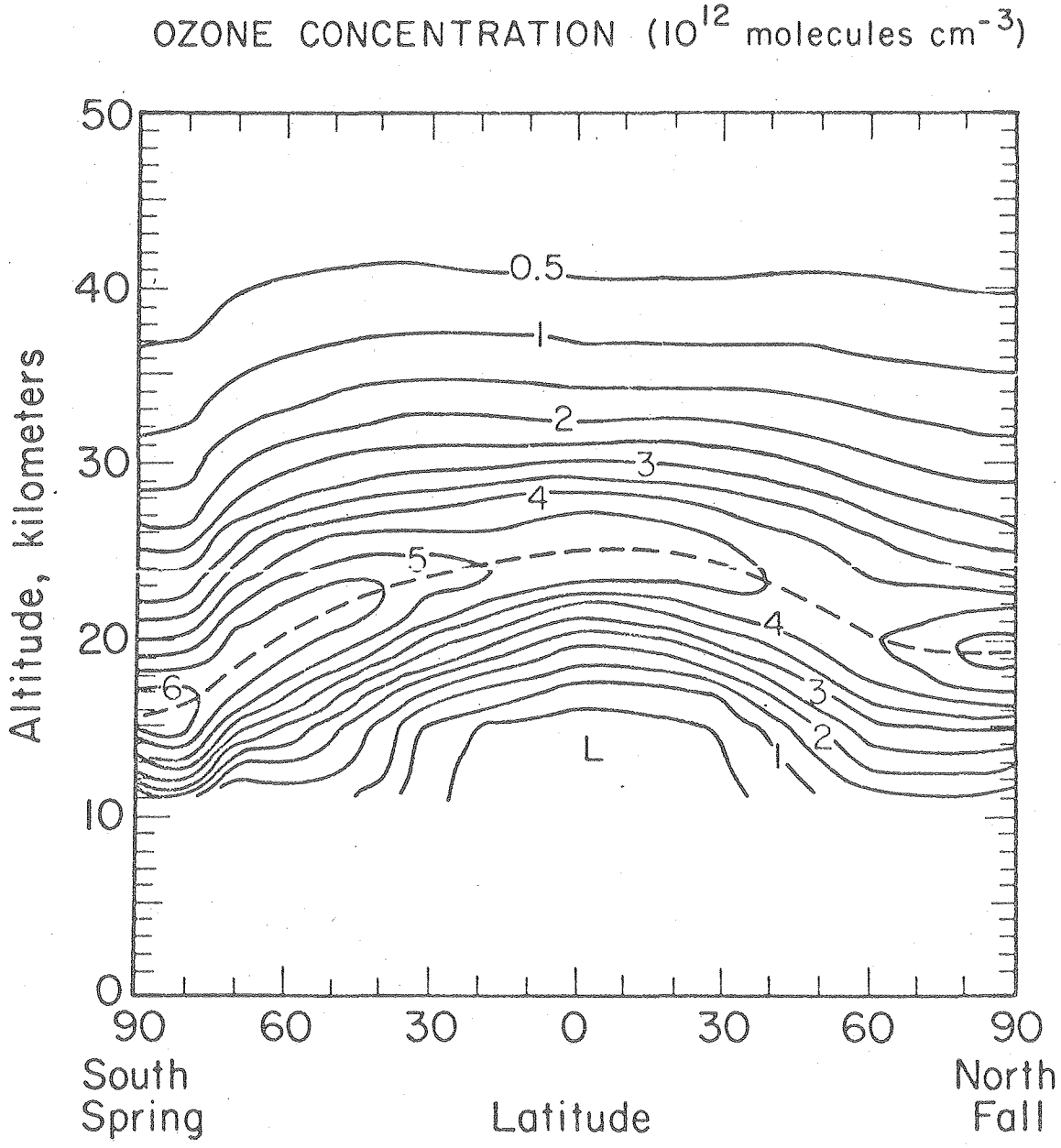

Fig. 4.4
H. S. Johnston

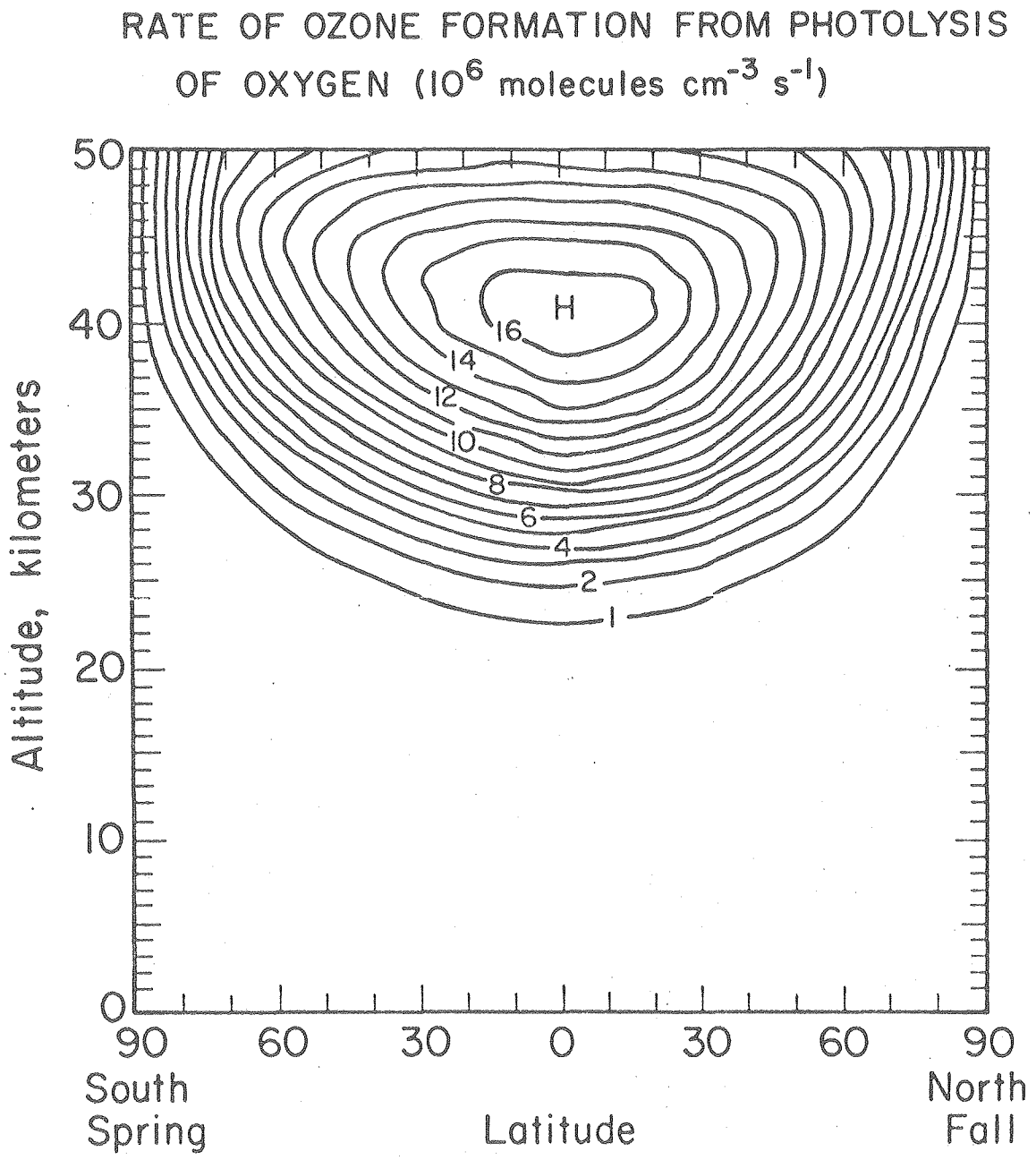

Fig. 4.5
H. S. Johnston

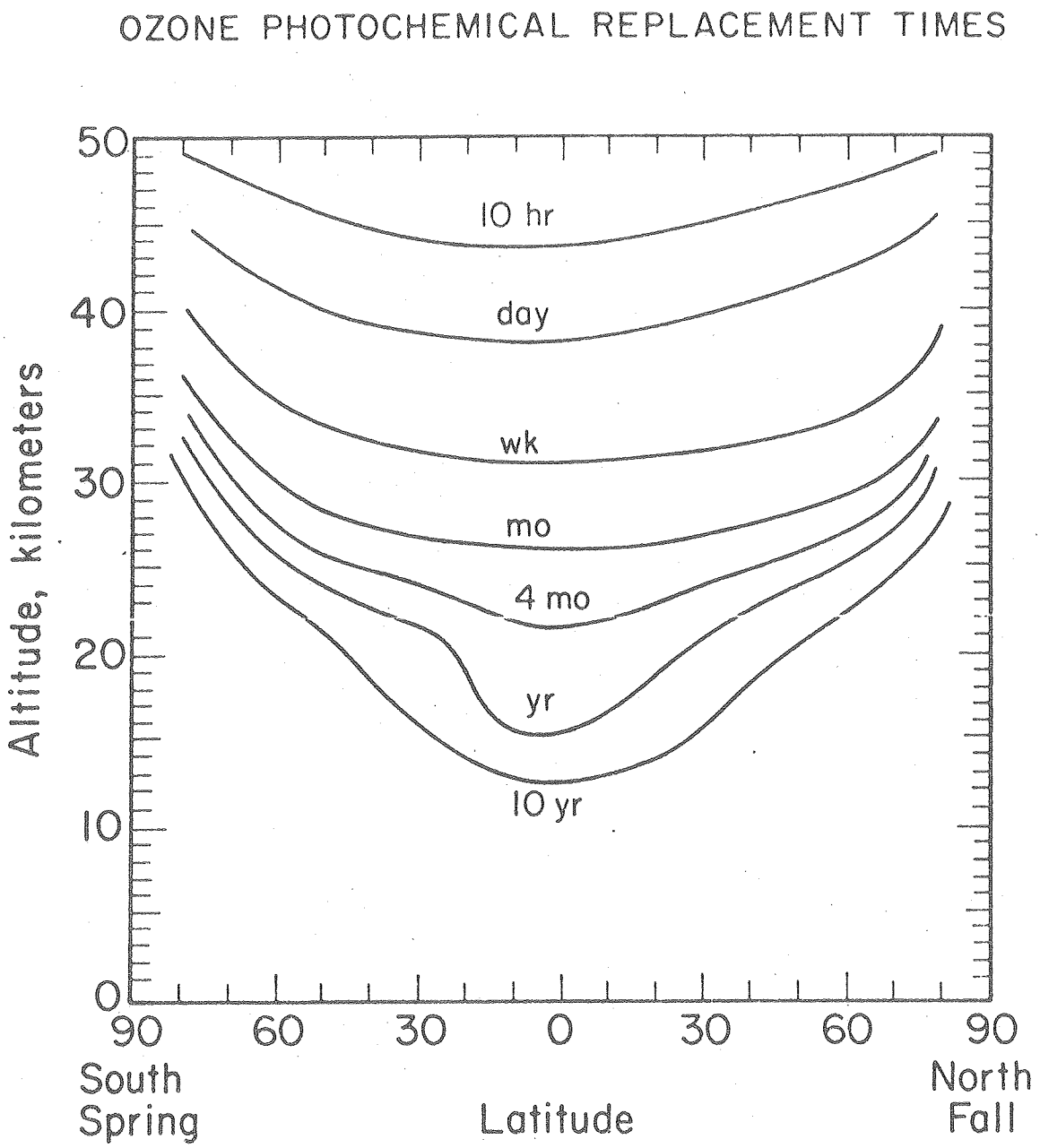

Fig. 4.6
H. S. Johnston

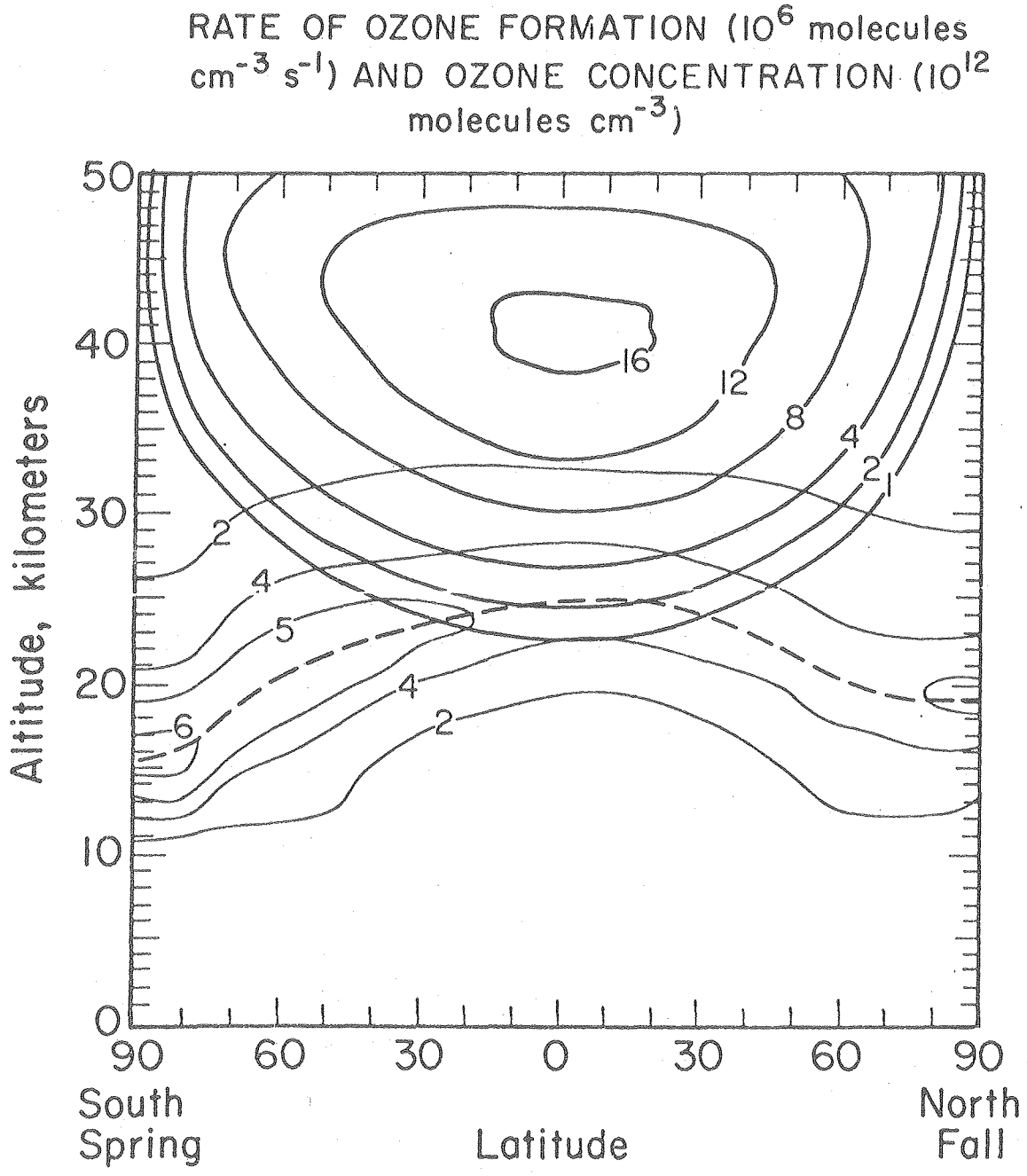

Fig. 4.7
H. S. Johnston

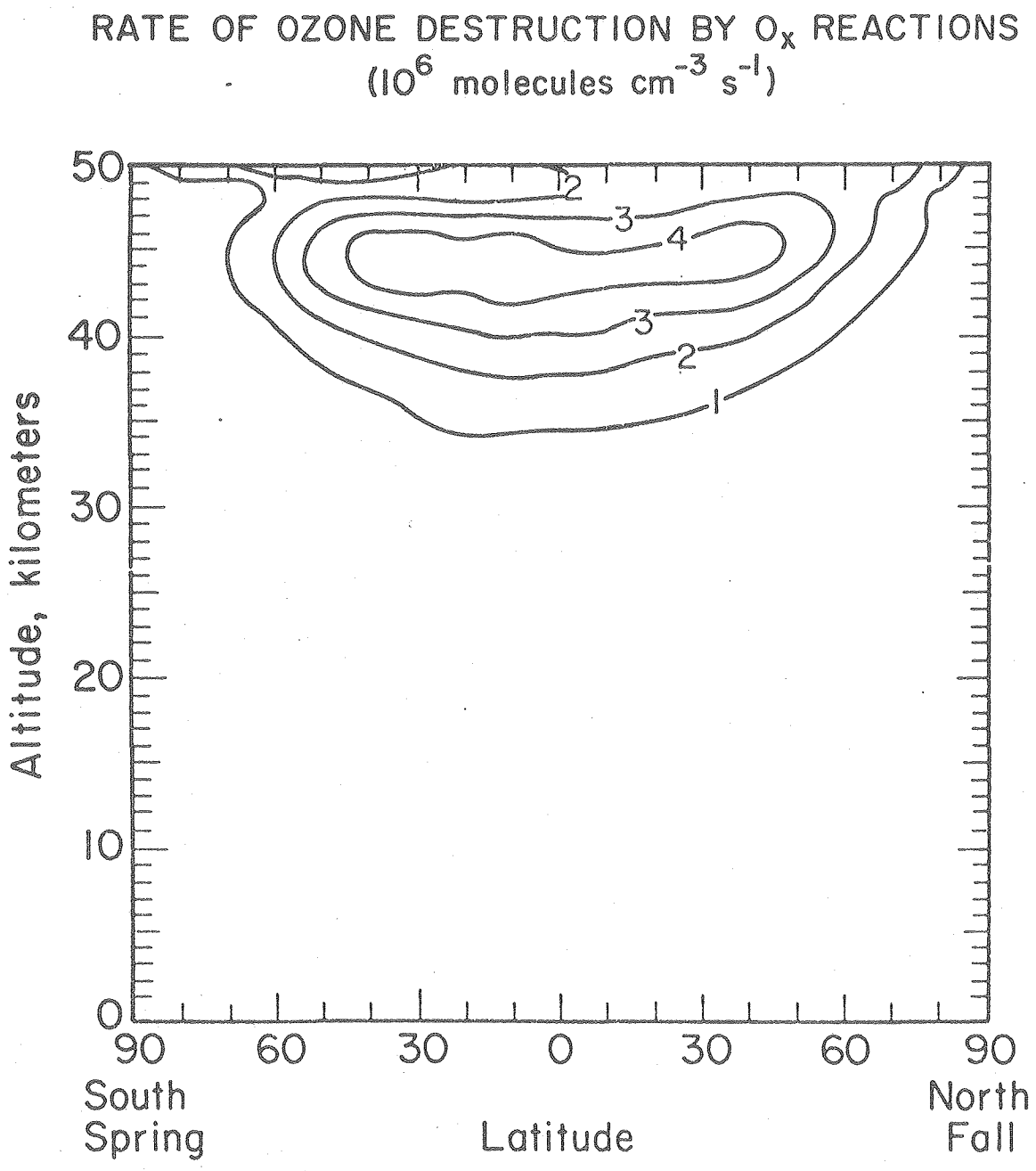

Fig. 4.8
H. S. Johnston

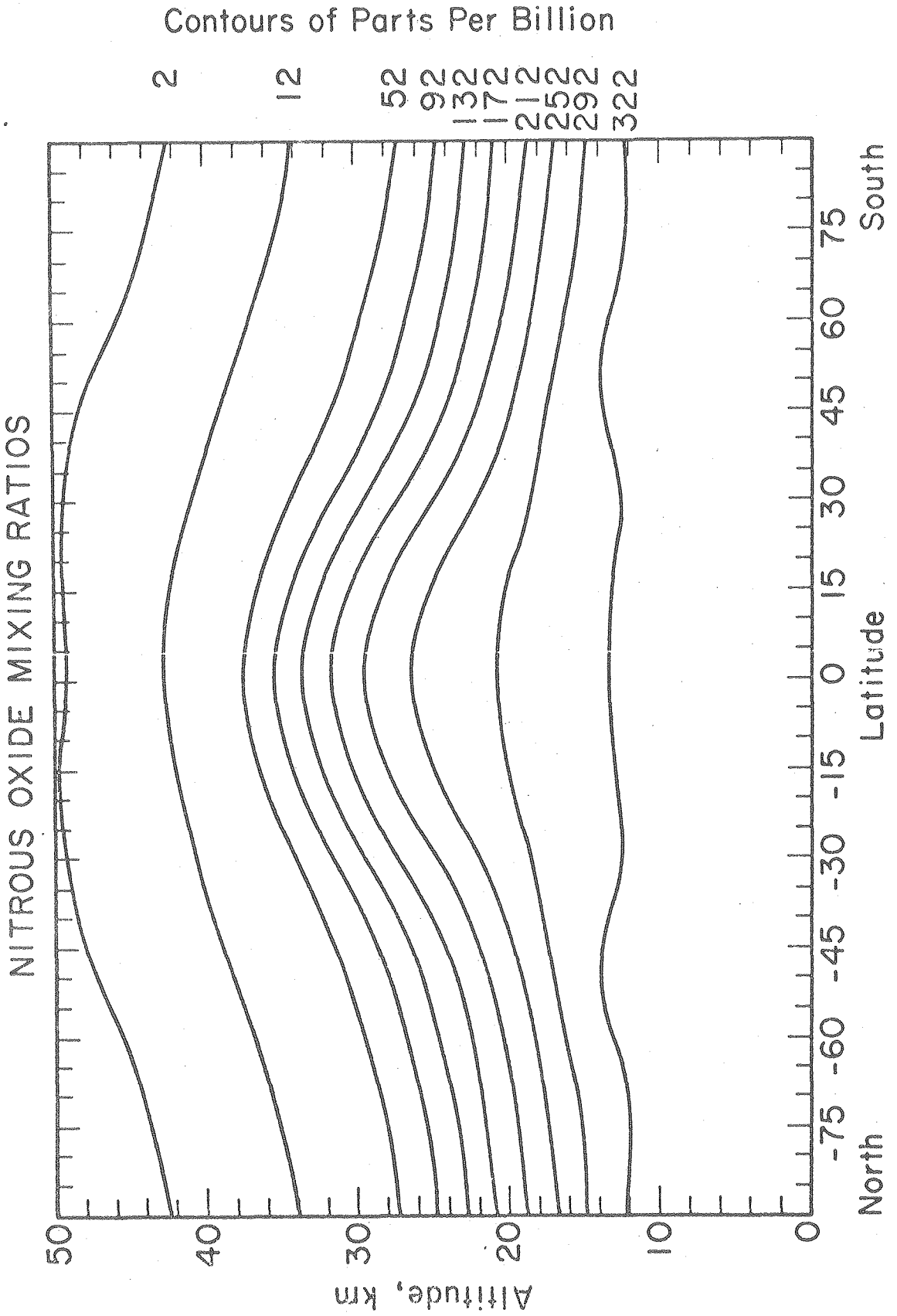

Fig. 4.9
H. S. Johnston

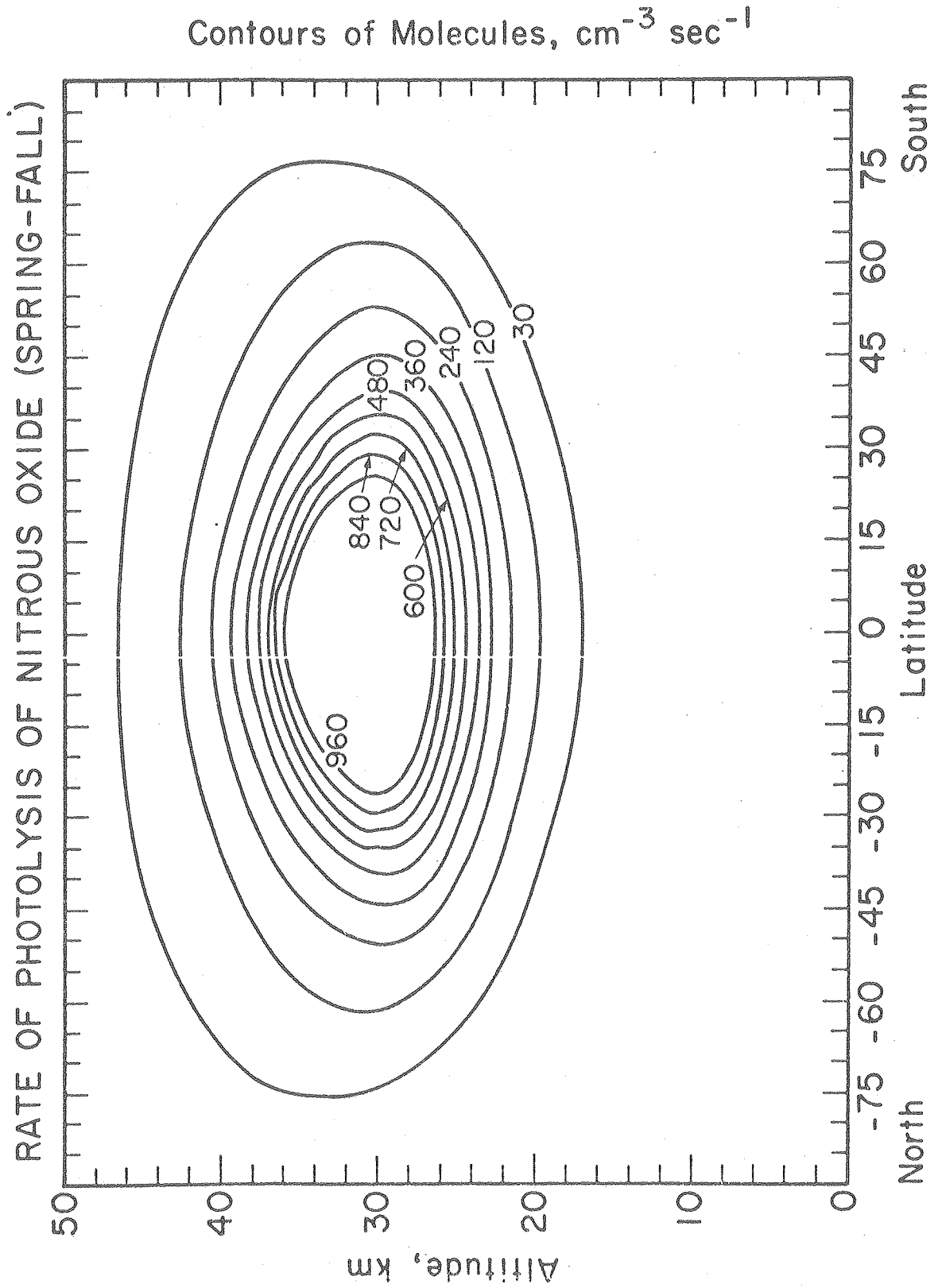

Fig. 4.10
H. S. Johnston

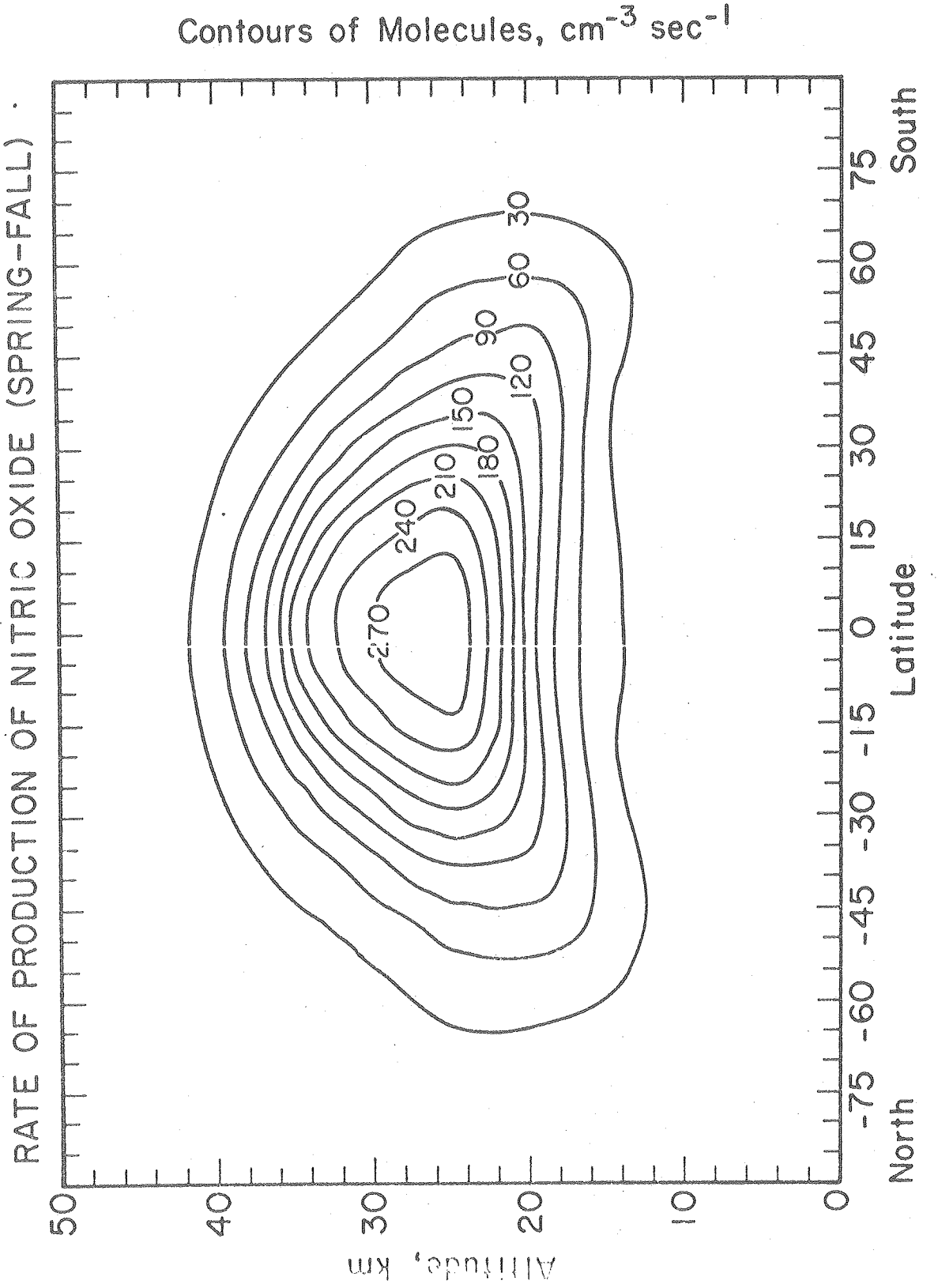

Fig. 4.11
H. S. Johnston

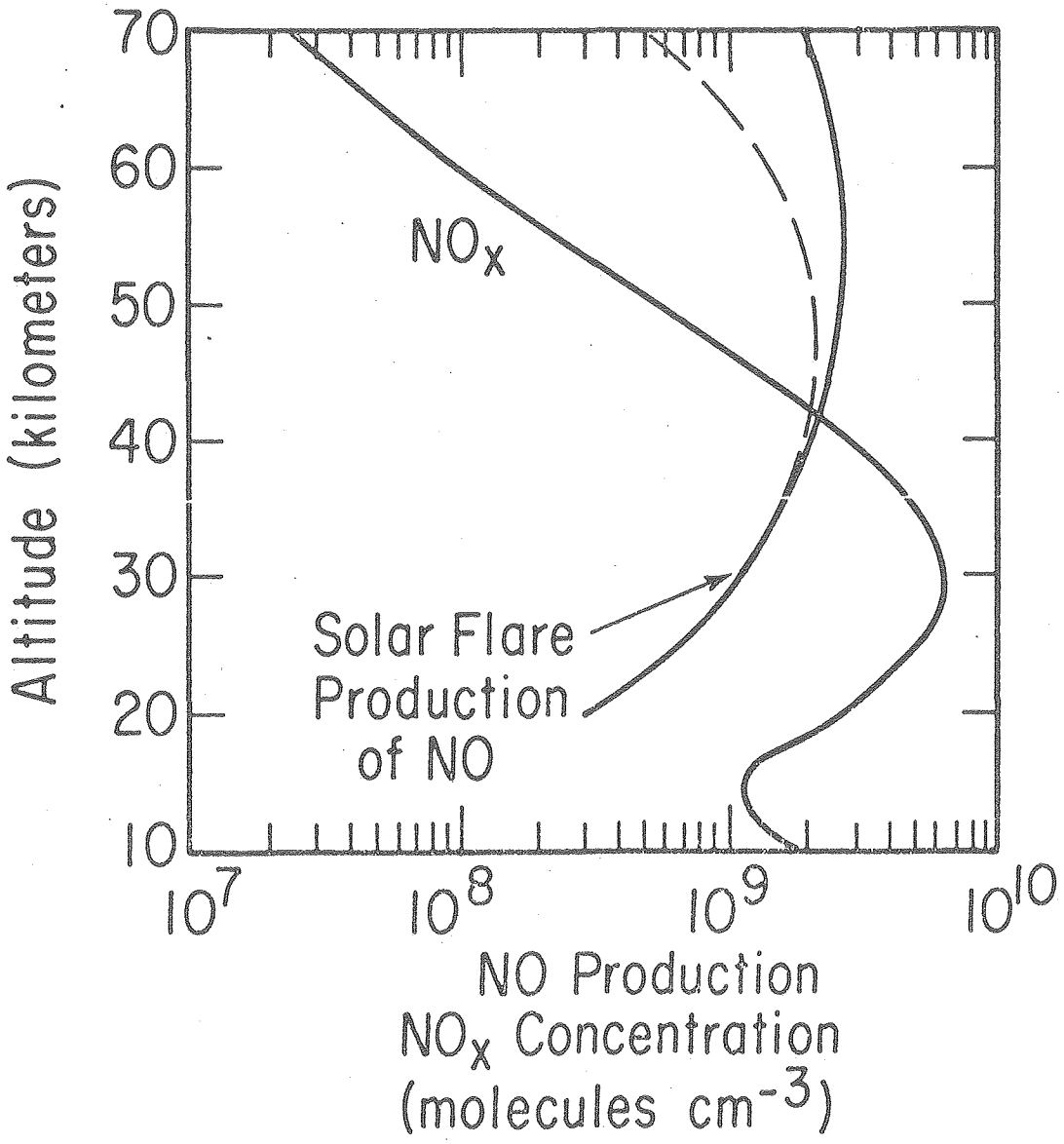

Fig. 4.12
H. S. Johnston

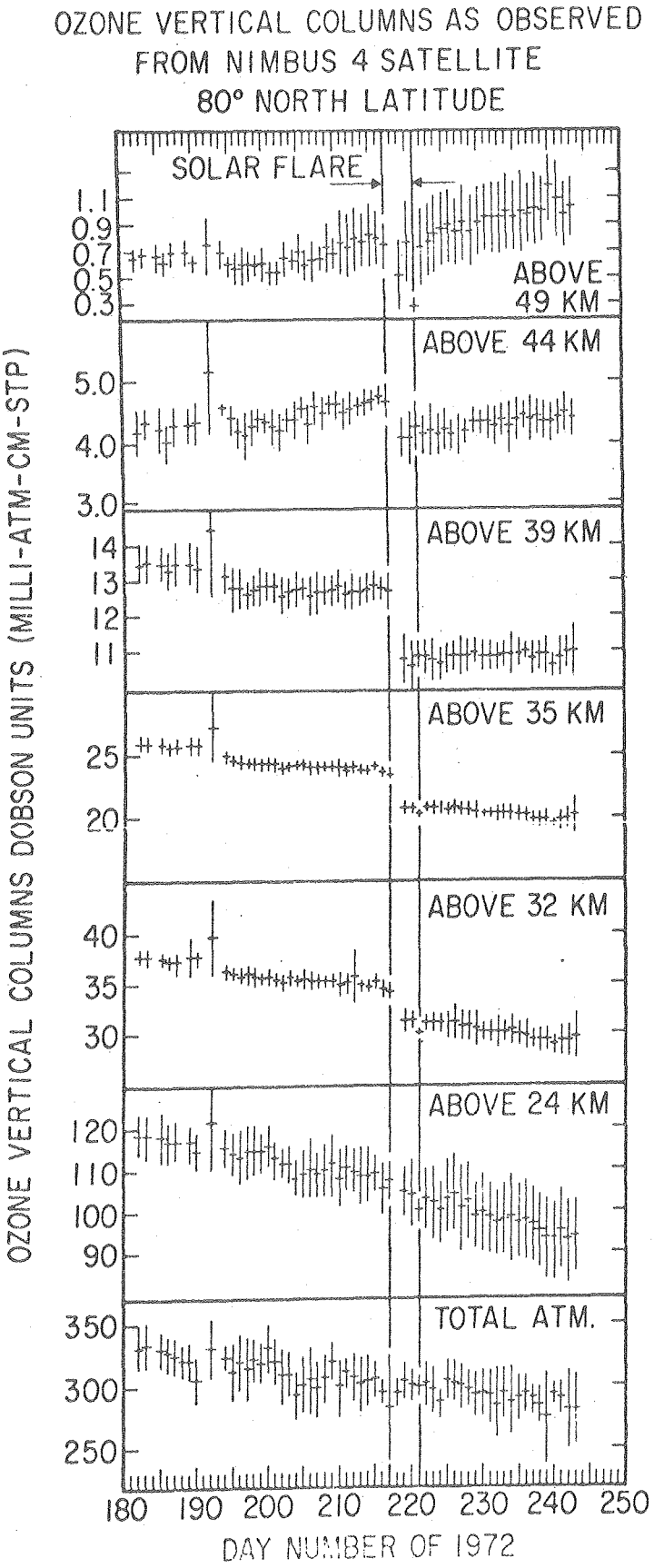

Fig. 4.13
H. S. Johnston

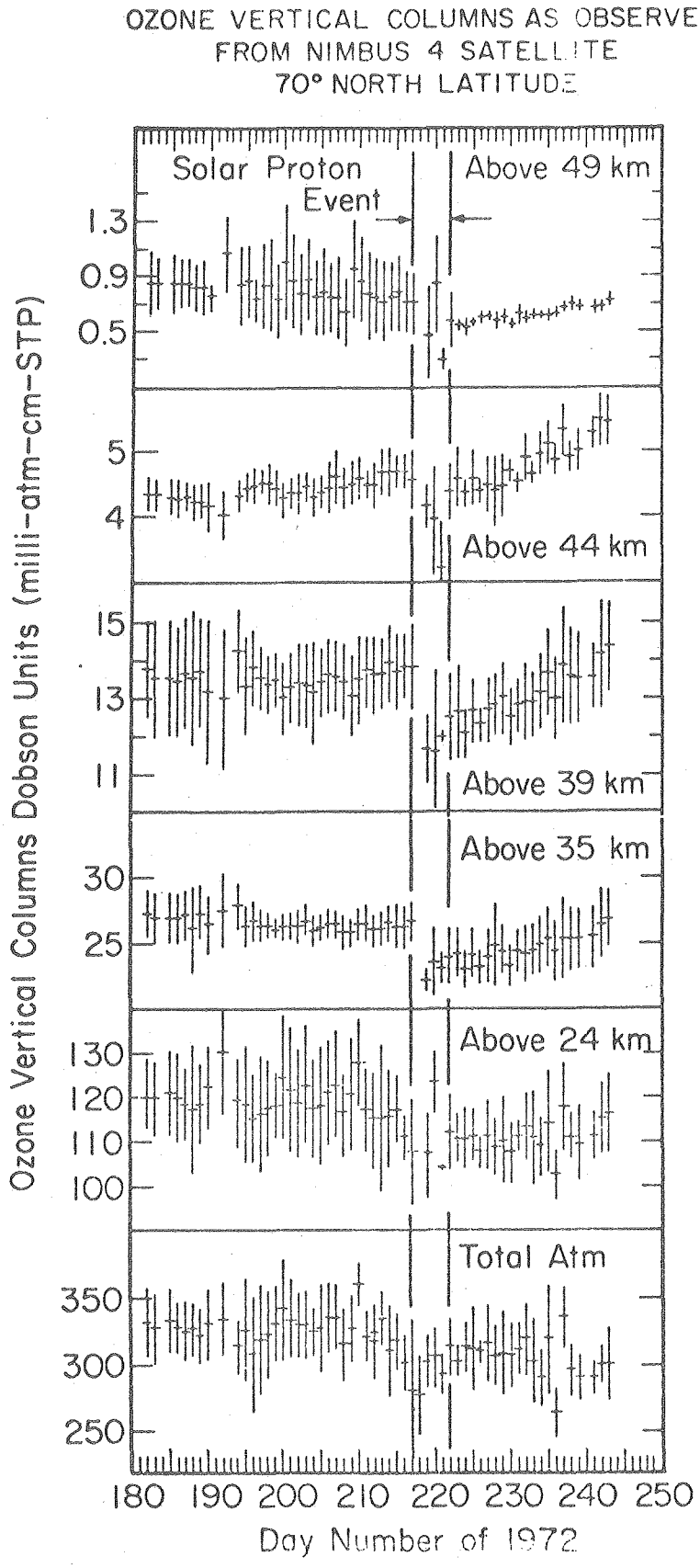

Fig. 4.14
H. S. Johnston

OZONE VERTICAL COLUMNS AS OBSERVED
FROM NIMBUS 4 SATELLITE
50° NORTH LATITUDE

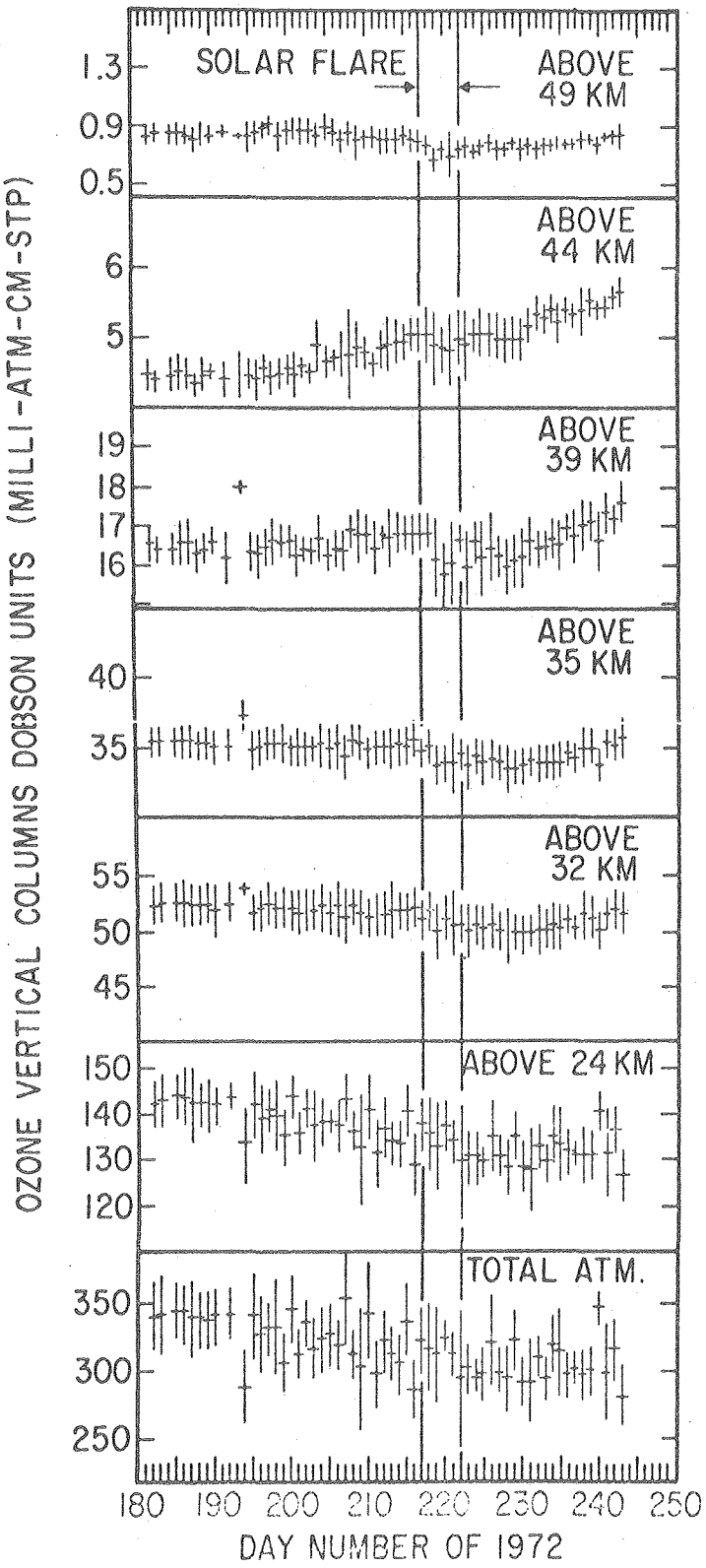

Fig. 4.15
H. S. Johnston

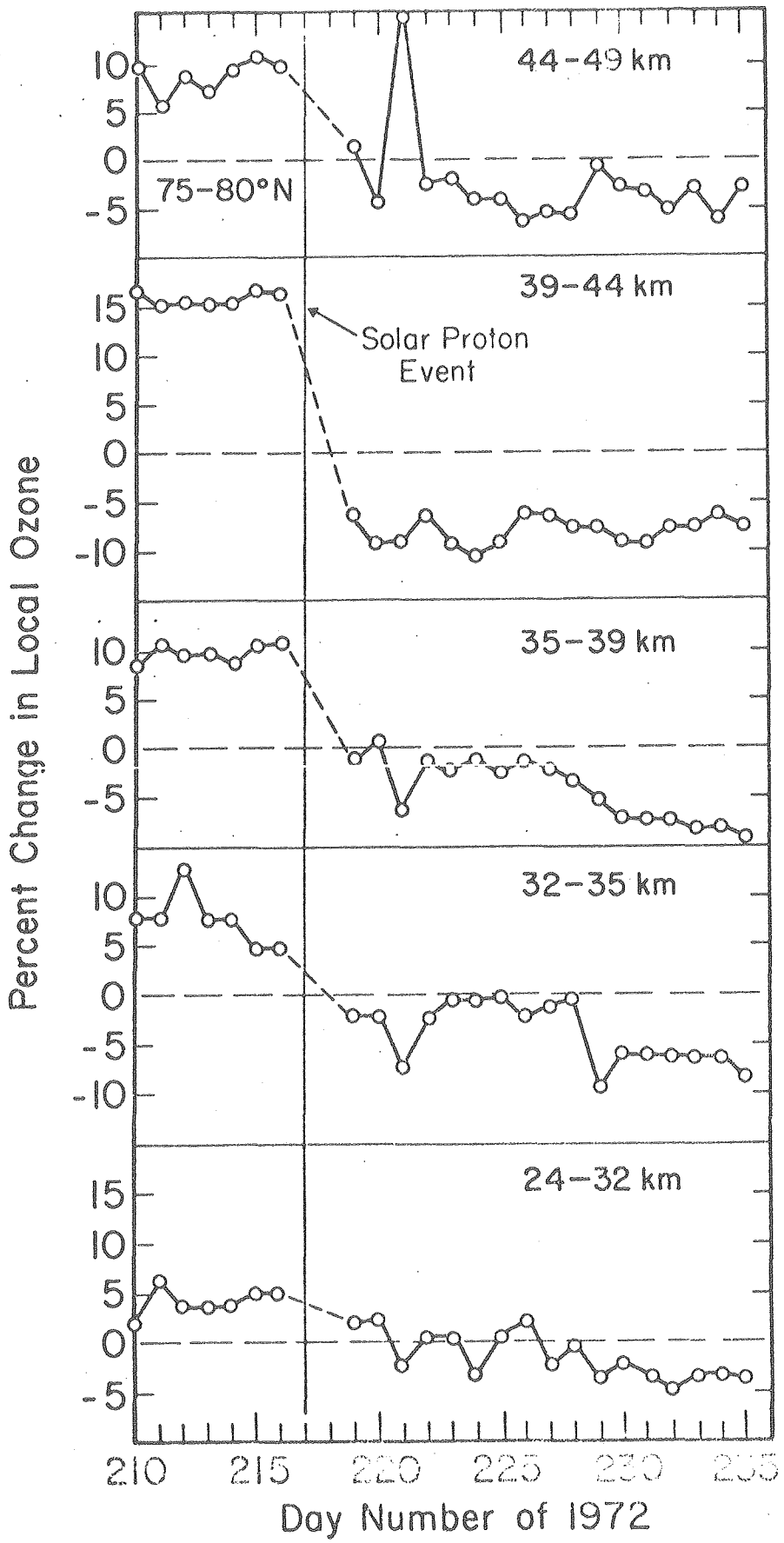

Fig. 4.16
H. S. Johnston

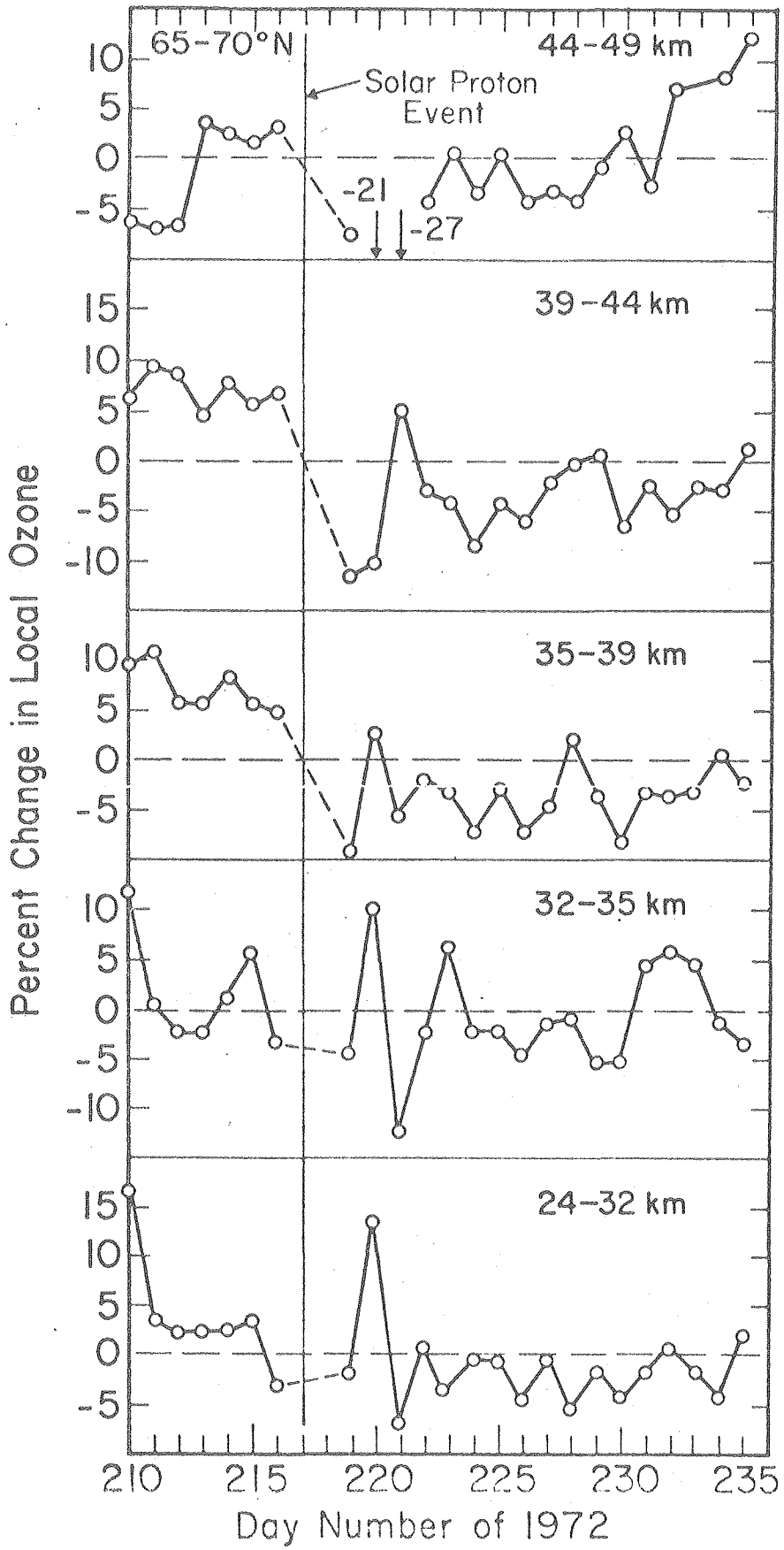

Fig. 4.17
H. S. Johnston

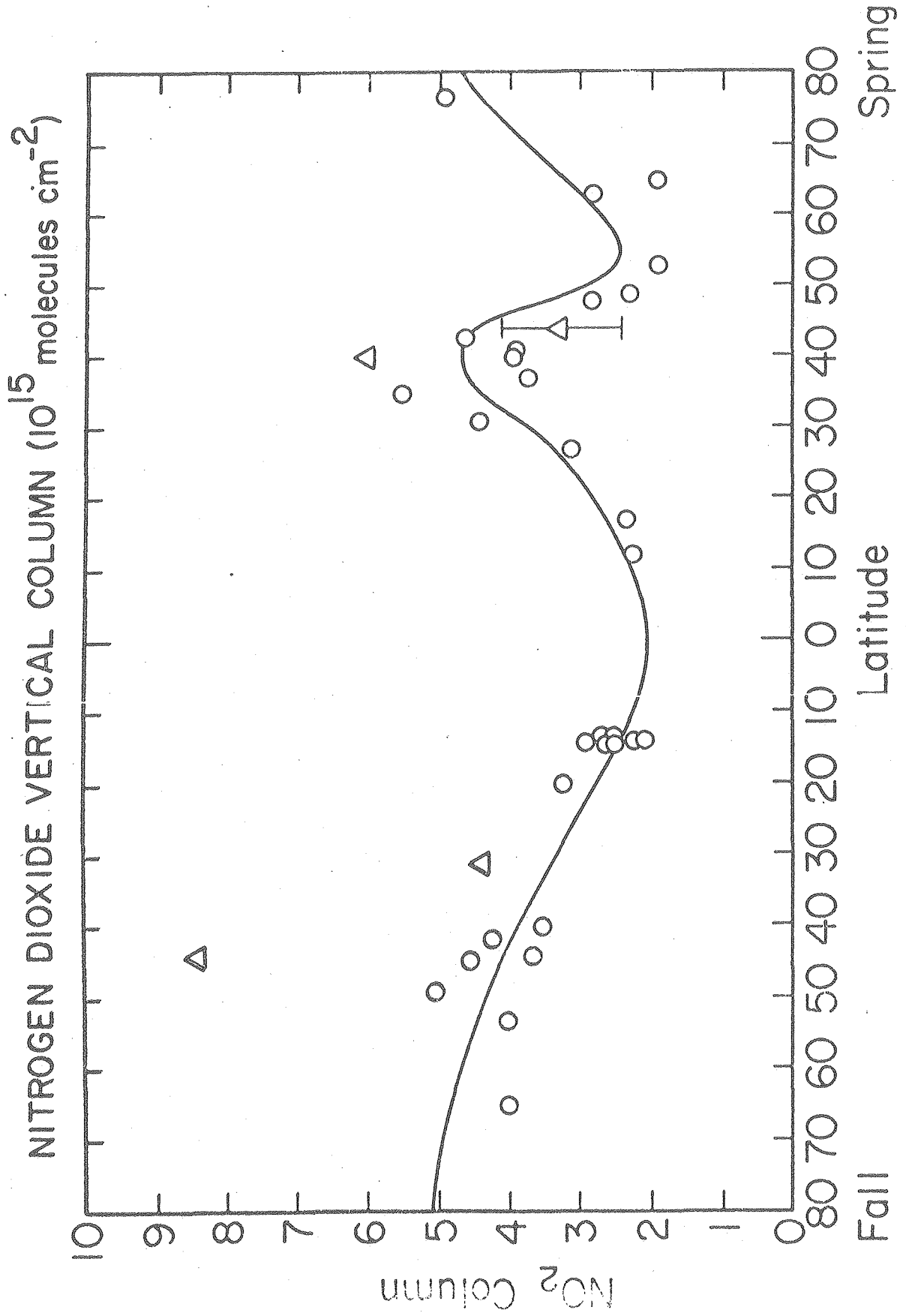

Fig. 4.18
H. S. Johnston

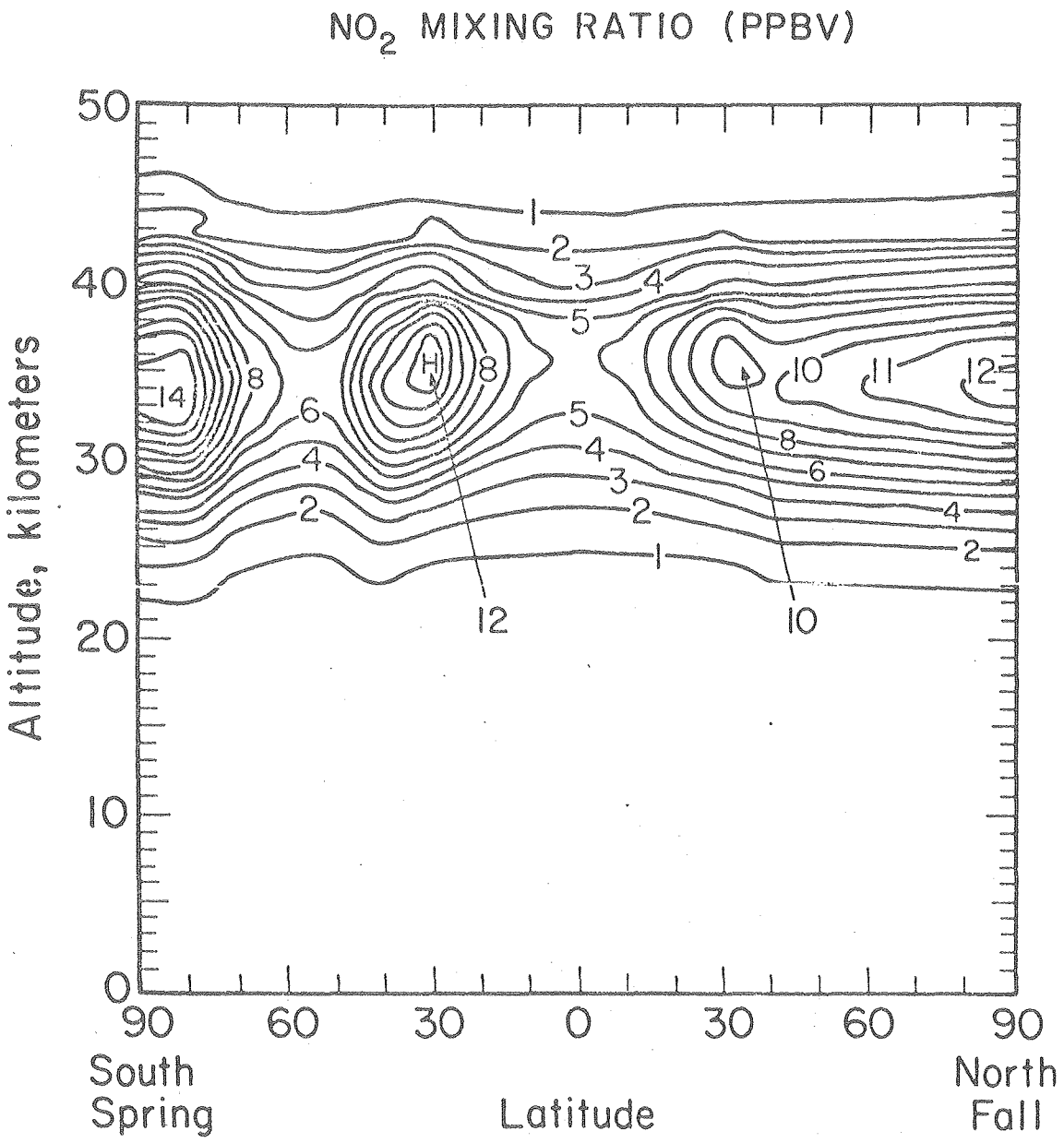

Fig. 4.19
H. S. Johnston

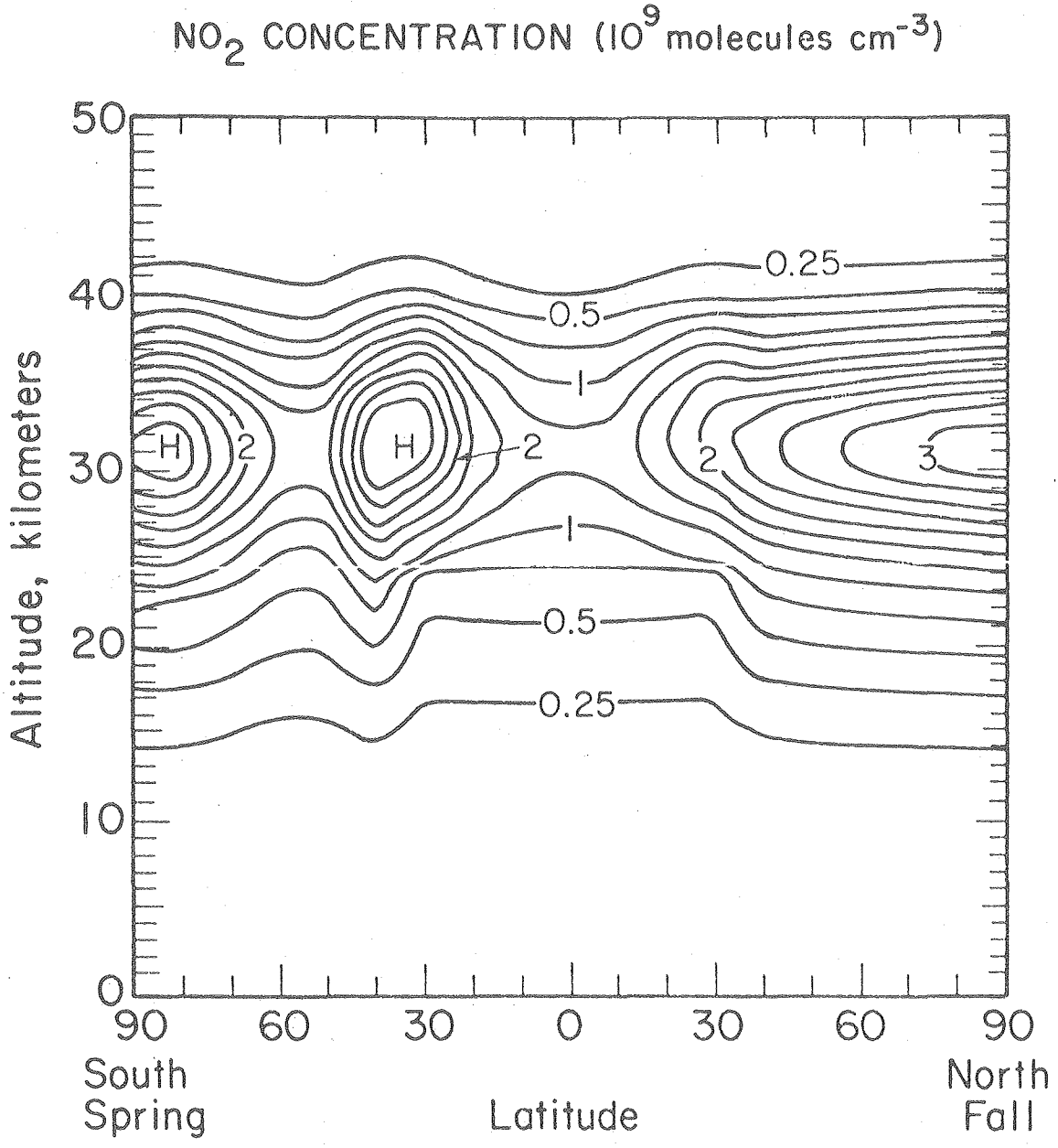

Fig. 4.20
H. S. Johnston

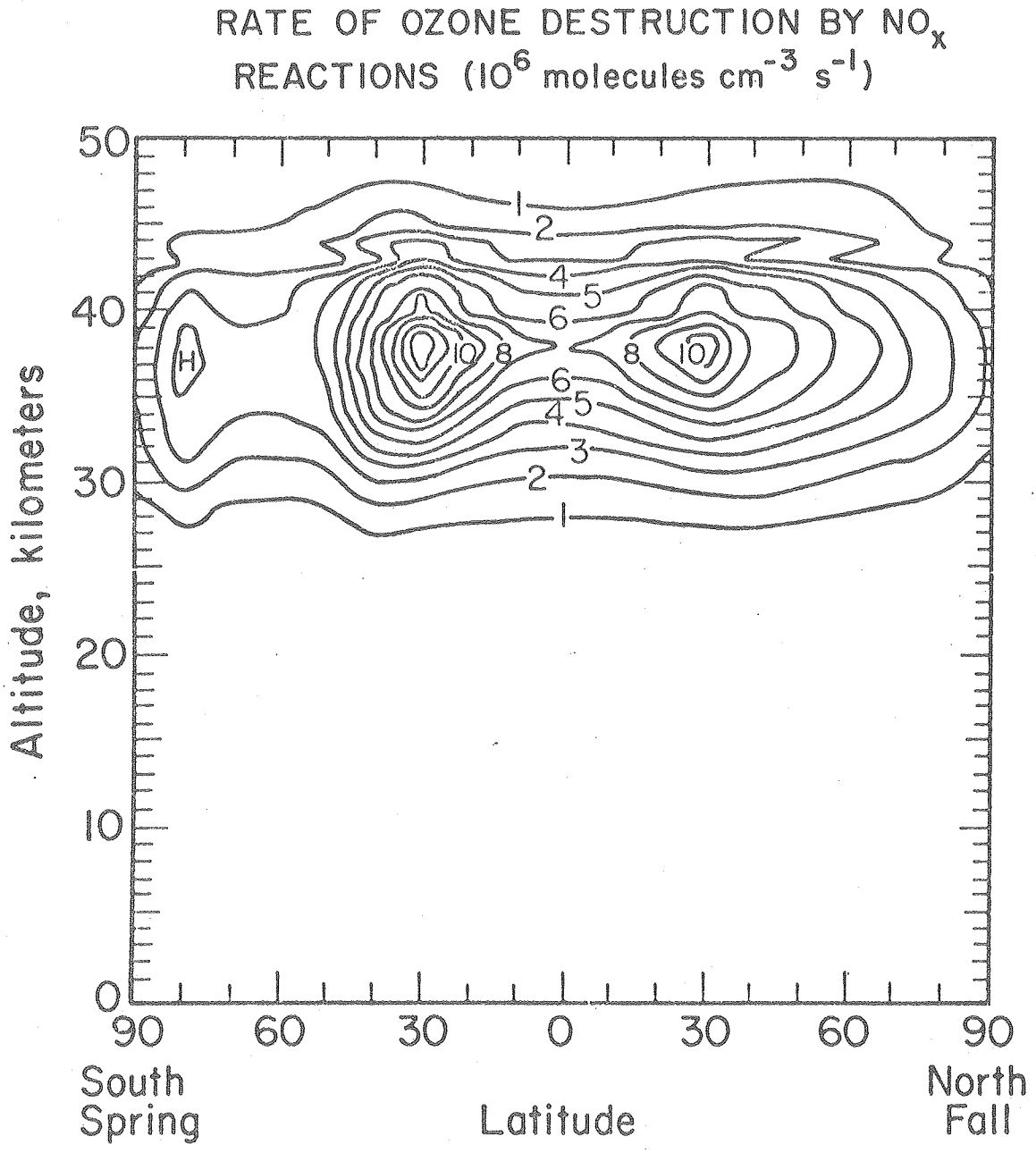

Fig. 4.21
H. S. Johnston

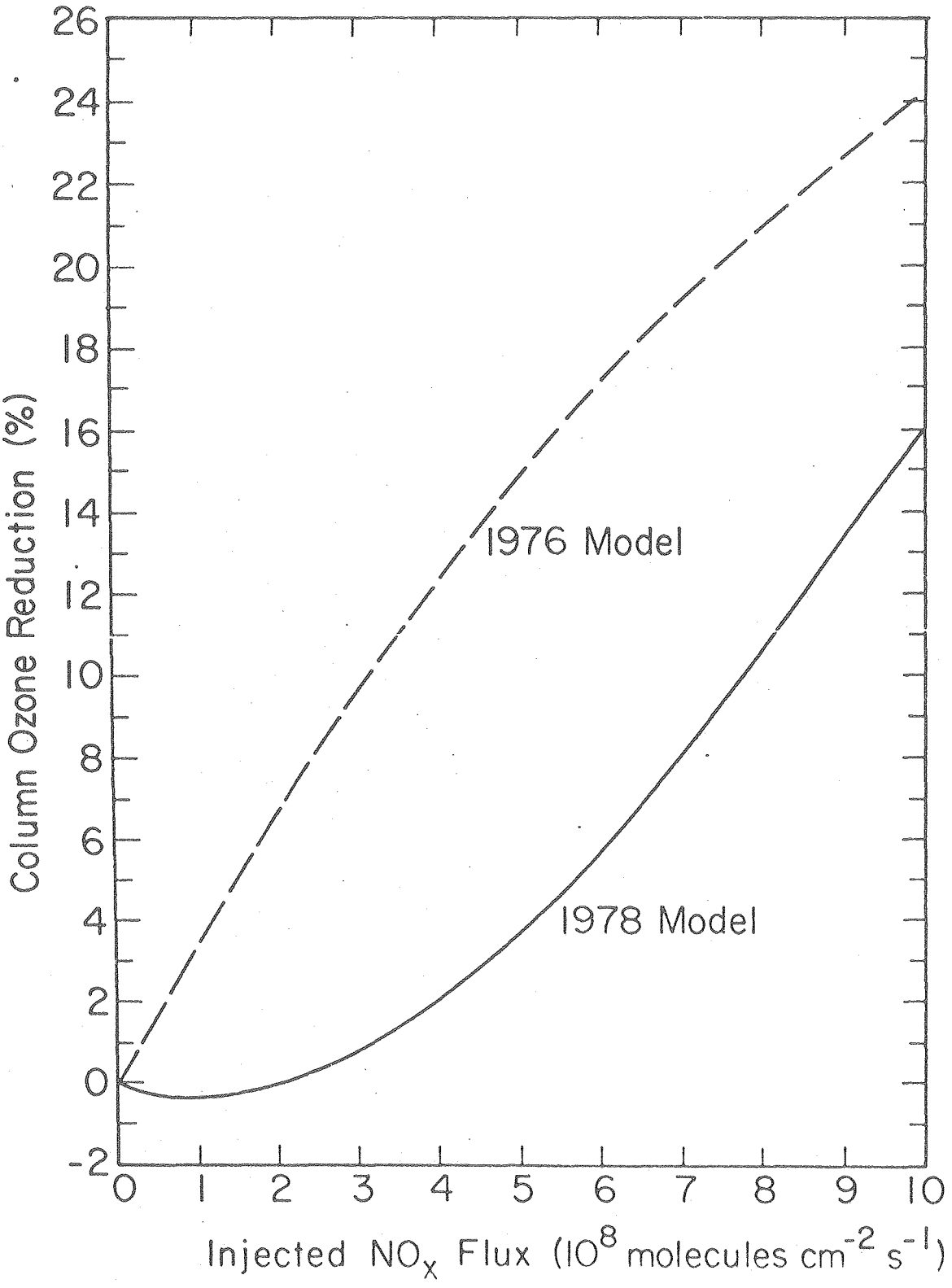

Fig. 4.22
H. S. Johnston

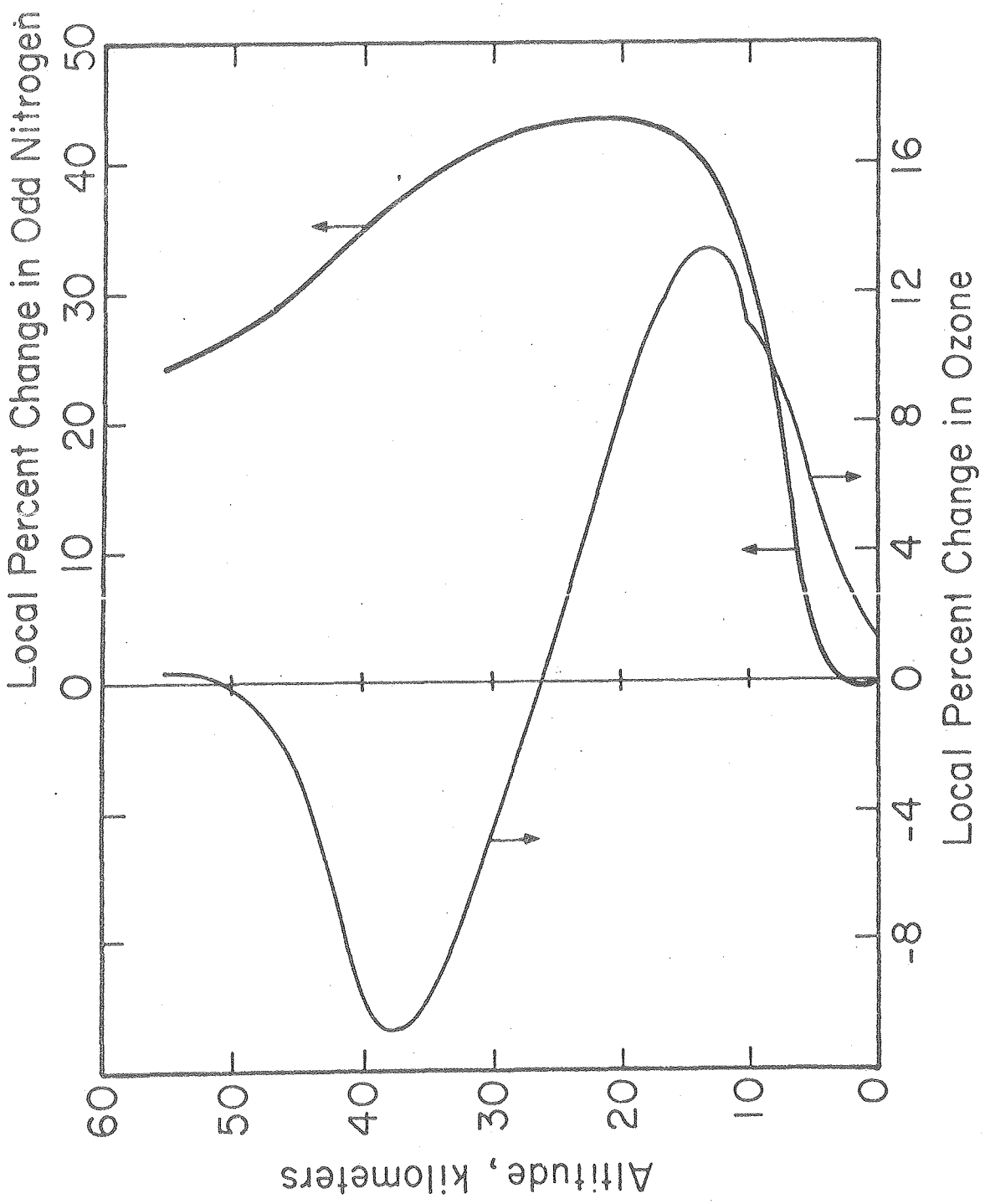

Fig. 4.23
H. S. Johnston

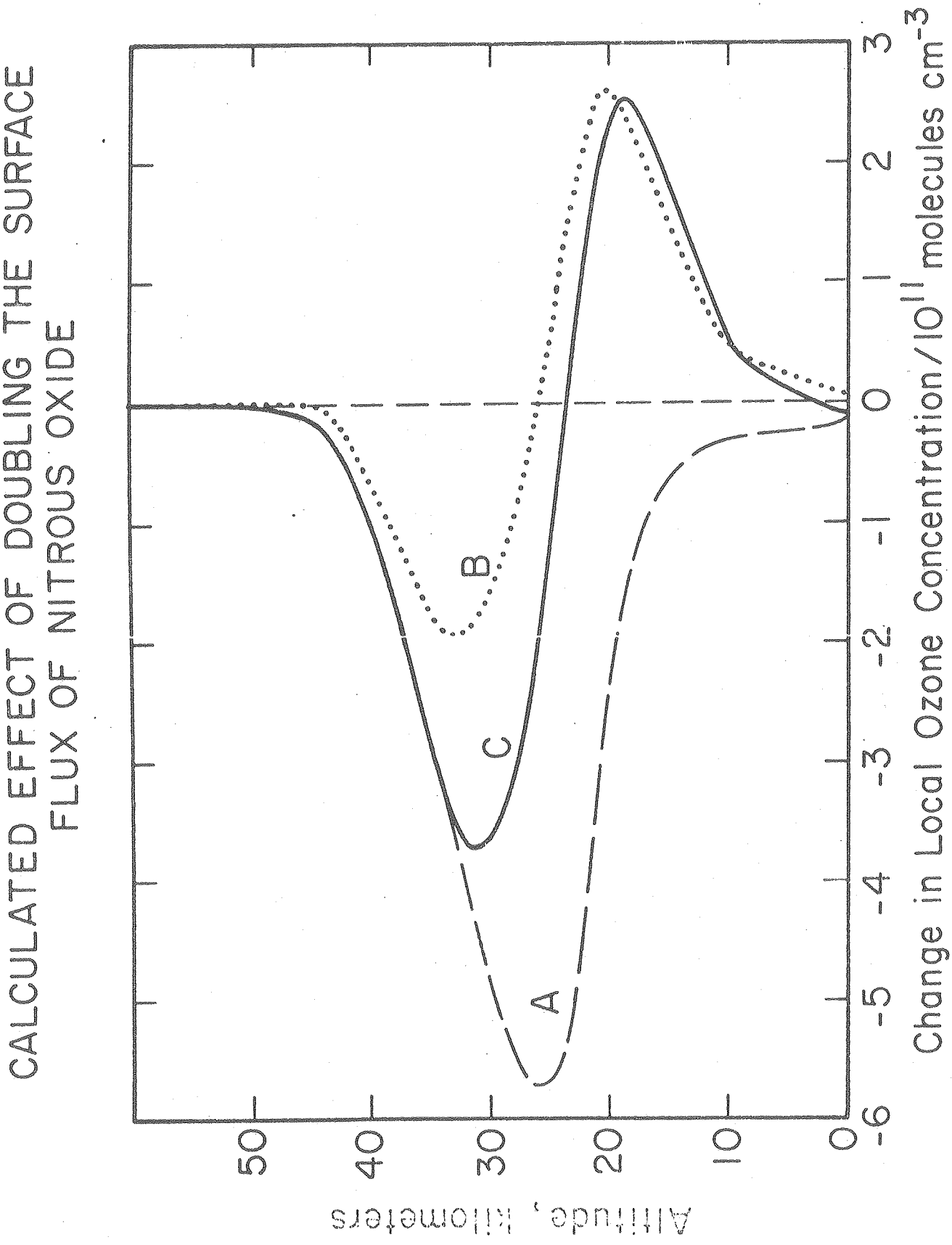

Fig. 4.24
H. S. Johnston

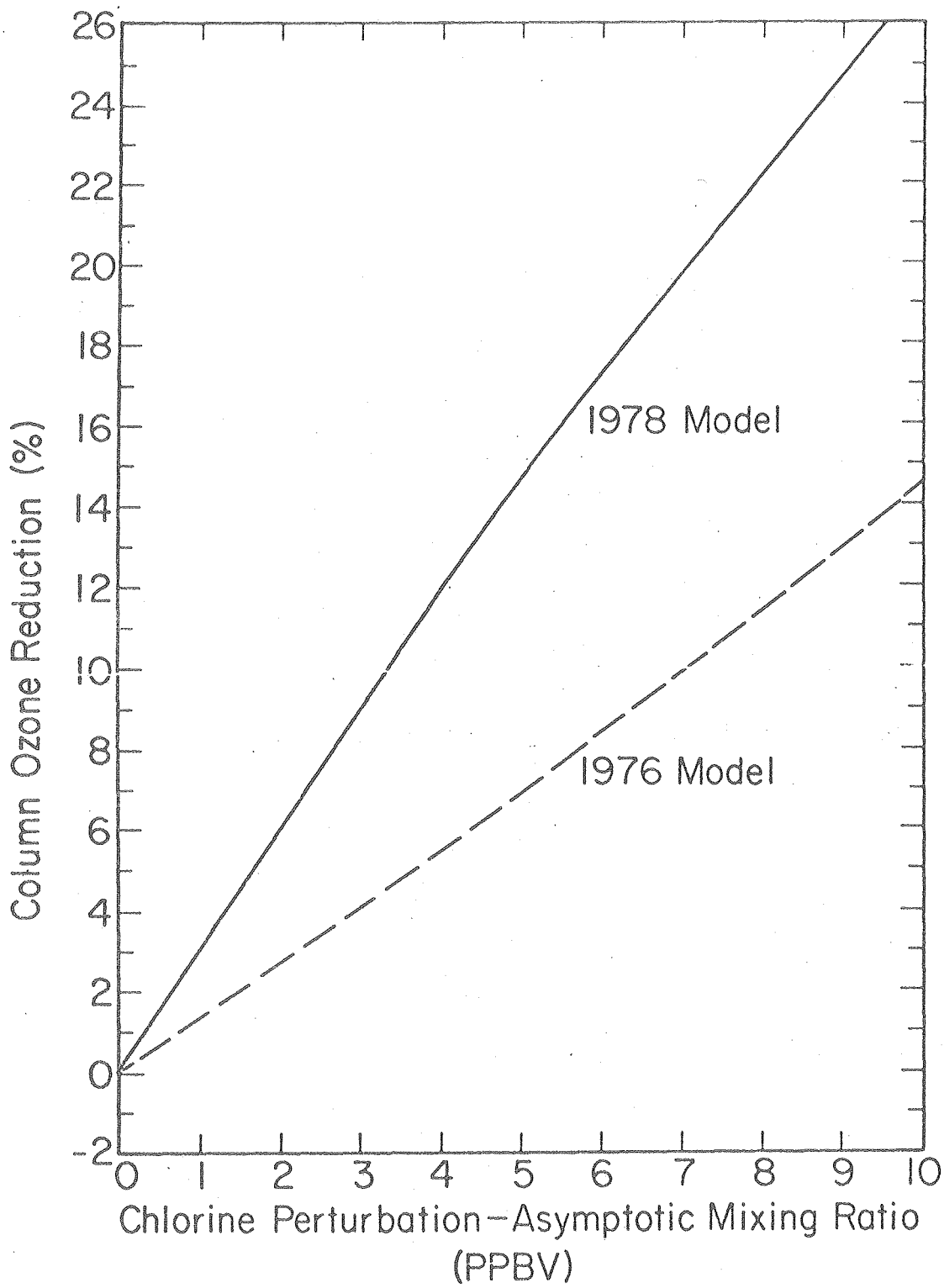

Fig. 4.25
H. S. Johnston

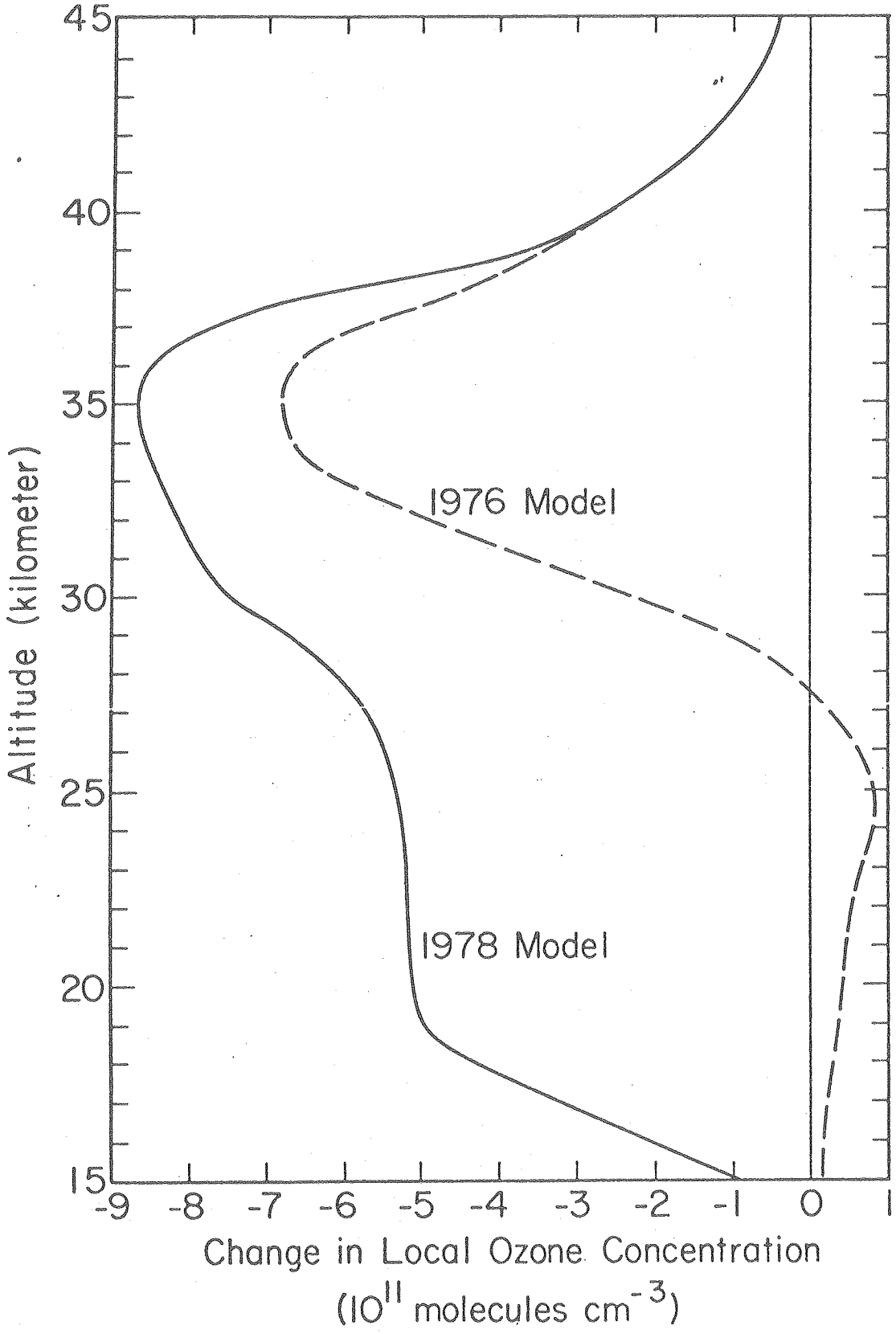

Fig. 4.26
H. S. Johnston

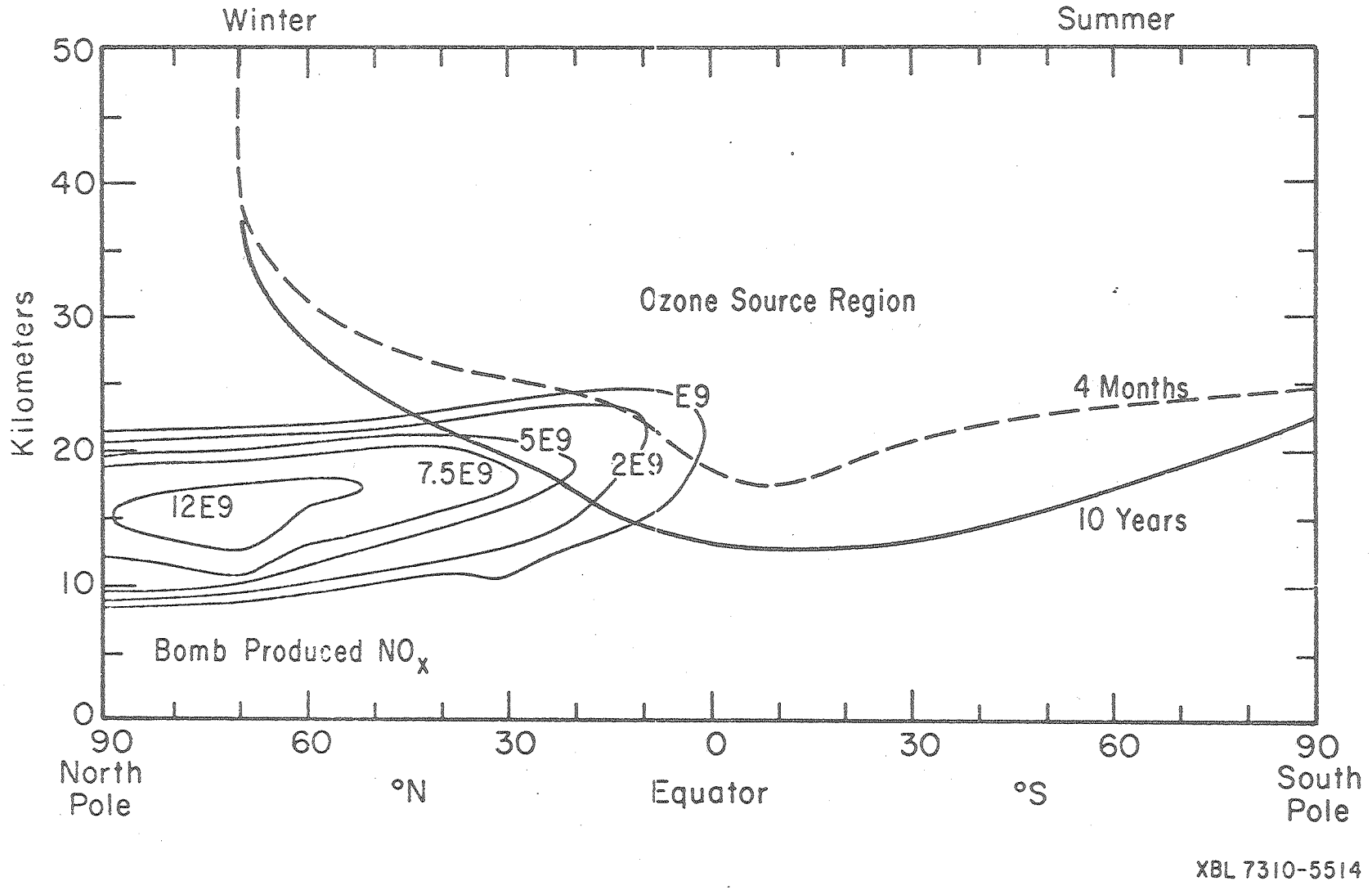

Fig. 4.27
H. S. Johnston

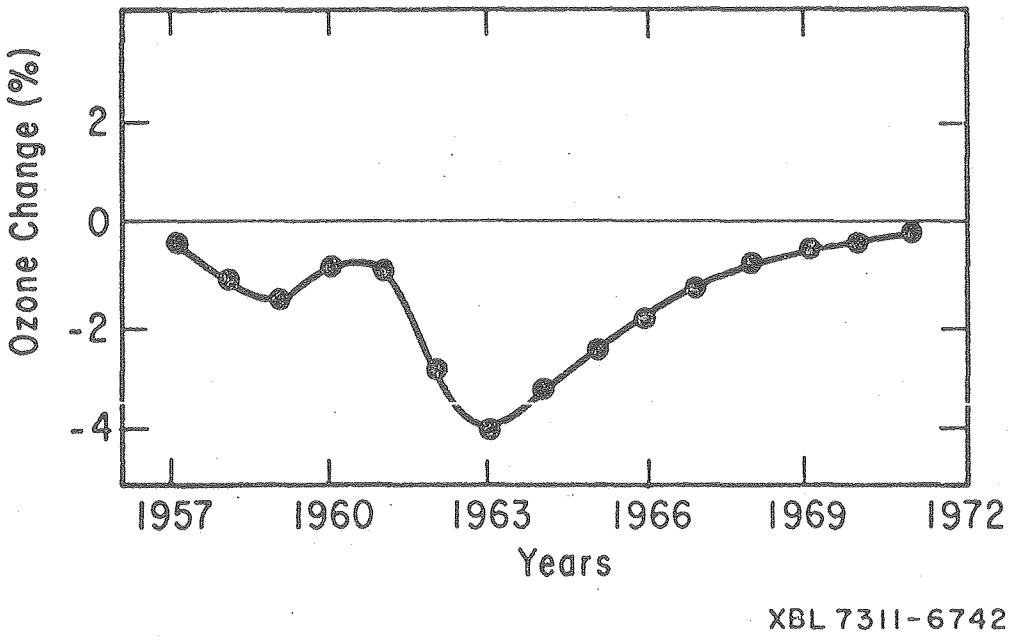

Fig. 4.28
H. S. Johnston

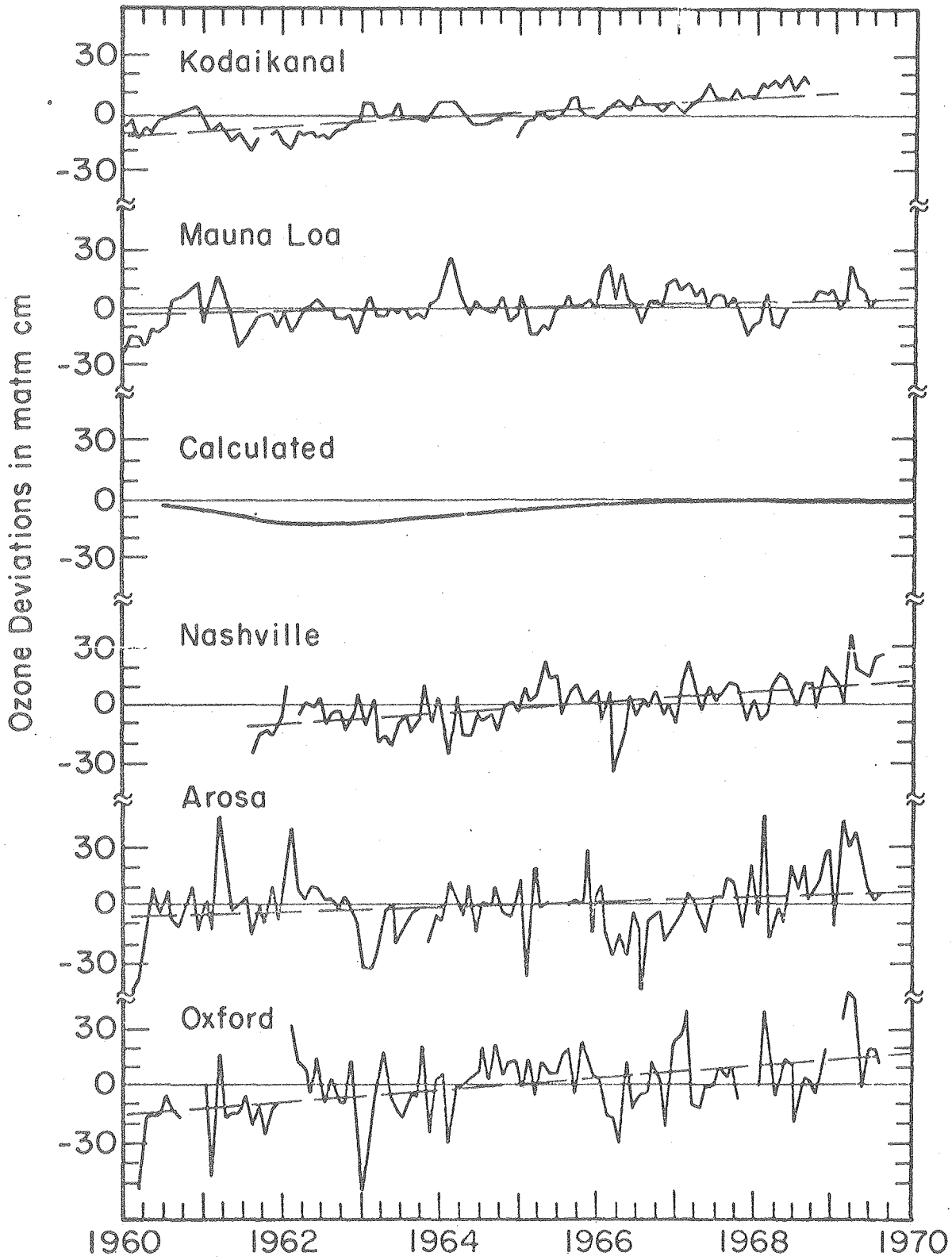

Fig. 4.29
H. S. Johnston

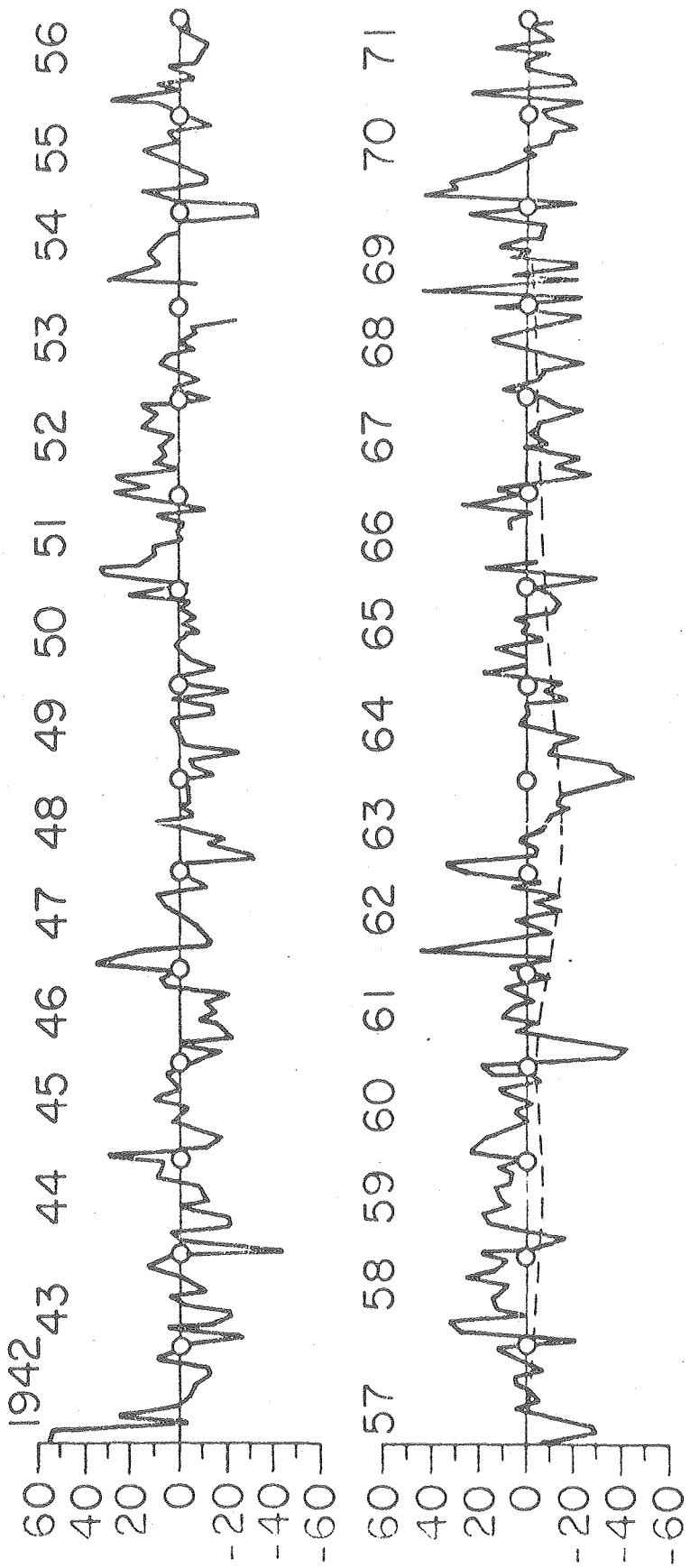

Fig. 4.30
H. S. Johnston

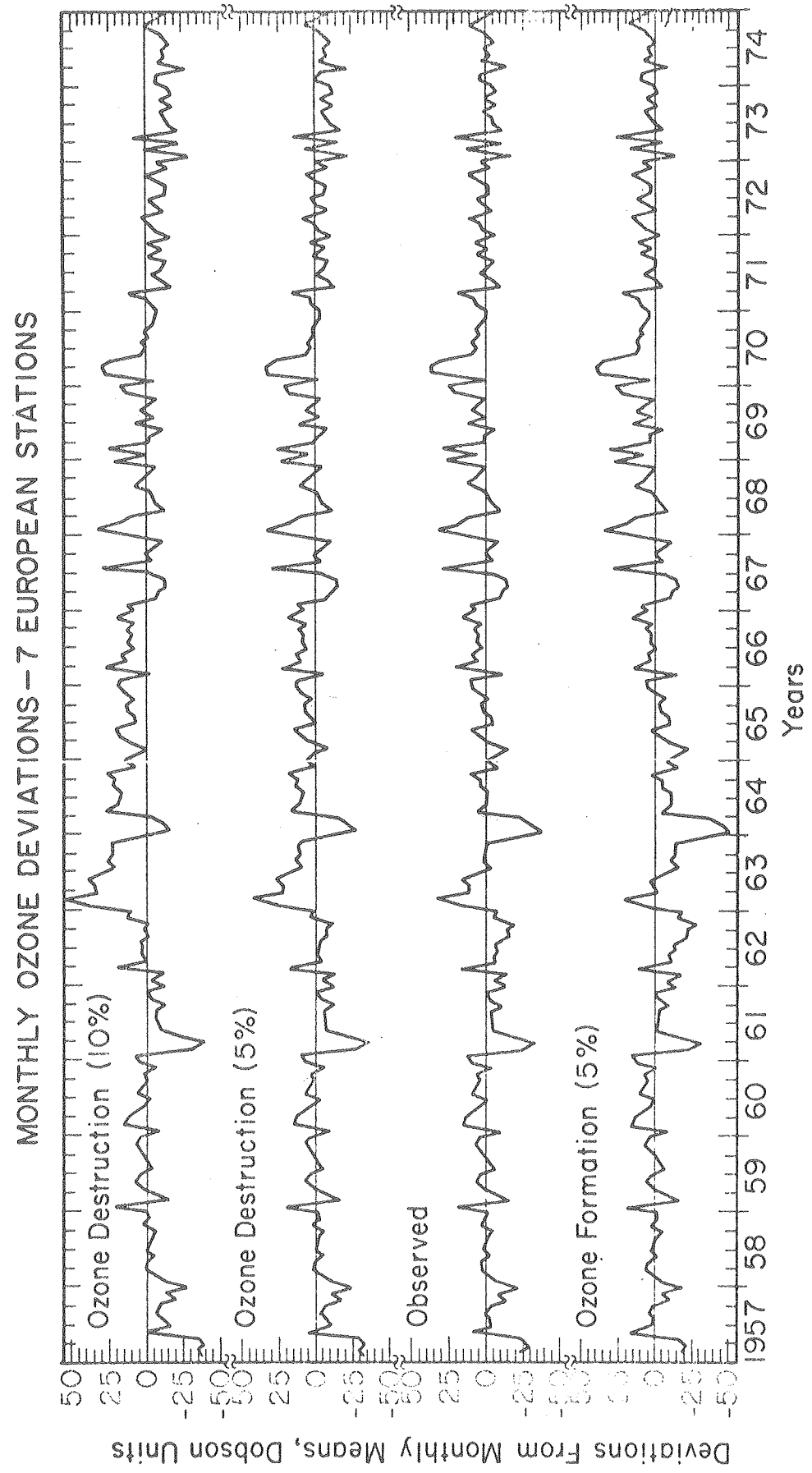

Fig. 4.31
H. S. Johnston

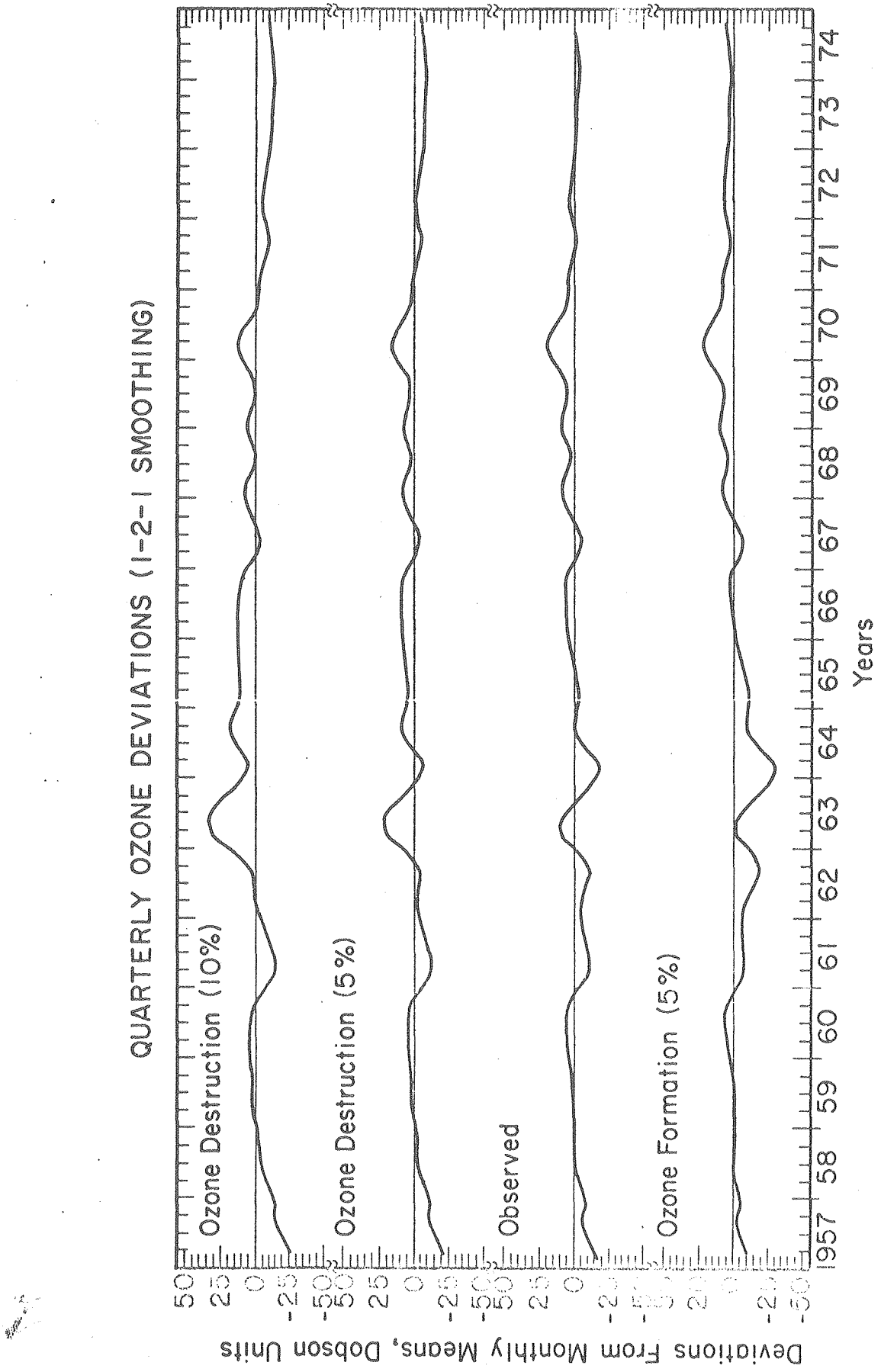

Fig. 4.32
H. S. Johnston

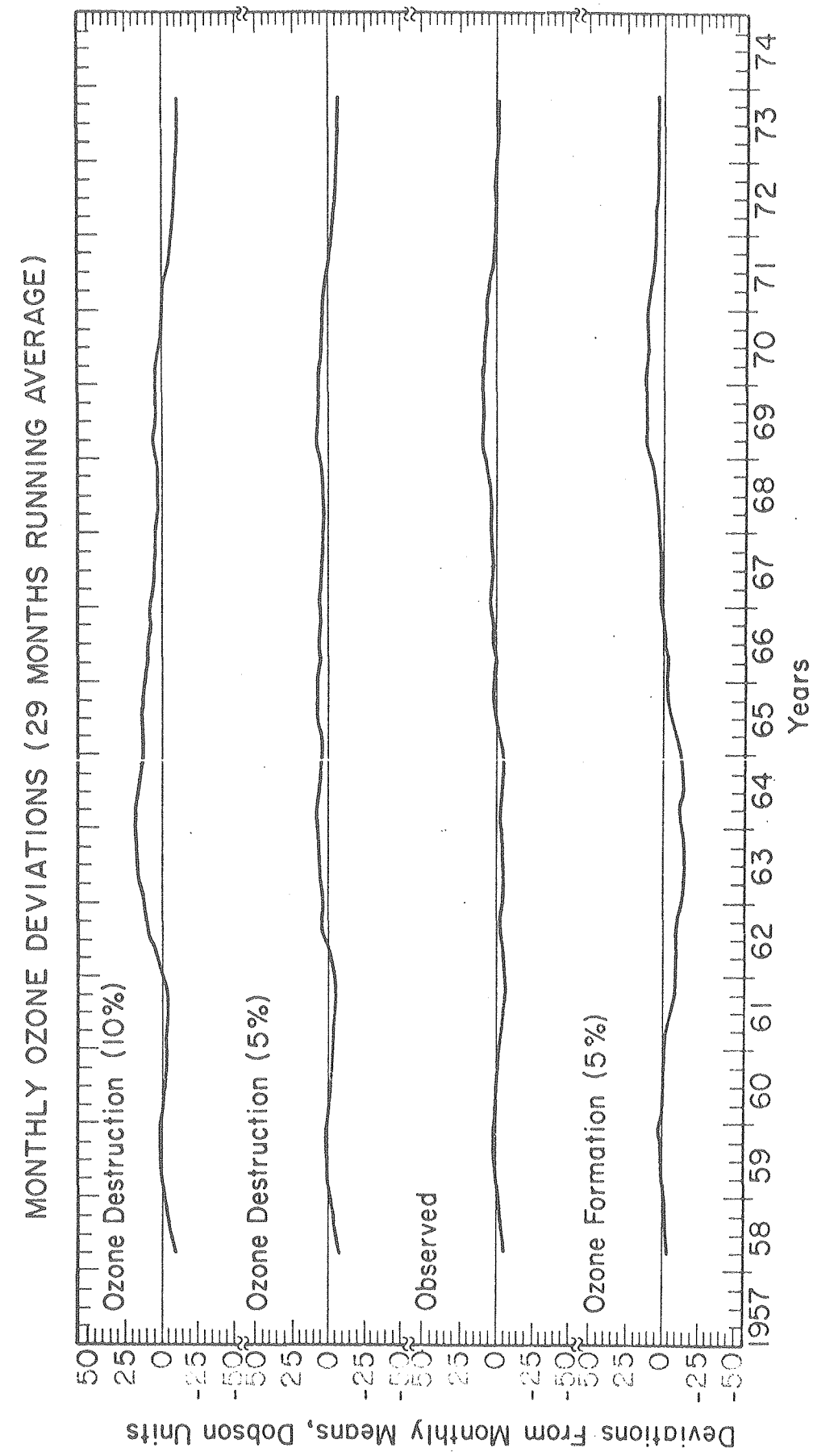

Fig. 4.33
H. S. Johnston

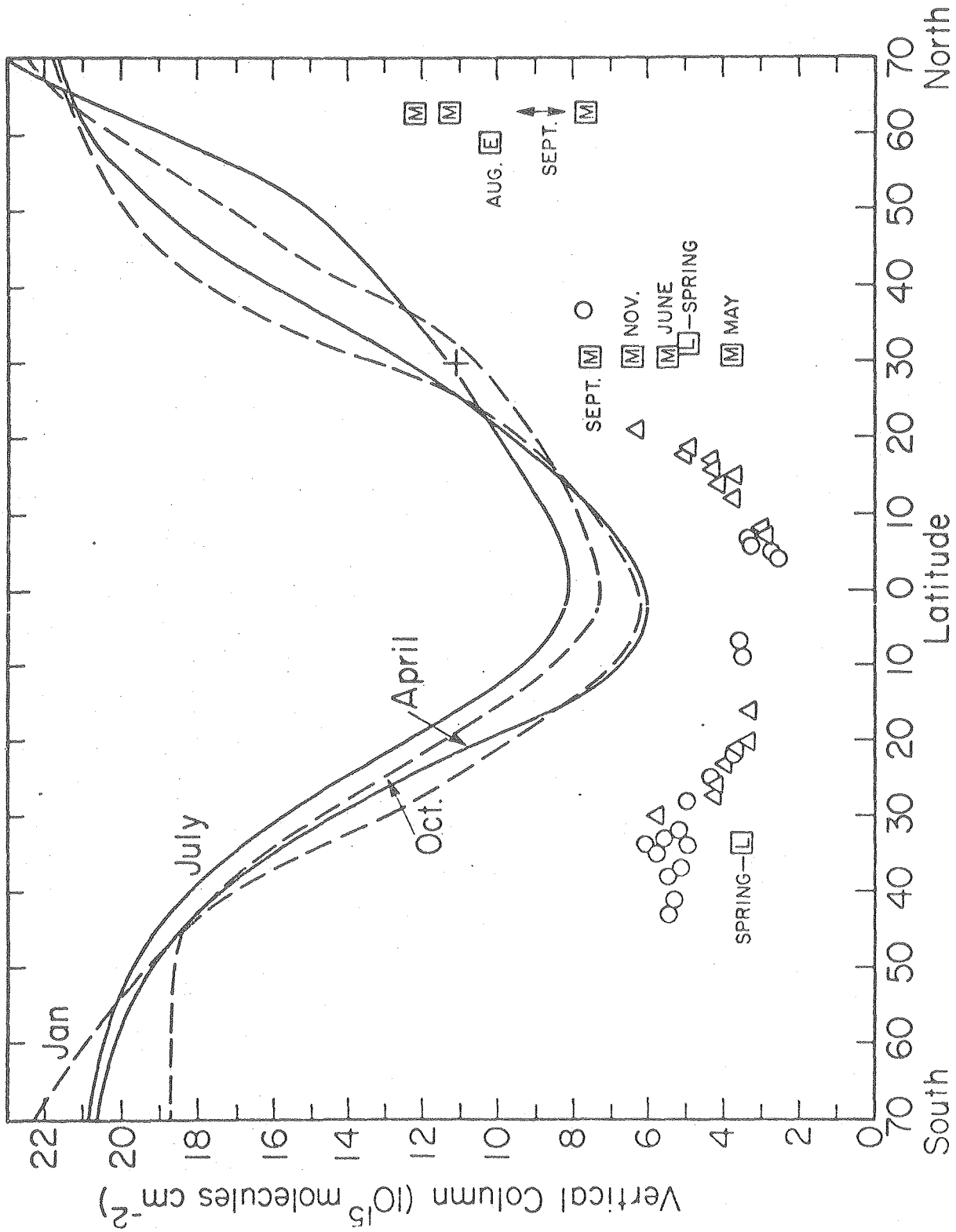

Fig. 4.34
H. S. Johnston

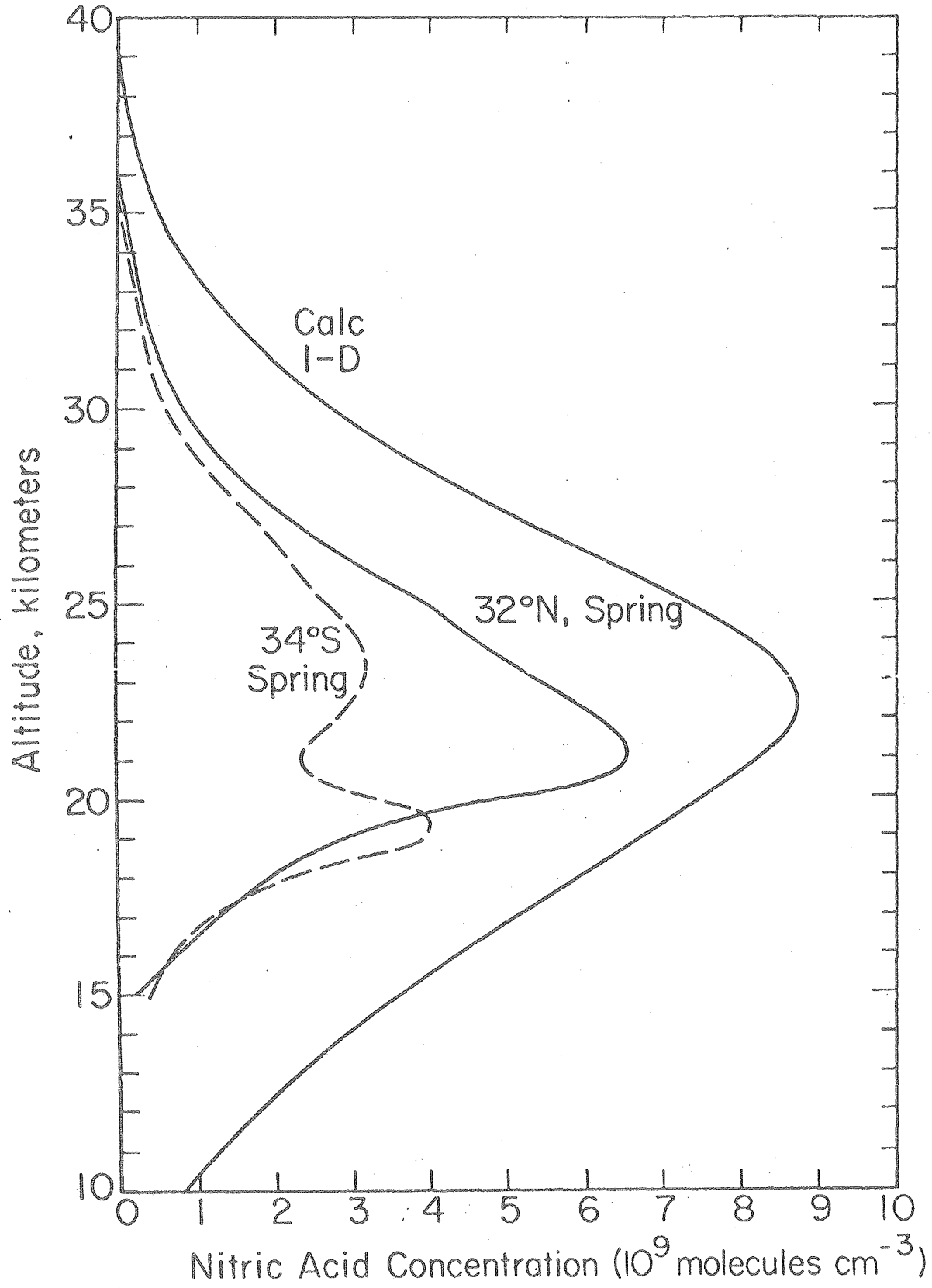

Fig. 4.35
H. S. Johnston

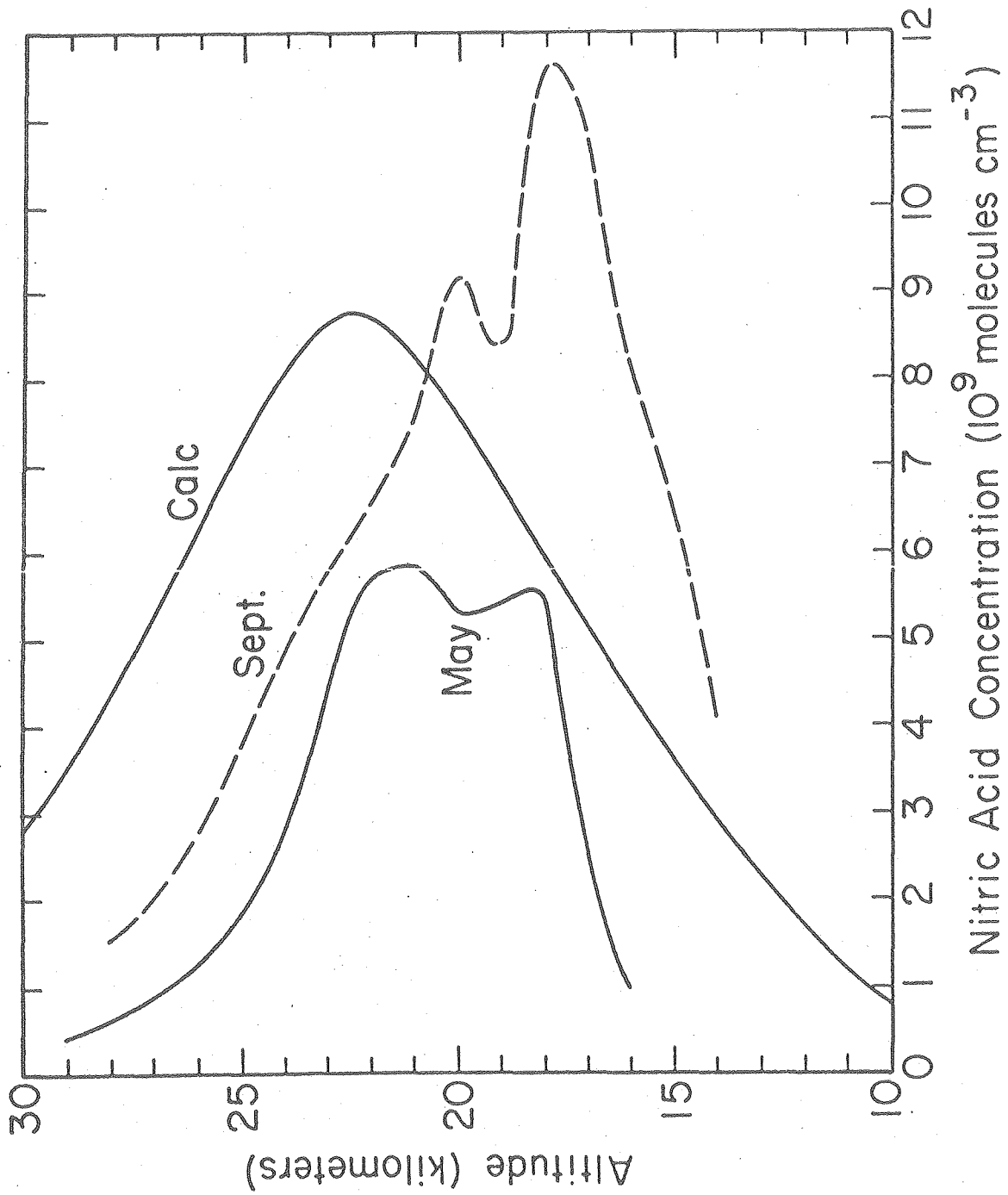

Fig. 4.36
H. S. Johnston

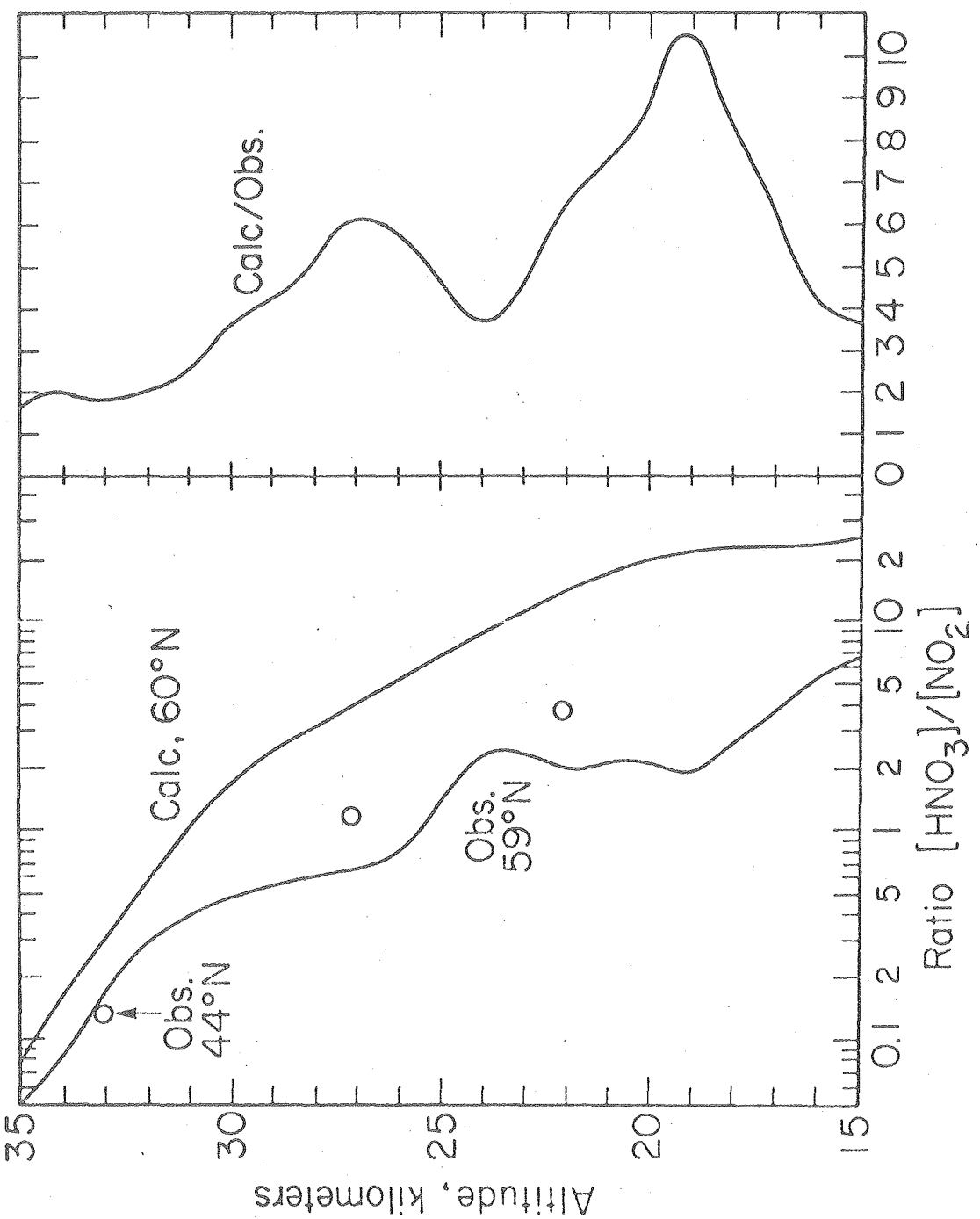

Fig. 4.37
H. S. Johnston

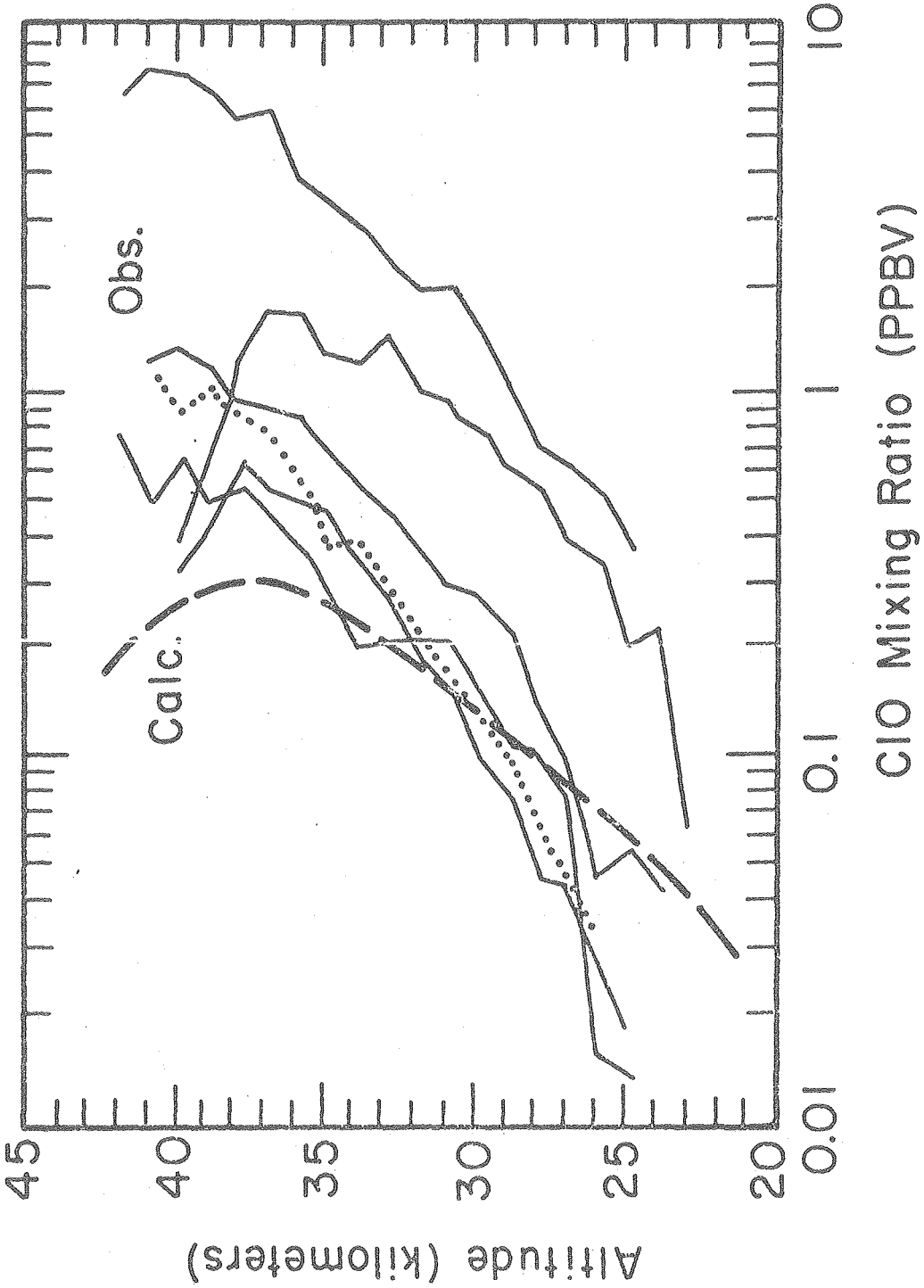

Fig. 4.38
H. S. Johnston